Suppression of hydrodynamic and severe slug flow by using surfactants in flowline-riser systems

J.M. van der Pol

Technische Universiteit Delft

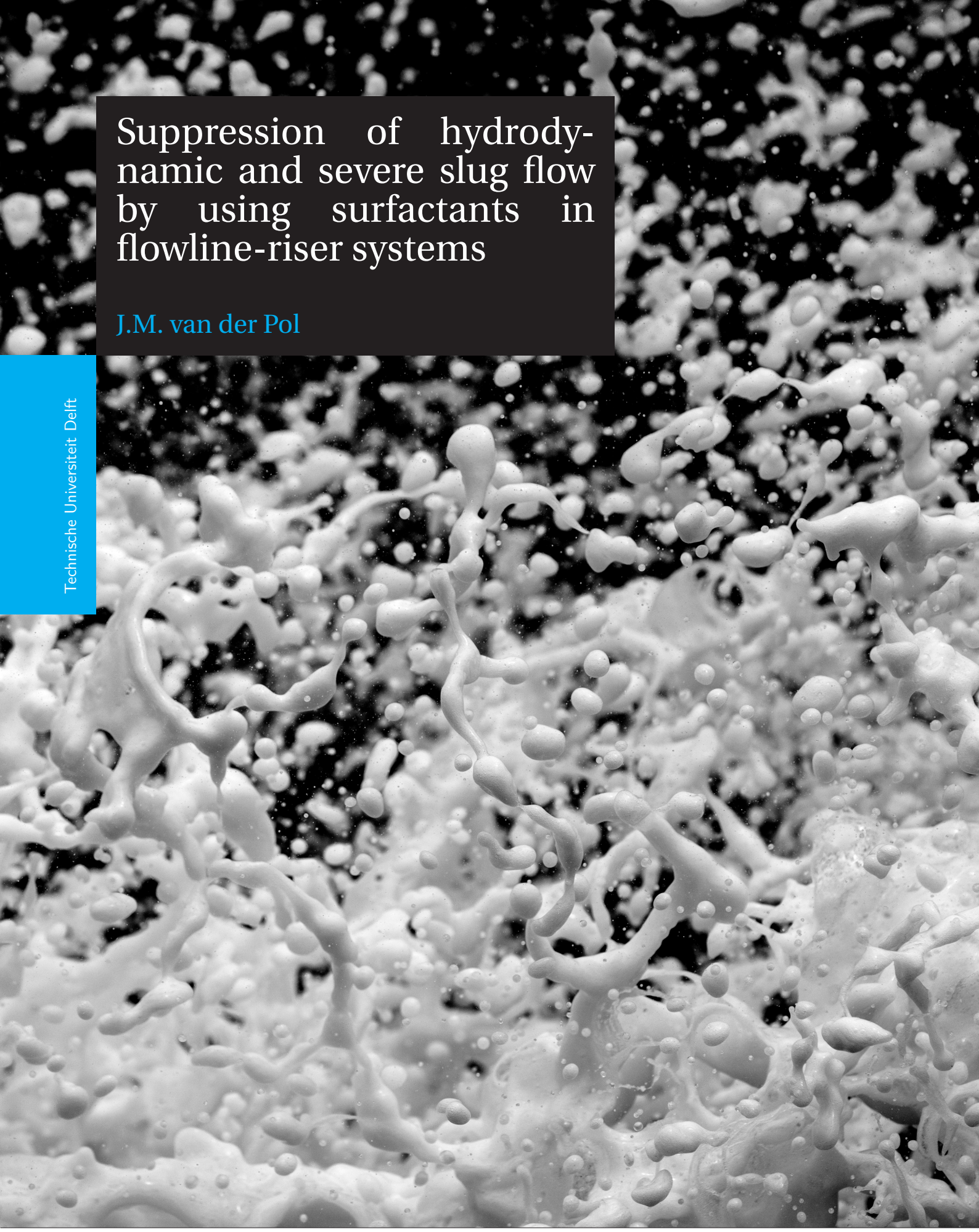

TU Delft Delft University of Technology

Challenge the future

SUPPRESSION OF HYDRODYNAMIC AND SEVERE SLUG FLOW BY USING SURFACTANTS IN FLOWLINE-RISER SYSTEMS

by

J.M. van der Pol

in partial fulfillment of the requirements for the degree of

Master of Science
in Mechanical Engineering

at the Delft University of Technology,
to be defended publicly on Wednesday March 20, 2019 at 13:30 AM.

Student number:	4084748	
P&E number:	2961	
Supervisor:	Prof. dr. ir. R.A.W.M. Henkes	TU Delft
Thesis committee:	G. Pagliuca MSc	Shell
	Dr. ir. W.P. Breugem	TU Delft
	Dr. ir. J.W. Haverkort	TU Delft

TU Delft Delft University of Technology

PREFACE

This project has proven to be a great learning experience for me, as it was the first time for me working with an experimental setup of these dimensions. It was also the first time using the Distributed Acoustic Sensing measurement technique and post-processing the data in order to quantify it and derive meaningful properties of the flow. A lot of hard work has been put into this thesis, which I could not have done without the help of several people. Of these people I would like to thank a few in particular.

First of all, I would like to thank my two supervisors from the TU Delft and Shell for supervising me throughout this project. Giuseppe Pagliuca was my daily supervisor who always gave great suggestions when I presented my progress and always made time to help me with getting the experimental setup up and running when a challenge did arise. My second supervisor was Ruud Henkes, who was both my TU Delft supervisor and Shell mentor. I would like to thank him for the opportunity to write this thesis as part of an internship at Shell, which he offered me after our first chat. He gave me very useful feedback and asked the right questions during our weekly meetings to let me perform at my best.

I would also like to thank Magdalena Wojtaszek for helping me with the post-processing tools of the Distributed Acoustic Sensing measurements. She debugged an existing code for the velocity tracking algorithm that made the quantitative results of the DAS possible.

J.M. van der Pol
Delft, March 2019

ABSTRACT

In the oil and gas industry the occurrence of slug flow in flowlines and risers can cause operational problems. Such flowline-riser systems are used to transport the oil and/or gas from the location of the wells to a production platform, where the fluids might be separated into single phases. Slug flow conditions impose fluctuations in the production rate, which may lead to the flooding of the separators, trips of compressors or pumps, and to increased loads on the supports of the pipeline and piping sections at the production platform. Therefore, measures have to be taken to mitigate the slugging, which can be a reduction of the production rate, making adjustments to the pipeline system, or adding surfactants to the flow. For vertical flow in production wells, the use of surfactants is a proven technology. Here the creation of a foam through adding a surfactant can increase the production life time, as the accumulation of liquid, which typically occurs when the reservoir pressure has decreased at the end of field life, is prevented. Far less is known yet about the effect of using surfactants for the mitigation of hydrodynamic slugs in a nearly horizontal flowline or the mitigation of severe slugs in risers.

From a previous Master's Thesis project by Pronk [1], in which lab experiments were carried out in the same flowline-riser facility as used in the present study, it was concluded that growing slugs could be suppressed by adding a surfactant to create foam. The surfactants also influence the characteristics of the severe slugging cycle, but they are not able to fully suppress it. Re-analysis of the measurement data by Pronk has turned out that instead of growing slugs, severe slugging was measured and therefore that severe slugging can be suppressed using surfactants and no conclusions can be drawn on growing slugs or hydrodynamic slugs from her research. There is limited literature on the effect of adding a surfactant to hydrodynamic slug flow in horizontal flowlines, but there are some indications that hydrodynamic slugs can be suppressed, though requiring a higher concentration of the surfactant than vertical flow. Suppressing slug flow using surfactants should eliminate the fluctuations in the flow and can lead to a lower pressure drop.

For this research experiments have been carried out in the Severe Slugging Loop at the Shell Technology Centre Amsterdam. This flow loop consists of a horizontal flowline of 50 m, a U-turn and a 15 m section. From there onward the pipe starts declining at an angle of -2.54° over a length of 35 m. Thereafter there is a short horizontal section of 5 m before arriving at the base of the riser, which has a height of 16.8 m and an internal diameter of 32 mm. The other sections have an internal diameter of 50.8 mm. For this research the configuration was used where air and water are connected through a Y-sprout at the start of the flow line. The air is supplied as pressurized air of 6 barg. The water is supplied by a pump, and it is separated from the air at a section at the top of the riser and recirculated through the system. The used surfactant is the household detergent Dreft.

At several points along the flowline and riser the flow conditions have been measured using pressure indicators and at two locations along the flowline the pressure difference over 3 m has been measured using differential pressure indicators. Through the inspection window at the end of the flowline the flow is recorded by using a GoPro camera. Furthermore, over a distance of 40 m the acoustic energy of the flow has been measured by a Distributed Acoustic Sensing (DAS) system. The DAS measurements have been used to determine the flow behaviour of the flow. In the case of slug flow, the velocity of the slugs was deduced from the DAS data.

Adding a 2000 ppm concentration of the surfactant Dreft Original has resulted in the full suppression of hydrodynamic slug flow. This has been verified using the pressure data, the video data and the DAS data in combination with the velocity tracking tool. The waves that were present without surfactant are decreased to a much smaller wave height when the surfactant is added; therefore, the flow pattern is changed from slug flow to wavy stratified flow. The severe slugging cycle can also be suppressed using 2000 ppm concentration of the surfactant Dreft Original. At the same flow conditions, the gas is able to lift more liquid through the riser.

The measurements by the DAS system were quantified using a velocity tracking algorithm. The measurement data can now be used to accurately measure the slug velocity and to determine whether slug flow or stratified flow is present in the system. This measurement method is ready for scale-up.

When the concentration of surfactant is sufficient to suppress slug flow, the flow can be described from visual observations as a threephase flow, containing gas, foam and liquid. The foam absorbs the stresses

imposed by the other phases, because of its non-Newtonian fluid properties. The waves are no longer able to grow until they reach the top of the pipe and are diminished into slow moving dampened waves of the foam layer.

CONTENTS

1

INTRODUCTION

1.1. MOTIVATION

In the upstream production process, hydrocarbon fluids are extracted from reservoirs and transported from there to the processing facilities. Often, the fluid consists of multiple phases while coming from the subsurface well and passing through flowline(s) and riser(s). Oil and gas are frequently produced in combination with water; the water is being separated at the production platform before being transported further or re-injected into the reservoir after extensive membrane filtering. A schematic overview of this process can be seen in figure 1.1.

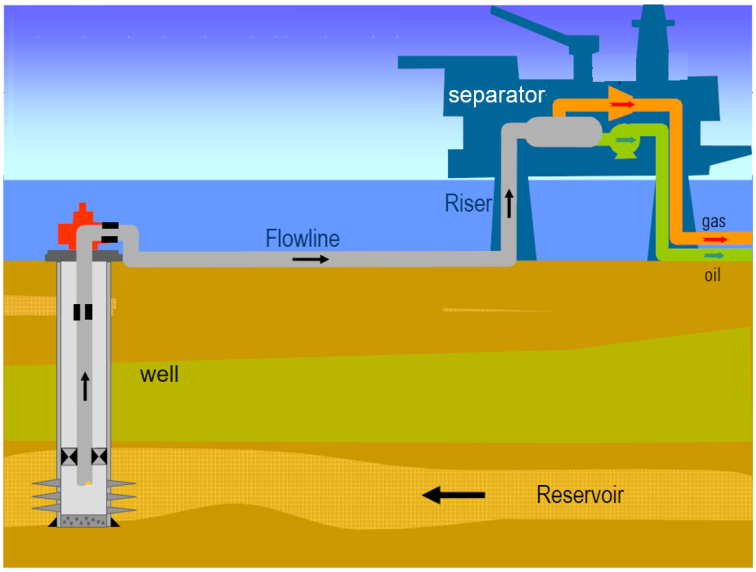

Figure 1.1: Illustration of the upstream production process [2]

Large savings can be made when the treatment of the fluids coming from the well is done on shore instead of at production platforms. In order to transport these fluids over longer distances, challenges induced by multiphase flow must be taken care of. One of these challenges is the reduction of slugging in the flowline and riser system. Large slugs can cause production problems, such as the flooding of the separation vessels, tripping of pumps and compressors, as well as vibrations in the flowline and riser system, which can impose safety risks to the employees working at the production sites.
The conventional techniques for slug mitigation are:

- Accept production losses. As many slug types occur in late field life when the production is relatively low, this can mean that the production is fully stopped.

- Increase the size of the slug catcher or separator: If the slugging behaviour is predicted up front, designing and building a larger slug catcher is an option. Although it is a radical solution, it mitigates the problem if separation is the main threat. The downside is huge costs for building a large slug catcher.

- Multiple small flow lines: Only an option during the design phase of a project. It is more costly than a single larger diameter pipeline.

- Riser-base gas lift: If there is slugging present in the riser section, injecting gas at the bottom of the riser may decrease slugging there. However the installation that has to be built is large and costly, and this thus is mainly an option during the design phase.

- Active or passive topside chocking: This also requires a turnaround for the installation and it is mainly able to mitigate slugging in the riser.

- Subsea separation: If the separator is relocated close to the well, the length of the flowline through which multiple phases have to be transported can be greatly reduced. Transporting gas or liquids in single phase form leads to a much lower pressure drop as well as less challenges concerning flow control when compared to the transport of multiple phases. The main downside is that building these facilities at the sea floor is very expensive. Also the maintenance is complex and costly. Leaks at these facilities impose a major threat, as stopping them is much more difficult subsea.

Adding surfactants to gas-liquid flows is an alternative to the conventional slug mitigation methods, as these seems to be able to decrease the pressure drop of multiphase flow and mitigate slug flow. Surfactants are chemicals that once added in a sufficient concentration to a gas-liquid flow, and once sufficiently agitated, will start to form a foam, where the gas forms bubbles within a network of thin liquid films.
The use of surfactants in vertical wells is a proven technology to mitigate slug flow [3]. Reduction of the pressure in the reservoir that occurs over its field life leads to an increase of the liquid hold-up in the well, which is the so-called liquification. Because of this, the flow becomes unstable and starts slugging. Adding surfactants at the bottom of the well leads to a reduction in the liquid hold-up fraction and leads to an increase of the interfacial friction between the gas and liquid phase. This allows the gas flow to lift the liquids to the well head at the surface again. If a sufficient large concentration of surfactant is used, it mitigates slug flow by changing the flow pattern to annular dispersed flow [4].
The same method can also be used to mitigate slug flow in inclined pipes and in vertical risers to mitigate slug flow[1] . When the incoming flow rates of liquid are larger than the amount that the gas is able to lift, slug flow also occurs in these pipelines. The same phenomena of decreasing the liquid hold-up fraction and increasing the interfacial friction between the gas and liquid phase also cause mitigation of slug flow in inclined and vertical pipelines [4].
For inclined (over 45°) and vertical pipelines the flow behaviour has been modelled by van Nimwegen et al. [5]. Their foam model for vertical flow is incorporated in the Shell Flow Correlations (SFC) and is able to predict the flow characteristics for foams containing a maximum of 34 vol% liquid. Van Nimwegen et al. introduced an effective concentration of surfactant that was measured using a shaking foamer test to make a comparison between the amount of foam produced for certain concentrations of different surfactants. This effective concentration was translated to the influence that a surfactant concentration has on the flow and it was used to predict the pressure drop reduction.
The available literature on the use of surfactants in multiphase flow in pipes with inclinations under 45° or for horizontal pipes is limited. Xia and Chai[6] carried out experiments that demonstrated a reduction of the pressure drop for slug flow in inclines pipes, but they were not able to achieve improvements for slug flow in horizontal pipes. Wilkens & Thomas [7] carried out lab experiments with surfactants that showed the suppression of hydrodynamic slug flow in horizontal pipes. They have carried out experiments for air-water flow with the added surfactant SDS (Sodium Dodecyl Sulfate) in a 52 mm horizontal pipe. This eliminated the occurrence of hydrodynamic slugs and replaced the slug flow regime by stratified flow, with a gas-liquid interface that consists of a bubbly layer (foam layer) [8].
Surfactants or foamers have also been used in field tests to increase the production rate by decreasing the pressure drop and mitigating slugging. In 2010 the NAM carried out a field test by injecting a foamer in a 12",

12 km wet gas pipeline in the Netherlands. Adding the foamer resulted in a decreased pressure drop over the pipeline by 15%, which led to an increase of the gas production 1.5%. In Egypt a field test in the flowlines of the West Delta Deep Marine had mixed results. For some of the wells the pressure drop decreased significantly leading to an increase of the production rate, while for other wells there was a significant pressure drop reduction, but that did not lead to a substantial increase of the production rate. In 2018 slugging in one of the flowlines in the Gulf of Mexico was mitigated through the injection of a surfactant into one of the wells without initiating adverse impact on the topside processes.

1.2. RESEARCH OBJECTIVE

The goal of this research is to test the following hypothesis:

> *With the use of surfactants, slugging in a horizontal flowline and in a flowline-riser system can be reduced or eliminated at certain flow rates and concentrations, leading to a reduction in the pressure drop and to a more stable multiphase flow.*

In order to verify this hypothesis, experiments have been conducted using the Severe Slugging Loop (SSL) at the Shell Technology Centre in Amsterdam. This experimental setup consists of 50 m horizontal flowline, followed by a 50 m partly horizontal and declined section as well as three risers of 16.8 m height. The fluids used during the experiments are air, water and a commercial surfactant called Dreft at ambient temperature and atmospheric pressure at the top of the riser.

1.3. PREVIOUS PROJECT

This research is an continuation of a previous Master Thesis project by Pronk [1], where the effect of surfactants in two-phase flow in flowlines and risers was investigated. She has used the same experimental setup and surfactant as in the present project.

From the previous research the following conclusions were drawn:

- Growing slugs in the flowline can be mitigated by adding a surfactant to the air-water mixture.
- The severe slugging cycle in a flowline-riser system is not prevented when a surfactant is added. The measured pressure drop over the riser height does change: the build-up of the liquid slug becomes irregular. This is because a significant amount of gas, which is present in the foam, enters the riser.
- Slugging in the riser cannot be mitigated by adding a surfactant to the air-water mixture. However, the differential pressure along the riser is decreased, due to the creation of foam.
- The development length of the air-water flow in a vertical riser is slightly increased when surfactants are added. The differential pressure measurements taken at two locations at the top of the riser showed differences. This is an indication that the air-water mixture flow has not fully developed yet.
- For low gas flow rates, surfactants decrease both the liquid and foam holdup. For high gas flow rates, the behaviour for the foam holdup changes. Two observations can be made from the experimental results and the simulation results with the Shell Flow Correlations. First, surfactants increase the foam holdup, due to a larger amount of foam that can be created with larger concentrations. Second, the foam holdup decreases with increasing gas and water flow rates. This is due to a change in foam structure: large flowrates create a foam with small bubbles, which results in a lower foam holdup.

Part of the current research is meant to reproduce the observed growing slugs, the severe slugging cycle and the slugging in the riser with the described effect of the added surfactant respectively. If no complete suppression can be found with the prescribed concentration, the surfactant concentration will be further increased.

On the outer side of the pipe in the experimental setup a Distributed Acoustic Sensing (DAS) system has been installed. This system measures the acoustic energy at multiple points along the flowline. It has been used to measure the flow characteristics qualitatively in the research by Pronk [1]. It is the objective of the present project to obtain quantitative and more accurate data of the slug characteristics using this measurement method.

2

GAS-LIQUID FLOW

2.1. INTRODUCTION

In the upstream production process, flows in flowlines consist of hydrocarbon gas and liquids often accompanied by water. However, due to constraints of our experimental setup, the focus of this report will be on gas-liquid flows containing air and water, without and with an added commercial surfactant. This chapter will explain the fundamentals of gas-liquid flows and the observed flow patterns[3][9].

2.2. GOVERNING EQUATIONS

Within the field of fluid dynamics the driving phenomena are the transfer of mass, momentum and energy. For each of these quantities there is a conservation law, which form the base of other derived equations. These laws state that a change in the amount of mass, moment and energy in a defined control volume over time, is only dictated by the fluxes over the boundaries of the control volume and to sink or source terms present within the control volume. The conservation laws for a single fluid in three dimensions and in their most general representation are:

$$\frac{D\rho}{Dt} = \frac{\partial}{\partial t}\rho + \nabla \cdot \rho\mathbf{u} = 0 \tag{2.1}$$

$$\left(\frac{\partial}{\partial t}\rho\mathbf{u} + \mathbf{u}\cdot\nabla\rho\mathbf{u}\right) = \nabla\cdot\tau + \sum\mathbf{F} \tag{2.2}$$

$$\rho\left(\frac{\partial}{\partial t}h + \mathbf{u}\cdot\nabla h\right) = \rho\dot{q} + \nabla\cdot\left(\frac{\lambda}{c_p}\nabla h\right) \tag{2.3}$$

Where ρ is the density, t is time, $\mathbf{u}$ is the velocity vector, τ is the stress vector, $\sum\mathbf{F}$ are all body forces, h is the enthalpy, $\dot{q}$ is the internal heat source, λ is the thermal conductivity and c_p is the heat capacity.

Equation 2.1 is the first conservation law, which is also known as the continuity equation and ensures that mass is conserved, as it cannot be created nor destroyed. The expression on the left hand side is also known as the material derivative.

In equation 2.2 the conservation law of momentum is stated, which is also known as Netwon's second law and is expressed per unit of fluid volume. The momentum in related terms of the fluid are stated on the left hand side, the stresses and forces acting on the fluid inside the control volume are given on the right hand side.

At last, the conservation of energy is given in equation 2.3, which can be ignored in our experiments, as the temperature can assumed to be constant.

2.2.1. SINGLE-PHASE FLOW

We start from equation 2.1 and use the assumptions that our flow is a single-phase flow and that the fluid used is an incompressible, viscous fluid without heat transfer. The right hand side of the expression follows from the material derivative, since the flow is assumed to be incompressible, i.e.:

$$\nabla\cdot\mathbf{u} = 0 \tag{2.4}$$

The equation that describes the motion of a viscous fluid is the Navier-Stokes equation:

$$\rho \frac{Du_i}{Dt} = \rho g_i - \frac{\partial p}{\partial x_j} + \frac{\partial}{\partial x_j}\left[\mu\left(\frac{\partial u_i}{\partial x_j} + \frac{\partial u_j}{\partial x_i}\right)\right] \tag{2.5}$$

This can be rewritten in vector form, while assuming that the variation of the viscosity with the location is negligible.

$$\rho \frac{D\rho}{Dt} = \rho \mathbf{g} - \nabla p + \mu \nabla^2 \mathbf{u} \tag{2.6}$$

The variables can be made dimensionless by using a characteristic length scale L, characteristic velocity U and density ρ_0:

$$\tilde{\mathbf{u}} = \frac{\mathbf{u}}{U} \tag{2.7}$$

$$\tilde{\rho} = \frac{\rho}{\rho_0} \tag{2.8}$$

$$\tilde{p} = \frac{p}{\rho_0 U^2} \tag{2.9}$$

$$\tilde{t} = \frac{tU}{L} \tag{2.10}$$

$$\tilde{\nabla} \cdot \tilde{\mathbf{u}} = 0 \tag{2.11}$$

By substituting equations 2.7-2.11 into equation 2.6, the Navier-Stokes equation in dimensionless form is obtained:

$$\frac{D\tilde{\mathbf{u}}}{D\tilde{t}} = \frac{1}{Fr^2}\mathbf{n} - \tilde{\nabla}\tilde{p} + \frac{1}{Re}\tilde{\nabla}^2\tilde{\mathbf{u}} \tag{2.12}$$

Where $Re = L\rho_0 U/\mu$ is the Reynolds number, $Fr = U/\sqrt{gL}$ is the Froude number and $\mathbf{n} = [0,0,-1]$ is the normal vector associated with the Froude number. This means that when for two different single-phase flows both the Reynolds and Froude number are equal, then the flows should behave equally.

2.2.2. TWO-PHASE FLOW

The behaviour of an isothermal gas/liquid two-phase flow conditions is fully determined by the equations of state of the phases, the conservation equations and the boundary conditions. Starting with the equations of state:

$$\frac{p_G}{\rho_G} = \text{const.} \tag{2.13}$$

$$\rho_L = \text{const.} \tag{2.14}$$

Then apply the mass conservation equations for the gas and liquid phases:

$$\frac{D\rho_G}{Dt} + \rho_G \nabla \cdot \mathbf{u}_G = 0 \tag{2.15}$$

$$\nabla \cdot \mathbf{u}_L = 0 \tag{2.16}$$

The Navier-Stokes equations for each point of the compressible gas and the incompressible liquid phase are:

$$\rho_G \frac{D\mathbf{u}_G}{Dt} = \rho_G \mathbf{g} - \nabla p_G + \mu_G \left[\nabla^2 \mathbf{u} + \tfrac{1}{3}\nabla(\nabla \cdot \mathbf{u})\right]_G \tag{2.17}$$

$$\rho_L \frac{D\mathbf{u}_L}{Dt} = \rho_L \mathbf{g} - \nabla p_L + \mu_L \nabla^2 \mathbf{u}_L \tag{2.18}$$

Assuming a constant surface tension at the gas-liquid interface, the normal and tangential stresses balance with the no-slip condition for velocities:

$$\left[-p_L + 2\mu_L\left(\frac{\partial u_z}{\partial z}\right)_L\right] - \left[-p_G + 2\mu_G\left(\frac{\partial u_z}{\partial z} - \tfrac{1}{3}\nabla \cdot u_G\right)\right] = \sigma\left(\frac{1}{R_1} + \frac{1}{R_2}\right) \tag{2.19}$$

$$\mu_G\left(\frac{\partial u_x}{\partial z} + \frac{\partial u_z}{\partial x}\right)_G = \mu_L\left(\frac{\partial u_x}{\partial z} + \frac{\partial u_z}{\partial x}\right)_L \tag{2.20}$$

$$\mu_G\left(\frac{\partial u_y}{\partial z} + \frac{\partial u_z}{\partial y}\right)_G = \mu_L\left(\frac{\partial u_y}{\partial z} + \frac{\partial u_z}{\partial y}\right)_L \tag{2.21}$$

$$u_G = u_L \tag{2.22}$$

Like what was done in the single-phase section, we can introduce a characteristic length L, velocity U and density ρ_L. The new equations become:

$$\frac{\tilde{p}_G}{\tilde{\rho}_G} = \text{constant} = Eu \tag{2.23}$$

$$\tilde{\rho}_L = 1 \tag{2.24}$$

$$\frac{D\tilde{\rho}_G}{D\tilde{t}} + \tilde{\rho}_G \tilde{\nabla} \cdot \tilde{\mathbf{u}}_G = 0 \tag{2.25}$$

$$\tilde{\nabla} \cdot \tilde{\mathbf{u}}_L = 0 \tag{2.26}$$

The Navier-Stokes equation for the gas phase then becomes:

$$\frac{D\tilde{\mathbf{u}}_G}{D\tilde{t}} = \frac{1}{Fr^2}\mathbf{n} - \frac{1}{\tilde{\rho}_G}\tilde{\nabla}\tilde{p}_G + \frac{1}{Re_G}\left[\tilde{\nabla}^2\tilde{\mathbf{u}} + \frac{1}{3}\tilde{\nabla}\left(\tilde{\nabla}\cdot\tilde{\mathbf{u}}\right)\right]_G \tag{2.27}$$

And the Navier-Stokes equation for the incompressible liquid phase:

$$\frac{D\tilde{\mathbf{u}}_L}{D\tilde{t}} = \frac{1}{Fr^2}\mathbf{n} - \tilde{\nabla}\tilde{p}_L + \frac{1}{Re_L}\tilde{\nabla}^2\tilde{\mathbf{u}}_L \tag{2.28}$$

Equations 2.19 to 2.22 can also be non-dimensionalized by substituting equations 2.23 to 2.26:

$$\left[-\tilde{p}_L + \frac{2}{Re_L}\left(\frac{\partial \tilde{u}_z}{\partial \tilde{z}}\right)_L\right] - \left[-\tilde{p}_G + 2\tilde{\mu}_G\left(\frac{\partial \tilde{u}_z}{\partial \tilde{z}} - \frac{1}{3}\tilde{\nabla}\cdot\tilde{u}\right)_G\right] = \frac{1}{We}\left(\frac{1}{\tilde{R}_1} + \frac{1}{\tilde{R}_2}\right) \tag{2.29}$$

$$\tilde{\mu}_G\left(\frac{\partial \tilde{u}_x}{\partial \tilde{z}} + \frac{\partial \tilde{u}_z}{\partial \tilde{x}}\right)_G = \frac{1}{Re_L}\left(\frac{\partial \tilde{u}_x}{\partial \tilde{z}} + \frac{\partial \tilde{u}_z}{\partial \tilde{x}}\right)_L \tag{2.30}$$

$$\tilde{\mu}_G\left(\frac{\partial \tilde{u}_y}{\partial \tilde{z}} + \frac{\partial \tilde{u}_z}{\partial \tilde{y}}\right)_G = \frac{1}{Re_L}\left(\frac{\partial \tilde{u}_y}{\partial \tilde{z}} + \frac{\partial \tilde{u}_z}{\partial \tilde{y}}\right)_L \tag{2.31}$$

$$\tilde{u}_G = \tilde{u}_L \tag{2.32}$$

Where n is the unit vector in the direction of g and the following dimensionless numbers are stated:

- Liquid Reynolds number:

$$Re_L = \frac{L\rho_L U}{\mu_L} \tag{2.33}$$

- Froude number:

$$Fr = \frac{U}{\sqrt{gL}} \tag{2.34}$$

- Weber number:

$$We = \frac{L\rho_L U^2}{\sigma} \tag{2.35}$$

- Euler number:

$$Eu = \frac{p_G}{\rho_G U^2} \tag{2.36}$$

- Dimensionless gas density:

$$\tilde{\rho}_G = \frac{\rho_G}{\rho_L} \tag{2.37}$$

- Dimensionless gas viscosity:

$$\tilde{\mu}_G = \frac{\mu_G}{L\rho_L U} = \frac{\mu_G}{\mu_L}\cdot\frac{1}{Re_L} \tag{2.38}$$

Two different two-phase flow conditions are similar when all six dimensionless numbers are equal for the two systems and if the ratio of mass fluxes is equal:

$$\frac{\dot{m}_G}{\dot{m}_L} = \text{constant} \tag{2.39}$$

2.3. PRESSURE GRADIENT

The pressure drop in a horizontal pipeline is the force required to counter balance the wall friction, which will increase as the volumetric flow rate is increased.

2.3.1. HORIZONTAL SINGLE PHASE FLOW

In a horizontal pipeline with single phase flow the pressure drop can be derived by using Newton's second law to obtain the momentum equation:

$$-A\frac{\partial P}{\partial x} = \frac{\partial}{\partial t}(\rho AU) + \frac{\partial}{\partial x}(\rho AU^2) + \tau S \tag{2.40}$$

Where t denotes the time, x the spatial coordinate in stream-wise direction, ρ the density, A the pipe cross section, U the fluid velocity averaged over the pipe cross section, P the pressure, S the pipe perimeter and τ the wall shear stress. When mass conservation is applied:

$$\frac{\partial}{\partial t}(\rho A) + \frac{\partial}{\partial x}(\rho AU) = 0 \tag{2.41}$$

Combining equations 2.40 and 2.41 gives:

$$\rho\frac{\partial U}{\partial t} + \rho U\frac{\partial U}{\partial x} = -\frac{\partial P}{\partial x} - \frac{\tau S}{A} \tag{2.42}$$

The wall shear stress τ can be modelled by non-dimensionalizing it using the Fanning friction factor f according to the definition:

$$\tau = f\frac{1}{2}\rho U^2 \tag{2.43}$$

The Churchill correlation is one of the many empirical relations present in literature and is used in the Shell Flow Correlations[10]:

$$\begin{aligned} f &= 2\left[\left(\frac{8}{Re}\right)^{12} + \frac{1}{(A^*+B^*)^{3/2}}\right]^{1/12} \\ A^* &= -\left\{-2.457\ln\left[\left(\frac{7}{Re}\right)^{0.9} + 0.27\frac{\varepsilon}{D}\right]\right\}^{16} \\ B^* &= \left(\frac{37530}{Re}\right)^{16} \end{aligned} \tag{2.44}$$

This correlation holds for both laminar and turbulent flow, ε is the pipe roughness, D the diameter and Re the Reynolds number.

$$Re = \frac{\rho UD}{\mu} \tag{2.45}$$

Where D is the internal pipe diameter and μ the dynamic viscosity. Further simplification of the equations is possible and known as the D^5-law:

$$\Delta p = \frac{32}{\pi^2}\frac{f\rho Q^2}{D^5} \tag{2.46}$$

With $Q = UA$ as the volumetric flow rate. Using equations 2.44 and 2.46 the wall roughness can be derived using iterations between these two equations and by knowing the pressure drop, pipe cross section and flow speed.[3] [9]

2.3.2. HORIZONTAL GAS-LIQUID FLOW

When there are more than one phases the momentum balance is split into separate equations for each phase and is derived similarly to the single-phase flow.

$$\begin{aligned} \frac{\partial}{\partial t}\rho_G A_G U_G + \frac{\partial}{\partial x}\rho_G A_G U_G &= -A_G\frac{\partial P}{\partial x} - \tau_G S_G - \tau_{LG} S_{LG} \\ \frac{\partial}{\partial t}\rho_L A_L U_L + \frac{\partial}{\partial x}\rho_L A_L U_L &= -A_L\frac{\partial P}{\partial x} - \tau_L S_G + \tau_{LG} S_{LG} \end{aligned} \tag{2.47}$$

These equations hold for the stratified flow regime, where gas flows as a separate layer on top of the liquid layer. The subscript "G" applies to the gas phase and the subscript "L" to the liquid phase. The nomenclature is equal to equation 2.40, apart from the subscripts. Mass conservation of the gas and liquid phase gives:

$$\begin{aligned} \frac{\partial}{\partial t}\rho_G A_G + \frac{\partial}{\partial x}\rho_G A_G U_G = 0 \\ \frac{\partial}{\partial t}\rho_L A_L + \frac{\partial}{\partial x}\rho_L A_L U_L = 0 \end{aligned} \tag{2.48}$$

And similar to the single-phase flow, combining equations 2.47 and 2.48 gives the following expressions:

$$\begin{aligned} -A_G\frac{\partial P}{\partial x} - \tau_G S_G - \tau_{LG} S_{LG} = 0 \\ -A_L\frac{\partial P}{\partial x} - \tau_L S_L + \tau_{LG} S_{LG} = 0 \end{aligned} \tag{2.49}$$

2.4. LIQUID HOLD-UP

To be able to make a comparison between experiments, the volumetric flow rates Q_L and Q_G are often scaled by the pipe cross section A. This gives the superficial velocities for the liquid and the gas part of the flow:

$$u_{SG} = \frac{Q_G}{A} \tag{2.50}$$

$$u_{SL} = \frac{Q_L}{A} \tag{2.51}$$

$$u_{mix} = u_{SG} + u_{SL} \tag{2.52}$$

The local gas holdup fraction per flow medium is derived by taking the ratio of the pipe cross section occupied by a fluid phase and the pipe cross section:

$$\alpha_G = \frac{A_G}{A} \tag{2.53}$$

$$\alpha_L = \frac{A_L}{A} \tag{2.54}$$

$$\alpha_G + \alpha_L = 1 \tag{2.55}$$

The actual velocity of the flow medium follows from the hold-ups and the superficial velocities:

$$u_L = \frac{u_{SL}}{\alpha_L} \tag{2.56}$$

$$u_G = \frac{u_{SG}}{\alpha_G} \tag{2.57}$$

2.5. FLOW PATTERNS IN HORIZONTAL FLOW

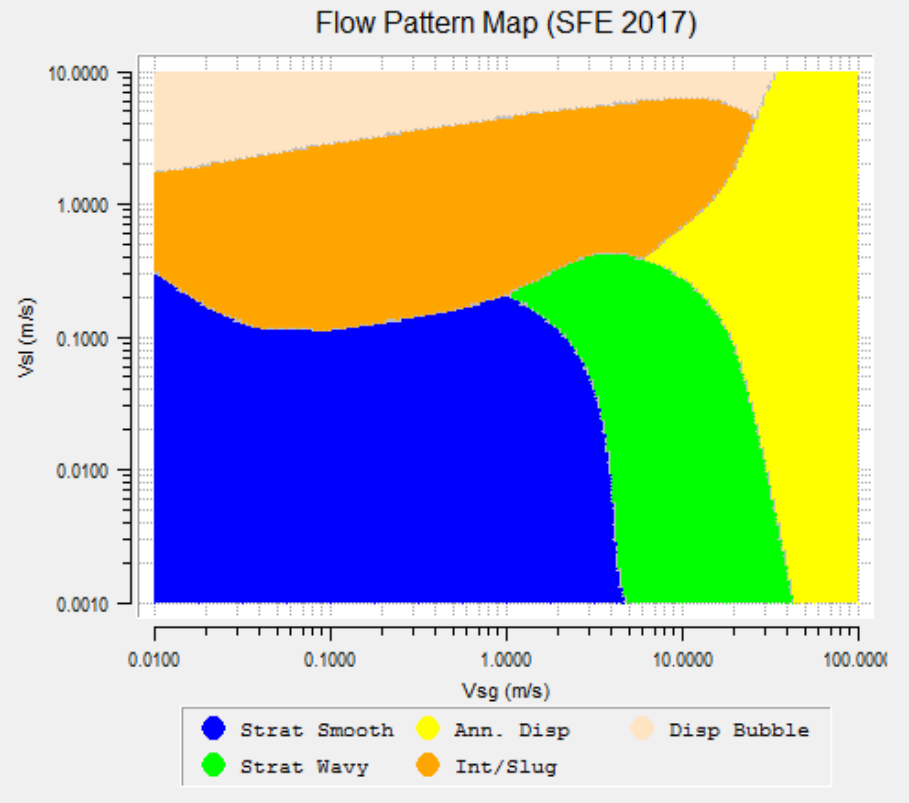

Figure 2.1: Flow pattern map by Shell Flow Explorer 2017 for water-air flow for the flowline section with a pipe diameter of 0.0508 m

In figure 2.1 the flow pattern map for the horizontal flowline of the severe slugging loop is shown. The superficial gas velocity is given on the x-axis and the superficial liquid velocity on the y-axis. The colours represent the different flow regimes. The boundaries between the different flow regimes in reality are not as sharp as plotted in this figure; they tend to be transition regions instead of sharp boundaries.

Different flow patterns can be distinguished; an illustration of the flow patterns in horizontal pipelines is given in figure 2.2. The annular dispersed flow regime is found for a high superficial gas velocity and a much lower superficial liquid velocity. The flow itself is characterized by a gas core with entrained droplets and a liquid layer at the wall of the pipe.
Stratified flow, either smooth or wavy, is a separated two-phase flow. It has the liquid flow at the bottom of the pipe and the gas flow on top. Stratified wavy flow has a rougher gas-liquid interface than the smooth alternative and some droplets can be carried by the gas flow. Slug flow (or intermittent flow) occurs when the superficial liquid velocity is increased, starting from stratified conditions. The most important phenomenon in hydrodynamic slug flow is the occurrence of waves which block the pipe cross section and they can grow in length up to about hundred times the pipe diameter. Within the liquid part of the slug, gas is dispersed as bubbles, especially at the tail of the liquid part of the slug. When the superficial liquid velocity is high and the superficial gas velocity is low, dispersed bubble flow is found. It consists of liquid with some dispersed gas bubbles.

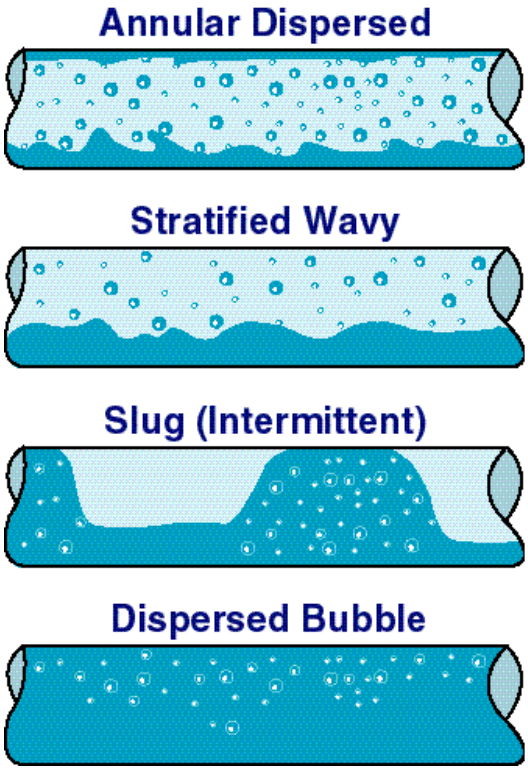

[3]

Figure 2.2: Illustration of the flow patterns for horizontal gas-liquid flows

2.5.1. SLUG FLOW

As mentioned earlier, the transition from stratified flow to slug flow can be determined using the Kelvin-Helmholtz stability analysis. If the difference in velocity between the gas and liquid layer is sufficiently large, the wave initiated at the surface becomes unstable and grows until the top of the pipe is reached. From this point on the slug grows and is pushed forward by the air flow. The instability grows only if the difference in velocity is sufficiently large [11]:

$$(u_G - u_L)^2 > \frac{2(\rho_G + \rho_L)}{\rho_G \rho_L} \sqrt{\sigma g(\rho_L - \rho_G)} \tag{2.58}$$

Where σ is the surface tension in N/m.
The nose of the slug moves even faster through the pipe than the mixture velocity. The velocity of the slugs can be estimated using the superficial velocities of the liquid and the gas according to Woods and Hanratty[12]

$$U_t = C_0 u_{mix} + C_\infty, \tag{2.59}$$

where U_t is the slug nose velocity in m/s, the drift velocity $C_\infty = 0.542\sqrt{gD}$ and C_0 is described by the following equation:

$$C_0 = \frac{K_0}{1 + (s-1)\epsilon}, \tag{2.60}$$

where $K_0 = 1.2$, s is the slip between the gas and liquid phases within the slug and ϵ is the void fraction. This void fraction is described by the following correlation found by Gregory et al.[13]:

$$\epsilon = 1 - \frac{1}{1 + \left(\frac{u_{mix}}{\alpha}\right)^\beta}, \tag{2.61}$$

where $\alpha = 9.48$ and $\beta = 1.26$ for a pipe diameter of 51 mm.

Woods et al. also introduced an intermittency factor with a derivation to a relation between the slug frequency, the pipe diameter and the superficial liquid velocity in a later paper [14]:

$$I = \frac{f_s L_s}{C} \approx \frac{u_{SL}}{u_{SL} + u_{SG}}, \tag{2.62}$$

in which f_s is the slug frequency and L_s is the fully developed slug length. These equations can be combined into:

$$\frac{f_s D}{u_{SL}} = 1.2 \left(\frac{L_s}{D} \right)^{-1}, \tag{2.63}$$

If the average value of $\frac{L_s}{D}$ is assumed to be a constant when the flow is fully developed, then:

$$\frac{f_s D}{u_{SL}} = \text{constant} \tag{2.64}$$

GROWING SLUGS

The observation of slugs with increasingly long lengths have been reported by Pronk [1] who used the same experimental setup. Growing slugs are observed in the region between plug, slug, stratified smooth and stratified wavy flow [15], as can be seen in figure 2.3.

These long liquid slugs appear at relatively low gas and liquid superficial velocities and are known to be either fully developed or growing. Our experimental facility is too short for most of these long liquid slugs to become fully developed as they can reach lengths of 500 pipe diameters or even more. The reason that they can reach these long lengths is the meta-stable flow behaviour at stratified conditions. This means that when a small disturbance is introduced, this can trigger the formation of a liquid slug that grows in length by picking up liquid as it moves through the pipe. Controlling these slugs is essential, as they can cause serious operational upsets due to their strong fluctuations in pressure and flow conditions.

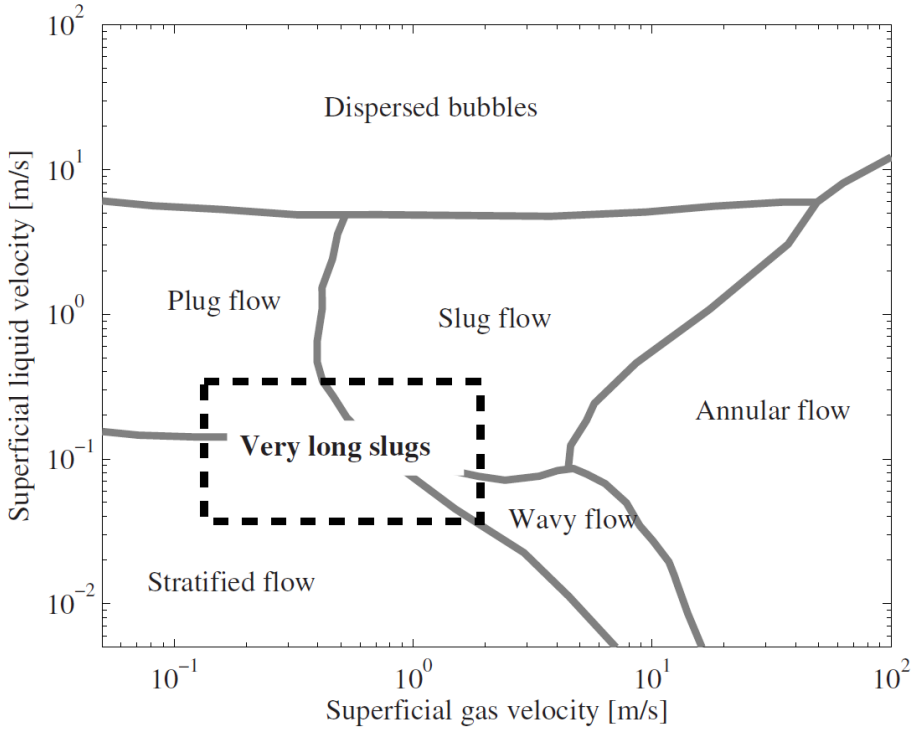

Figure 2.3: Flow pattern map with indication of very long slugs region [15]

2.6. FLOW PATTERNS IN VERTICAL UPWARD FLOW

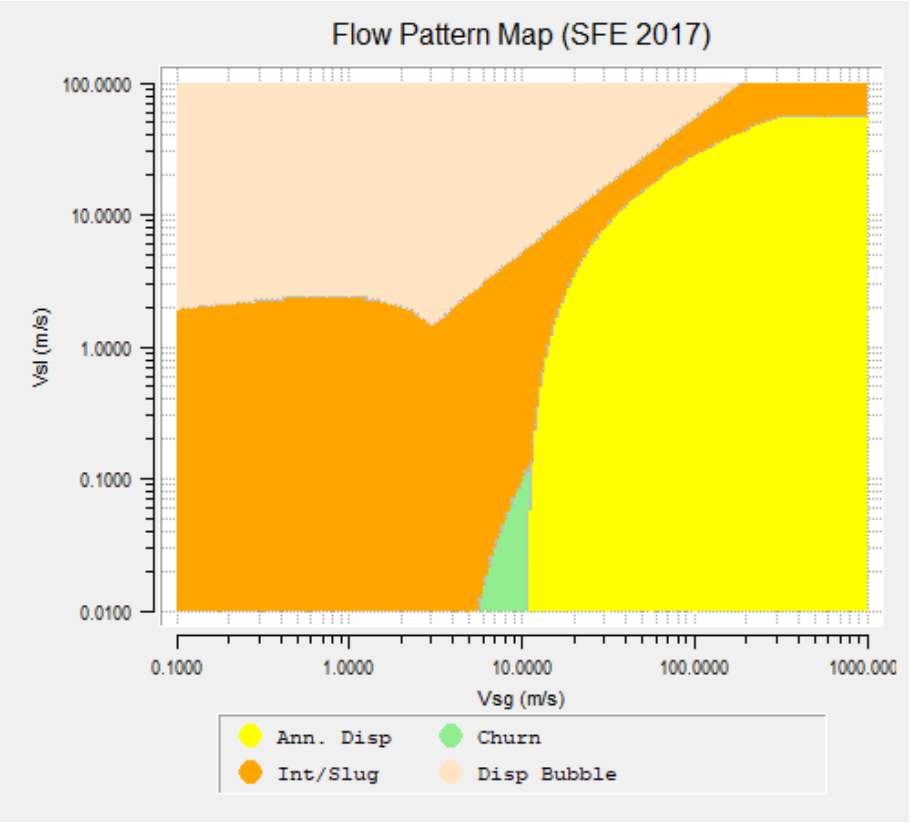

Figure 2.4: Flow pattern map by Shell Flow Explorer 2017 for water-air flow for the riser section with a pipe diameter of 0.044m

The flow pattern map for the vertical riser of the Severe Slugging Loop is shown in figure 2.4. An illustration of the flow patterns in vertical pipelines is given in figure 2.5. At high liquid flow rates combined with a low gas flow rate the flow pattern is bubble flow. Here the liquid is forming a continuous phase with small gas bubbles flowing inside the liquid.
When decreasing the liquid flow rate, while keeping the gas flow rate relatively low, the small gas bubbles will form large gas bubbles. The gas bubbles can grow to such a large size that they create hydrodynamic slug flow (or intermittent flow).
At higher gas flow rates combined with low liquid flow rates the large gas bubbles can become unstable. This creates a chaotic flow regime with gas bubbles of various shapes and sizes inside the liquid, also known as the churn flow regime. This regime is most of the time treated as slug flow, as most of the models do not make a distinction between the two flow regimes.
Increasing the gas flow rate further, while keeping the liquid flow rate low, leads to a transition to annular dispersed flow. In this flow regime the gas flow is the continuous phase with small droplets of liquid entrained in the core, and a liquid film is formed along the wall. If the gas flow is even more increased, the liquid film will disappear and only the liquid droplets remain; this is known as annular mist flow. Table 2.1 lists the model types for the different flow regimes.

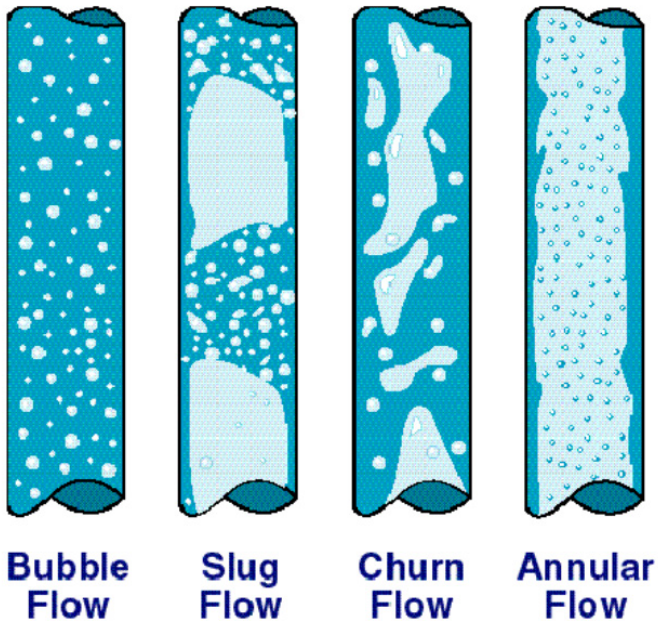

Figure 2.5: Illustration of the flow patterns for vertical gas-liquid flows [3]

Table 2.1: Different models and submodels used to calculate properties of flows with dispersed bubble, separated and intermittent flow patterns. [9]

Flow pattern	Models and Submodels
Dispersed bubble flow	Drift flux Model Wall friction Distribution parameter Bubble rise velocity
Separated flow (stratified/annular)	Two-Fluid Model Wall friction Interfacial friction Interfacial velocity Interface shape Liquid entrainment
Intermittent flow	Drift-Flux & Two-Fluid Model Wall friction Distribution parameter Bubble rise velocity Intermittent flow Void fraction in liquid slug body Slug frequency Length of liquid slug with gas bubble Bubble shape

2.7. SEVERE SLUGS

Severe slugs, also known as riser-induced slugs, are initiated by a liquid blockage at the riser base. The process of severe slugging is characterized by a strong cyclic behaviour, which starts with a long period in which there is low gas and liquid flow at the top of the riser, followed by the passing of the liquid slug with a length longer than the riser height, and finally the breakthrough of a strong gas surge. The cycle time depends on the system

size and flow conditions. The cycle of severe slugging consists of five characteristic stages, as can be seen in figure 2.6:

1. Blocking of the riser base: at low flow speeds the riser will operate in the hydrodynamic slugging regime, in which liquid falls back and blocks the riser, initiating the severe slugging cycle.

2. Growing of the slug: Liquid accumulates at the riser base, leading to growing of the slug in the direction of the riser and upstream into the flow line. The outflow at the top of the riser breaks down completely, as the incoming gas will only build up pressure upstream of the slug in order to balance the hydrostatic head.

3. Liquid outflow: The severe slug grows until the riser is completely filled with liquid. When the slug reaches the top of the riser, it will flow out on the top of the riser and the liquid production starts.

4. Fast liquid flow: As the liquid part of the severe slug leaves the riser at the top, the hydrostatic pressure decreases, which leads to an acceleration of the flow.

5. Gas blow-down: After the liquid leaves the riser, the remaining pressurized gas is released.

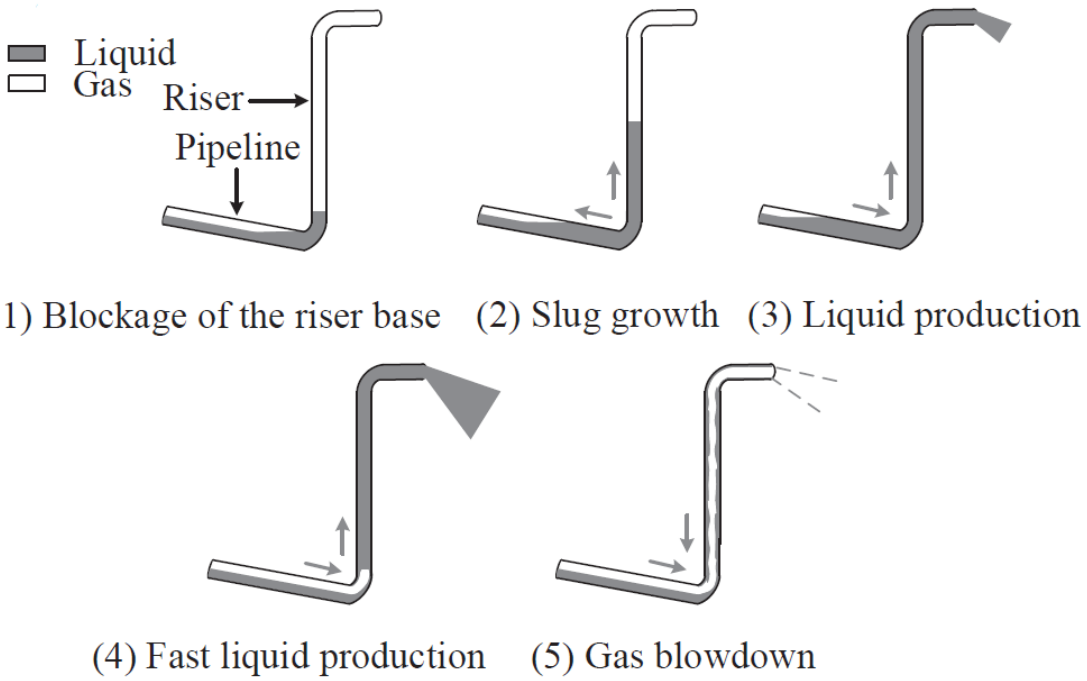

Figure 2.6: Illustration of severe slugging cycle [16]

Severe slugging occurs once the following four conditions are satisfied:

1. The severe slugging number $\Pi_{ss} < 1$.

$$\Pi_{ss} = \frac{\left(\frac{dp}{dt}\right)_{flowline}}{\left(\frac{dp}{dt}\right)_{riser}}$$

$$\left(\frac{dp}{dt}\right)_{flowline} = \frac{P_N}{(1-\alpha_f)L_f} u_{SG,N,flowline}$$

$$\left(\frac{dp}{dt}\right)_{riser} = (\rho_L - \rho_G) u_{SL,riser} g \sin\varphi$$

$$\text{GLR} = \frac{u_{SG,riser}}{u_{SL,riser}} \frac{P_{actual}}{P_N} \frac{T_N}{T_{actual}} = \frac{u_{SG,N,riser}}{u_{SL,riser}} = \frac{Q_{G,N}}{Q_L}$$

$$u_{SG,riser} = \frac{A_{risers}}{A_{flowline}} u_{SG,flowline} = n_{risers} \left(\frac{D_{flowline}}{D_{riser}}\right)^2 u_{SG,flowline}$$

$$\Pi_{ss} = \frac{P_N}{(1-\alpha_f)(\rho_L - \rho_G) n_{risers} \left(\frac{D_{flowline}}{D_{riser}}\right)^2 g L_f} \text{GLR} \tag{2.65}$$

where:

- P_N is the pressure at normal conditions, which is 1 bar,
- α_f is the liquid holdup fraction in the flowline,
- L_f is length of the flowline upstream of the riser,
- T_N is the temperature at normal conditions, which is $273.15K$,
- u_{SG} is the superficial gas velocity,
- u_{SL} is the superficial liquid velocity.
- g is the gravitational acceleration,
- φ is the angle of riser with respect to the horizontal,
- ρ_L and ρ_G are the densities of the liquid and gas,
- n_{risers} is the amount of risers used,
- $D_{flowline}$ and D_{riser} are the hydraulic diameters of the flowline and riser respectively,
- GLR is the gas to liquid ratio at normal conditions,
- P_{actual} and T_{actual} are respectively the actual pressure and the actual temperature of the flow.

2. The pipeline has a layout such that the riser bottom is the lowest point at which liquid blockage may occur.

3. The flowline is operated in such a way that the flow pattern is stratified or annular flow, but not hydrodynamic slug flow.

4. The riser flow is unstable. A decrease in production will lead to a higher rather than a lower pressure drop over the riser. This phenomenon occurs at flow rates where the pressure drop becomes gravity dominated (with hydrodynamic slug flow as the flow regime) rather than friction dominated (with annular flow as the flow regime). When the flow is unstable, less production will lead to an increased liquid holdup in the riser, which causes an increase of the hydrostatic head. A rough indication for the onset of unstable flow is when the densimetric gas Froude number is smaller than one:

$$Fr_G^* = \sqrt{\frac{\rho_G}{(\rho_L - \rho_G)} \frac{u_{SG}^2}{g D_{riser}}} < 1 \tag{2.66}$$

3

SURFACTANTS IN TWO-PHASE FLOWS

3.1. SURFACTANTS

Surfactants, which is short for surface active agents, are amphiphilic or amphipathic molecules constisting of a non-polar hydrophobic tail which is attached to a hydrophilic head. The head is a polar or ionic head group which interacts strongly with water molecules and makes the surfactant soluble in water. On the other hand, the water molecules avoid contact with the hydrophobic part. This leads to a tendency to squeeze the hydrophobic tail out of the water by the accumulation of the surfactants at the interfaces or in the solution to form micelles. In these micelles, the surfactant hydrophobic tails are directed toward the interior of the aggregate and the hydrophilic heads are directed toward the solvent. Due to these properties, the surfactants can adsorb at the interfaces of gas-liquid flows and lower the surface tension γ (which has the unit mNm^{-1}). It should be noted that commercial surfactants will contain a variety of chemicals; in those surfactants, the tail exists as a mixture of chains of different lengths and the same holds for the hydrophilic head group.

3.1.1. CRITICAL MICELLAR CONCENTRATION

Once a certain concentration of the surfactant has been added to the liquid, stable aggregates are formed, which prevent the hydrophobic tail parts to touch the liquid. This threshold is called the critical micellar concentration (CMC). Commonly, aggregates will form a micelle formation, with the tails pointing to each other, while the hydrophilic heads are directed to the water, as illustrated in figure 3.1. The shape of the aggregate depends on the chemical structure of the surfactants used and on the concentration of the surfactant.

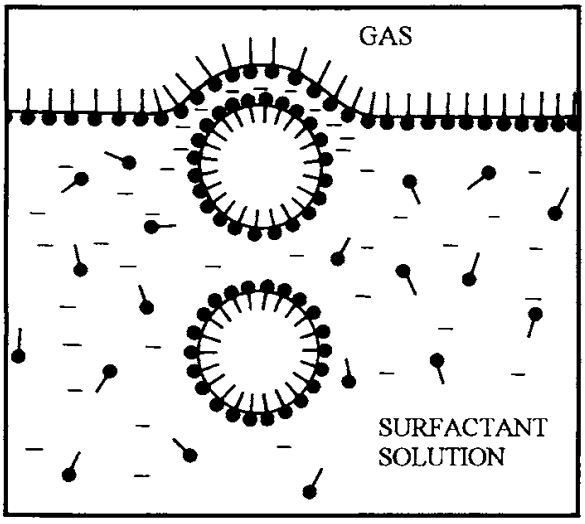

Figure 3.1: Illustration of the formation of a foam film when the bubble reaches the surface of a surfactant solution [17]

3.1.2. SURFACE TENSION

The larger attraction between water molecules (cohesion) than between water and gas molecules (adhesion) leads to the elastic tendency of the interface between the fluids, also known as surface tension or as interfacial tension. Surfactant molecules are adsorbed at the interface between gas and liquid, leading to a reduction of the surface tension.
For a pure liquid and gas, the surface tension is a static value, depending only on the chemical composition of the fluids and of the temperature and pressure. When a surfactant is added to the pure fluids assuming no flow, the surface tension will increasingly drop, as the surfactant molecules adsorb at the interface. When the concentration is increased and gets closer to the critical micellar concentration, the surface tension reduction is slowed down, as less molecules are able to adsorb at the interface.
When a liquid with a surfactant concentration is disturbed, the time that it takes to restore the static situation depends on the adsorption rate of the surfactant at the interface and on the diffusion rate of the surfactant molecules to the surface (assuming no convective flow). The latter depends on various quantities, such as the viscosity of the fluid, the temperature and the geometry of the molecules of the surfactant. This dependency is called the dynamic surface tension and describes how quickly the surfactant is able to influence the interface after the mixture has been established.
Above the critical micellar concentration, the static surface tension is constant. The dynamic surface tension, however, can still become smaller. This is caused by the micelles, where molecules can also adsorb at the surface after a disruption of the mixture [18]

3.2. FOAM

When surfactants are sufficiently agitated and their concentration is high enough, foam is formed. Foam is a dispersed system consisting of gas bubbles, separated by thin liquid layers[17].
Currently there is no general theory available to explain the mechanism of the stability of foams, nor is there a commonly accepted test that is able to evaluate the properties of the foam formed by the different surfactants[19]. The Bartsch (shaking test), the Ross-Miles (pouring) and the Bikerman (sparging gas) methods are most commonly used methods to determine the foamability of a surfactant [20]. Experiments using the Bartsch method proposed and conducted at the TU Delft by Bechan[21] and by van Boven[22] with multiple surfactants, including SDS and Dreft, have led to a foam scaling factor. This factor is based on an experimental setup that created similar foam bubble sizes as in the experiments with vertical air-water flow in the churning flow regime. This makes it possible to conduct experiments with similar foamability while using different surfactants.

3.3. THE APPLICATION OF SURFACTANTS

Surfactants or the foam created by surfactants have many applications, for example at home as a detergent or within the oil and gas industry as a production enhancer. One of these applications in the industry is gas well deliquification, where surfactants are injected in wells that have problems to produce gas due to an increasing liquid holdup. As the pressure in the reservoir reduces over time when gas is being produced, the gas velocities decline and the effectiveness of the gas to be able to lift the liquid decreases. Liquid then accumulates in the well, which is called liquid loading or liquification, and this is a major threat to produce the maximum potential of the gas well.
By injecting surfactants inside the well, foam is formed. This leads to an increase of the interfacial drag between the gas core and the liquid/foam in the annular flow regime in comparison with the original state, which makes it possible to lift the liquids with the gas and to prevent transition to churn or slug flow[23].
In the field, for each application a surfactant with specific properties is required. The surfactant has to be effective at the actual operational conditions in the well, flowline or riser. Ideally, a stable foam is created which survives high temperatures and pressures. It should also be compatible with the liquid phase and stable in the presence of hydrocarbon condensate which acts as a defoamer. In wells, the surfactant should not affect the reservoir rock. In pipelines, it should not corrode the pipe wall and it should not freeze when stored at low temperatures. Another important requisite is the availability of a chemical defoamer, such that the foam can be mitigated when it is no longer required. Finally, the surfactant should also not create oil-water emulsions or there must be a demulsifier available to prevent this [4].

3.4. LITERATURE ON TWO-PHASE FLOW WITH SURFACTANTS

Recently an other Master student, Emily Pronk, has investigated the influence of surfactants on horizontal and vertical flow using the same experimental setup at the Shell Technology Centre Amsterdam[1]. She has reported the following conclusions:

- Growing slugs can be mitigated using surfactants.
- Severe slugging cannot be suppressed, only the frequency can be influenced.
- Slugging in vertical flow can be mitigated by adding a surfactant, however the pressure drop increases with higher concentrations.

Van Nimwegen has carried out experiments[4], and later van Nimwegen et al. made a model[24], for the use of surfactants in upward inclined and vertical gas-liquid flow. The foam model for vertical flow has been incorporated into the Shell Flow Correlations (SFC). Three different pipe diameters of 34, 50 and 80 mm were used in the experiments, as well as five different surfactants including SDS (Sodium Dodecyl Sulfate) and Dreft. It was shown that the effect of the five different surfactants on the flow was equal when incorporating a scaling factor to obtain the effective concentration. Adding a surfactant to create foam replaced the churn flow regime by the annular flow regime. The foam decreased the density of the film layer along the wall and created an increased interfacial stress. This reduced the hydrostatic head, giving a lower pressure drop. An optimum surfactant concentration is reported; a further increase of the surfactant concentration leads to an increased pressure drop due to the increasing frictional pressure drop.

Only a few publications have appeared that cover the influence of surfactants on two-phase horizontal pipe flow. The influence of the surfactant Aliquat 221 on the flow pattern map was investigated by Weismand et al. in 1979[25]. They used pipe diameters of 11.5, 25 and 51 mm with horizontal co-current air-water flow. The main effect of adding the surfactant that was observed is the delay of the transition from smooth stratified flow to wavy stratified flow to much higher gas flow rates.

Hand et al. used Chemtreat 271 in co-current air-water flow in a pipe with a diameter of 93.5 mm[26]. It was concluded that the transition from smooth stratified to wavy stratified flow occurred at higher air velocities. The following conclusions were drawn:

- No effect was found on the transition to stratified and roll wave flow.
- The onset of entrainment occurred at lower air velocities.
- The liquid holdup increased between air flow rates of 0.02 and 0.07 $m^3 s^{-1}$
- The pressure drop was reduced for air flow rates between 0.02 and 0.08 $m^3 s^{-1}$
- The surfactant damped the capillary wave formation by accumulating at the liquid interface.

Later Spedding and Hand have revised their analysis[27], in which they concluded that the justification for the reduction in pressure drop was not at all convincing and they conducted further experiments in the same experimental setup. From these experiments it was concluded that the formation of ripple waves was suppressed and the range of the smooth stratified regime was extended. Furthermore, it was found that the liquid holdup was increased by the surfactant, leading to a lower pressure drop. Drag reduction also occurred with other flow regimes: the slug and plug flow patterns formed at higher liquid flow rates and had a lower pressure drop, caused by suppression of turbulence in the liquid nose region. In the annular flow regime the drag was also reduced, which was caused by the damping of waves in the annular film.

In 2006 Wilkens et al. conducted research on the subject of reducing the occurrence of slug flow using surfactants [8]. SDS was used as surfactant with 220 and 1340 ppm concentrations in demi water and 1140 ppm concentration in tap water. Also the surfactant LAS (linear alkyl benzene sulphonate) with 1375 ppm concentration in tap water. The pipe diameter is 50.8 mm and the superficial velocities were u_{sl} = 0.03-1.2 m/s and u_{sg} = 0.07-7 m/s. To be able to explain the changed flow pattern transitions, new flow patterns have been proposed which can be seen in figure 3.2:

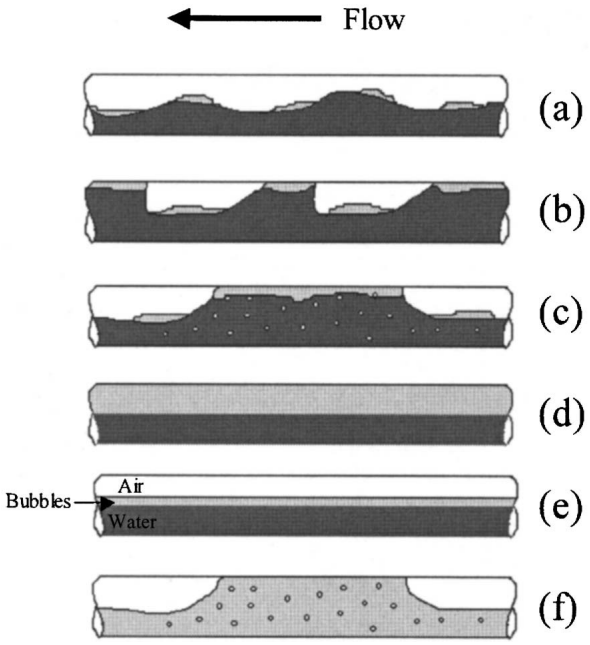

Figure 3.2: Illustration of the new flow patterns proposed by Wilkens et al., (a) stratified wavy with bubbles, (b) intermittent bubble top plug, (c) intermittent bubble top slug, (d) stratified bubble-liquid, (e) stratified gas-bubble-liquid, (f) intermittent bubbly slug [8]

As the concentration of SDS was increased, the range of superficial velocities at which slug flow exists is decreased, namely only up to a to up to a superficial liquid velocity of 0.2 m/s. The plug and pseudoslug flow patterns above this speed are replaced by stratified gas-bubble-liquid and dispersed bubble flow patterns. This suppression of the intermittent flow patterns with SDS is more effective when the water is hard (tap water) instead of deionized (demi water). Furthermore, the experiments with 1375 ppm LAS resulting in a surface tension of 30 mN/m agree better with the results using the 1340 ppm SDS in demi water (surface tension = 48 mN/m) than with the results for the 1140 ppm concentration of SDS in tap water (surface tension is 30mN/m). From this it is concluded that the surface tension alone is not a conclusive prediction factor for flow pattern changes. There were indications that it could be also related to the foam tendency of the mixture with surfactant. At last, there was no surface tension effect observed for the flow pattern transitions from any other flow pattern to annular or dispersed bubble flow, as was expected from mechanistic models for horizontal flow.

Using the same setup and superficial gas velocities of 3.8, 5.2 and 6.6 m/s Wilkens and Thomas [7] found that a pressure drop reduction of up to 40% is possible for superficial liquid velocities of up to 1 m/s when using SDS concentrations of 400, 800 and 1000 ppm. It should be noted that the 1000 ppm concentration caused unreliable measurement data as too much foam was formed. Another important conclusion is that there were no surfactant effects reported during the single phase experiments, in which they compared the water-surfactant mixture with the pure water pressure drop for a superficial liquid velocity range of 0 to 1.2 m/s.

Wilkens and Thomas also proposed a new method to determine the slug frequency using pressure measurements. By determining the minimal pressure drop required for a slug to exist in horizontal pipelines, using data from slugs in inclined pipes up to 11° and the assumption that the pressure drop for a slug should be larger in horizontal pipelines compared to inclined pipelines, they derived a minimum slug length [28]:

$$\frac{L_s}{D} \geq 10U_{SL} + 5 \tag{3.1}$$

This expression can be used to determine the minimum pressure drop over the slug:

$$-\Delta P_{\text{one slug}} = 4f\frac{L_s}{D}\frac{\rho_s U_s^2}{2} \tag{3.2}$$

4

EXPERIMENTAL SET-UP

4.1. SEVERE SLUGGING LOOP

The flow loop used to conduct the experiments for this research is called the Severe Slugging Loop and it is located on the outer plot of the Shell Technology Centre Amsterdam; figure 4.1 shows a photo of the flow loop. The flow line of the SSL consists of three sections: a horizontal, declined and vertical section, as can be seen in the schematic overview in figure 4.4. For this research the configuration was used where the air and water are connected through a Y-sprout at the start of the flow line. The horizontal part consists of a 50 m section, a U-turn and a 15 m section. From there on the pipe starts declining at an angle of -2.54° over a length of 35 m. Thereafter there is a short horizontal section of 5 m before arriving at the base of the riser. There are three vertical pipes which can be operated separately or together by adjusting the corresponding valves at the bottom of the risers. The horizontal section is made of galvanized steel with an inner diameter of 50.8 mm, the declined section has the same diameter, but is made of plexiglass and the risers are also made of plexiglass, but have a inner diameter of 32 mm or 44 mm. Right before the U-turn at the horizontal section, there is an inspection glass installed, through which the flow is visible and is recorded by using a GoPro camera.
After the flow has passed through the three sections, it enters the top vessel (V-201), which is directly connected to the separation vessel (V-202). The gas and liquid are separated by gravity; the air is vented into the atmosphere and the water is re-injected into the flowline. At the air exhaust a flexible hose has been installed to prevent the foam from exiting uncontrollably; instead it is redirected to V-103. This has the advantage that surfactants are now used in a closed system.

Figure 4.1: Photo of the Severe Slugging Loop at STCA

Figure 4.2: Photo of the inspection glass at the flowline of the SSL

Figure 4.3: Photo of the water vessel, where the surfactant is added and mixed with the water

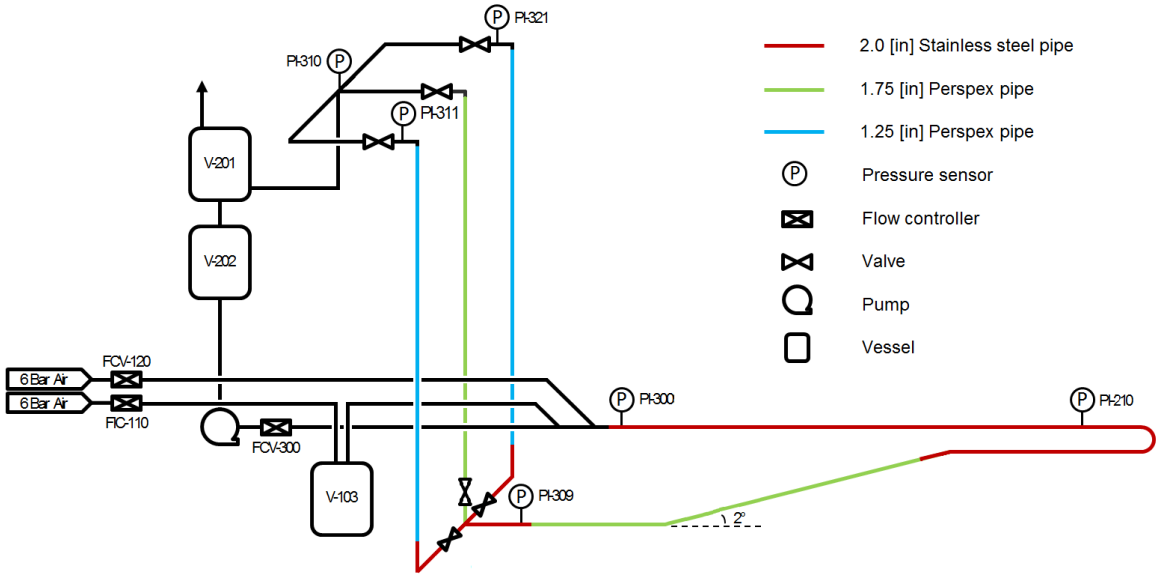

Figure 4.4: Overview of the used configuration of the Severe Slugging Loop [29]

4.1.1. PREPARATIONS

Just before the experiments were performed, the loop did have its 5-yearly inspection during which every aspect of the SSL has been checked on the safety and operational status. The piping was extensively flushed with alternating air and water, the differential pressure indicators were recalibrated and DPI-210 was replaced as the performance was outside the allowable offset. Furthermore, the influence of rain water entering vessel V-103 was minimized as much as possible. The lid was closed at all times, unless the concentrations was changed or experiments with a high surfactant concentration were run, the latter only when it was not raining.

Furthermore it should be noted that the ambient temperature is not constant, which has an effect on the viscosity of the water and on the effectiveness of the surfactant. A temperature sensor will be used during

the experiments and the viscosity is corrected by making use of the New International Formulation for the Viscosity of H2O [30]. The inside of the pipes has to be clean enough to prevent any influence on the results. This is verified by estimating the height of the wall roughness using Shell Flow Explorer 2017 for single phase water flow while specifying the measured pressure drop. The resulting wall roughness is in the range of the expected wall roughness for commercial steel of 46 micron.

4.1.2. EXPERIMENT PROTOCOL

To ensure reliable results, all experiments have been conducted using the same approach (protocol).
The experimental plan describes which superficial velocities and corresponding volumetric flow rates are desired for each individual experiment. Using the temperature and pressure during the experiment, the desired normal volumetric gas flow rate is derived from the preferred superficial gas velocity. The adjustment of the volumetric flow rates of both the gas and liquid flow is done by slightly opening or closing the FCV-300sp valve for water, the FIC-110 valve for the low gas flow rates and the FIC-120 valve for the large gas flow rates. The experiment is started once the flow has the right averaged value and steady state was reached, or in the case of severe slugging, once at least 3 severe slugging cycles had been completed. All experiments have a duration of 15 minutes, which was derived by the balance between statistical relevant data, the scope of the project to explore a large variety of flow rates and concentrations, as well as the time constraint of this research project.

4.1.3. ADDING SURFACTANT CONCENTRATION

The water vessel (V-140) at the bottom of the tower is used to mix the surfactant and water before the mixture is injected into the flow loop. After each concentration change the vessel is completely drained, flushed and refilled with the appropriate ratio of the water to the surfactant. To speed up the filling process, one of the fire hoses from the GTL building is used. The process of introducing a new surfactant concentration to the system is:

- Flush and drain the water vessel completely.
- Fill the watter vessel half way.
- Add the appropriate amount of surfactant to the water in the water vessel, while slowly filling the water vessel further with the fire hose under water to prevent excessive foaming and ensuring that all surfactant droplets have been completely dissolved by moving the fire hose around under the water surface. Keep on filling the vessel until the height needed to have the appropriate amount of water in the vessel for the chosen concentration is reached.

The volume of the vessel is estimated by measuring the dimensions at the bottom and top of the vessel, while keeping in mind that the slope of the walls is constant. At the bottom the dimensions are 1800 mm in length and 1150 mm in width, at the top 2000 mm in length and 1350 mm in width, and the height difference between the top and bottom is 900 mm. Here the rounded edges and unevenness of the bottom of the vessel have been assumed to be negligible when a large amount of water is used, i.e. more than 1 cubic meter. The height h of the water-surfactant solution is the only remaining variable, which is used in the following expression to determine the volume of the water in the vessel:

$$V = LWH = (180 + \tfrac{1}{9}h)(115 + \tfrac{1}{9}h)h \tag{4.1}$$

The volume of water needed for a specified amount of surfactant and a chosen concentration is:

$$V_{total} = \frac{V_{surfactant}}{c_{surfactant}} \tag{4.2}$$

Since the volume and concentration of the surfactant are chosen, the water height needed to match this concentration can be derived.

4.2. MEASUREMENT EQUIPMENT

At the Severe Slugging Loop several pressure and differential pressure indicators have been installed; five pressure indicators and two differential pressure indicators have been used. The first pressure indicator is located at the start of the flowline; it is indicated as PI-300 (Endress+Hauser Cerabar M PMC41). The range of the sensor is from 0 to 10 bar and it has an accuracy of ±0.2% over the full range, or ±20 mbar.

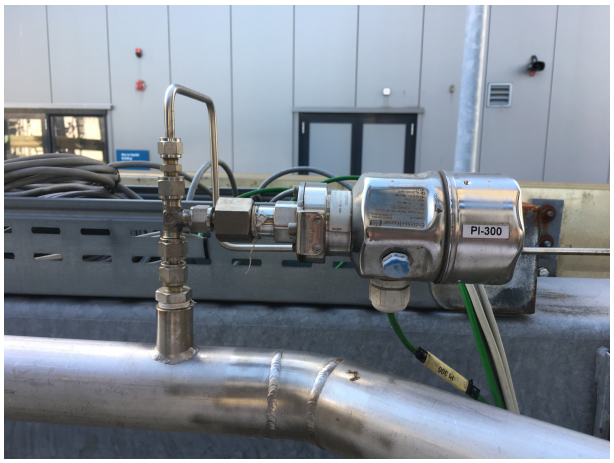

Figure 4.5: Pressure sensor PI-300 at the start of the flowline

Going downstream of this sensor, along the flowline, at a distance of 10.5 m from the air injection point, the first differential pressure indicator is located. This sensor is called DPI-430 (Endress+Hauser Deltabar S PMD75) and it measures the differential pressure over 3 meters with an accuracy of 0.075% over the calibrated range of 0 to 50 mbar. This results in an accuracy of 3.75 Pa over the sensor or 1.25 Pa/m for the pressure drop.

Figure 4.6: Differential pressure sensor DPI-430 along the flowline

At a distance of 46.7 m upstream of the air-injection point, the differential pressure indicator DPI-102 is located. This sensor has been replaced, as the old sensor did not pass the calibration test. The new sensor is from Endress+Hauser and of type Deltabar S PMD70. It is calibrated similar to the DPI-430 sensor and has the same accuracy range.

Figure 4.7: Differential pressure sensor DPI-102 near the end of the flowline

The PI-210 sensor is located at the end of the tubing to the DPI-210 sensor, which is at a distance of 48.2 m from the air-injection point. It is of the same type as the PI-300 sensor and is also calibrated similarly.

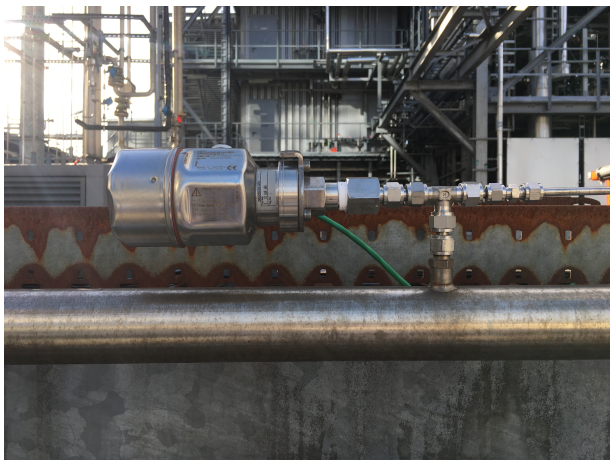

Figure 4.8: Pressure sensor PI-210 near the end of the flowline

The water entering the flow loop is pumped from the storage vessel V-202 and passes the flow controller FCV-300 and mass flow indicator FI-300. The amount of water entering the flow loop is influenced by the opening of the FCV-300 valve and by the back pressure inside the system. The resulting flow ranges from 0.15 to 6 m^3/hr with an accuracy of 0.02 m^3/hr.
The air inflow comes from the STCA air supply, which contains pressurized air at 6 bar. The amount of air entering the system is regulated by the two mass flow controllers: FIC-110 of type Brooks Instrument 5853E with a range of 0-48 Nm^3/hr and the FCV-120 of type Endress+Hauser Prowirl 72 with a range of 30-200 Nm^3/hr. The combined accuracy of the two controllers is 1.0 Nm^3/hr and they are both insensitive to

temperature fluctuations or back pressure.

Figure 4.9: Volumetric flow meter of the water inflow

FI-110

Figure 4.10: Volumetric flow meter of the air FI-110 with a low range

To convert the normal gas conditions to actual gas conditions the following equation is used:

$$Q_{g,normal} = Q_{g,actual} \frac{P_{normal}}{P_{actual}} \frac{T_{actual}}{T_{normal}} \tag{4.3}$$

4.3. DISTRIBUTED ACOUSTIC SENSING (DAS)

The DAS measurement system is based on a fibre-optic technology that transforms an ordinary Telecom fibre into a distributed sensor that can measure acoustic disturbances along the entire length of the fibre. The flow induced acoustics can be filtered from the sensor data. Apart from the fibre, DAS only requires an interrogator and no other electronics. DAS has many applications including flow monitoring in wells and pipelines [31].

4.3.1. DESCRIPTION OF THE MEASUREMENT TECHNIQUE

In the interrogator the laser emits light pulses at a wavelength of 1550 nm. The speed of light in the fibre can be derived from the speed of light in vacuum c and the refractive index of the fibre n:

$$v = \frac{c}{n} = \frac{3 \cdot 10^8}{1.5} = 2 \cdot 10^8 \text{ m/s} \tag{4.4}$$

The light that travels through the core of the optical fibre is subjected to a total internal reflection according to Snell's law, as the core of the optical fibre has a larger refractive index than its surrounding cladding. The

length of the fibre is limited by the speed of the light pulse in the fibre v and the pulse rate F_p. The next light pulse can only be launched after the previous pulse has travelled over a distance L from the interrogator to the end of the fibre and back:

$$L = \frac{v}{2F_p} \tag{4.5}$$

The length d of the light pulse in the fibre, depends both on the speed of sound v in the fibre and on the duration Δt of the pulse:

$$d = v\Delta t \tag{4.6}$$

The time it takes for the light pulse to travel to some point z along the fibre, reflect at that point and travel back to the interrogator is equal to:

$$t = \frac{2z}{v} \tag{4.7}$$

From the pulse duration Δt and the speed of light in the fibre v, the spatial resolution Δz can be approximated:

$$\Delta z = \frac{v\Delta t}{2} \approx 10^8 \cdot \Delta t \tag{4.8}$$

In order to achieve a spatial resolution of 1 m, a pulse duration of 10 ns will be needed.

4.3.2. DAS MEASUREMENT PRINCIPLE

Light is backscattered from inhomogeneities in the fibre, more when the fibre is deformed and less when there is no strain on the fibre. These inhomogeneities are the result of the manufacturing process of the fibre, in which density fluctuations are frozen into the glass and therefore will exist in any optical fibre. They are essential for fibre-optic sensing techniques such as DTS and DAS.
For the DAS measurement technique, the same frequency of light is measured as with which it was emitted. This backscattered light is called Rayleigh scattering: this returns the same intensity regardless of the temperature or static strain on the fibre. The other two scattering categories are called Brillouin, which returns different frequencies with changing temperature and static strain, and Raman, which gives in the lower frequency range more intense scattering when the temperature is increased. A schematic overview of all three backscattering categories is given in figure 4.11 (see [31]).

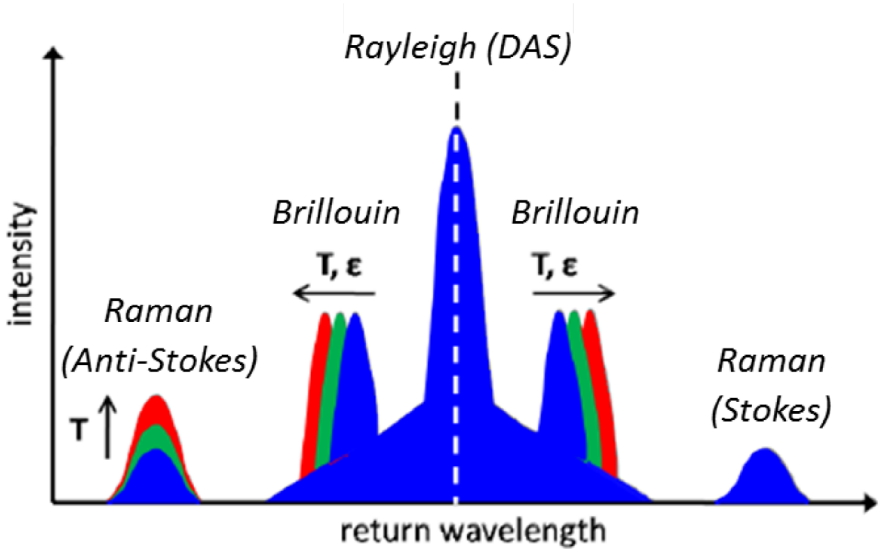

Figure 4.11: Spectrum of backscattered light; intensity versus wavelength for Rayleigh, Brillouin and Raman backscattering

The fibre on our experimental set-up is in total 932 m long. It has been installed 9 times directly onto the flowline over sections of 40 m length, and coiled in between. The fibre has been installed three times at the top, side and bottom of the pipe. Around the flowline at the location where the fibre has been installed, the pipe is insulated with insulation material all around. A schematic overview of the ordering of the fibre is shown in figure 4.12; this ordering also appears in the measured data.

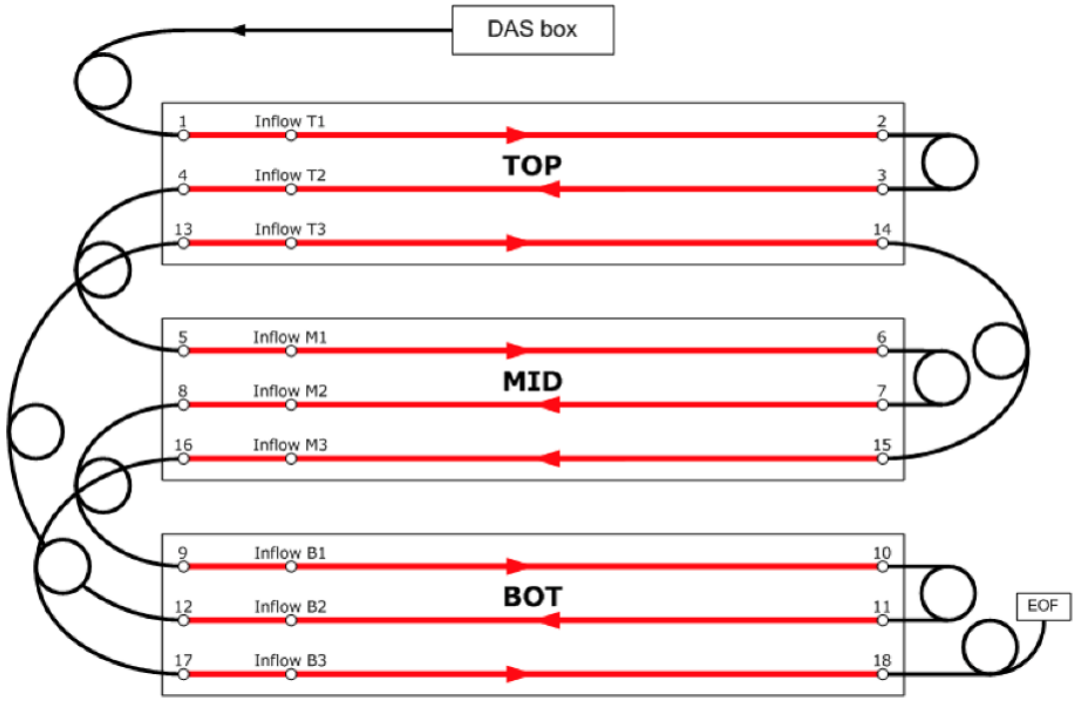

Figure 4.12: The schematic layout of the DAS fibres along the flowline

4.3.3. DAS INTERROGATION MODES

With the current state of the DAS technology two interrogation modes can be used depending on the type of measurement: single pulse and dual-pulse, which are showed schematically in figure 4.13.

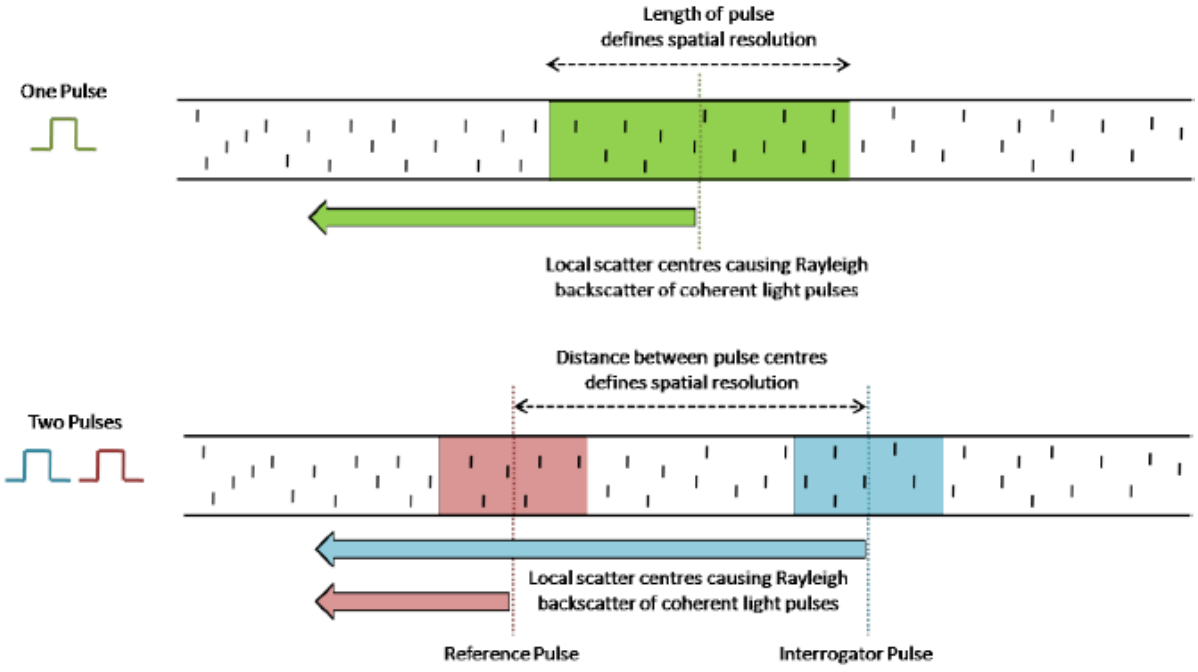

Figure 4.13: Schematic overview of the single and dual pulse interrogation modes

In single pulse mode a light pulse is emitted by the laser at fixed intervals and the amplitude of the

backscattered light is measured, which results in a series of independent acoustic samples along the length of the fibre. The change of the signal over time represents the acoustic signal at a certain location. The length of the light pulses determines the spatial resolution as shown in equation 4.6. The minimum distance between the light pulses is determined by the sample rate, which is related to the length of the fibre as mentioned in equation 4.5.
When the interrogator is set in dual pulse mode, two pulses are emitted per measurement and the phase change is measured by comparing the interrogator and reference pulse at a slightly different frequency. For each measurement more time is needed, since there are now two pulses and a certain time between these pulses needed. This extra time results in a larger spatial resolution of the DAS measurement when the dual phase mode is used.
For DAS measurements over short distances, the single phase pulse is preferred, as the spatial resolution is smaller. The downside of this method is that non-linear effects are growing with distance. The dual-pulse method is not affected by this and therefore will lead to more accurate measurements, provided the increased spatial resolution is not a problem. For our set-up both methods were considered, but the minimum spatial resolution of 8 m for the dual-phase mode is unfortunately too large for our purpose, and therefore the singe-pulse mode was chosen.

4.3.4. SLUG ANALYSIS USING DAS

Using the DAS system the velocity and frequency of acoustic events can be determined with 1D FFT (Fast Fourier Transform) or 2D FFT, depending on the number of channels measured and on the typical velocities of the events that are being tracked. In practice 1D FFT is used to track slow moving events, such as slugs and 2D FFT is used to determine the velocity of events that move with the speed of sound in different media. Also it should be noted that 1D FFT has a speed advantage over 2D FFT, as it requires significantly less computational power. [32] [33] [34] For the input of the velocity tracking, either sensor data or Frequency Band Extraction data can be used. The latter type provides filtered sensor data and uses only the frequency bands from the original sensor data in which the relevant acoustic signals show up. Using FBE data has the advantages that some of the noise is filtered out and that the time required to determine the velocity and frequency of the events is drastically reduced. However, using the sensor data directly will increase the accuracy of the measurement.
For the tracking of the slugs in the experimental data, 1D FFT on FBE data has been chosen as the best option to start with, keeping in mind the background noise of the area around the flow loop and the feasibility in terms of hardware and software. The method is based on the velocity tracking algorithm developed by Paleja[35] [36], which has been altered and tweaked to get the best results for the measurement data. After reading the FBE data and extracting only the relevant channels, the data for each channel are split into windows to enhance the accuracy of the velocity tracking. This window size should be large enough such that a typical event exists over the full length of the measured part of the fibre. This size depends on the slug velocity, the length of the fibre and the sampling frequency:

$$\text{window}_{min} = \frac{1.3 U_{mix}}{L_{channels} \cdot F_s} \tag{4.9}$$

For every window the algorithm compares two channels at a defined distance, cross correlates the signals and if the measurement meets the thresholds, a feature is detected and the velocity is measured. The criteria consist of a cross correlation threshold of 0.8 and an index threshold of 2 time steps to filter out cases where the lag is equal or very close to zero. These thresholds may vary from set-up to set-up. They have been found to give the best results in terms of false positives and filtered out data by trial and error. Since our data are discrete, the velocity measurements have a finite accuracy. This depends on the time step and measurement distance, as it divides the distance of the measurement by the time lag with the highest correlation. Short distance measurements have a lower accuracy than long distance measurements. The features, however, are more likely to have a more identical acoustic footprint for shorter distances. Hence, using a fixed distance in the measurement is a trade-off between these two factors. Figure 4.14 shows what the velocity tracking algorithm returns for one of our measurements using a distance of 3 channels in the measurement. These data have already been filtered from negative velocities, as these are physically not possible in our experiments and the axis has been limited to a maximum velocity of 20 m/s.

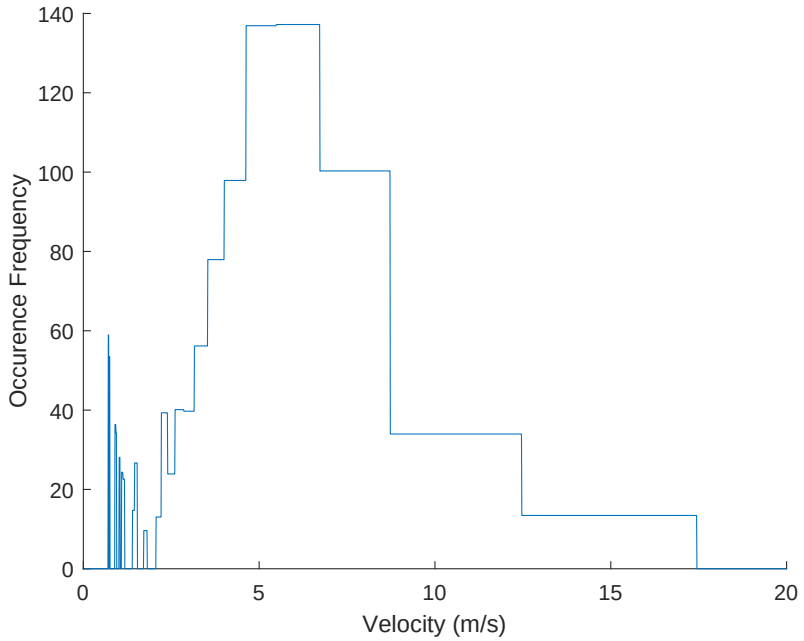

Figure 4.14: Velocity histogram for a distance measurement with a difference of three channels

The bin sizes and locations of the start and end of these bins varies with the distance used. Estimating the velocities for all the possible channel distances results in a range of velocity distributions that have a similar shape; this can be seen in figure 4.15.

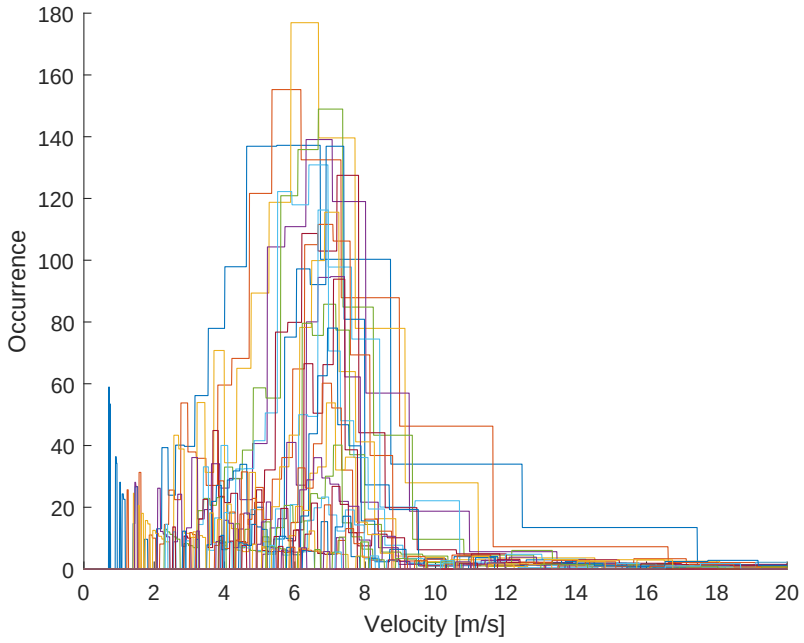

Figure 4.15: Velocity distribution for all distance measurements

Combining these velocity histograms leads to an overall velocity distribution produced by the velocity tracking algorithm, as can be seen in figure 4.16. All distances which are able to produce the most likely slug velocities have been used; in other words, the distances of 1 and 2 channels have been neglected. The peak represents the most likely velocity of the slugs travelling through the flow loop and the large number

of measured occurrences indicates that slug flow is likely. Drawing other conclusions from a single velocity distribution should be done with care, as each experimental set-up can possibly influence the shape of the distribution. However, comparing different velocity distributions from the same experimental set-up could lead to new insights. The slug detection can be seen as a new feature of the velocity tracking algorithm, for which the purpose until now was only to roughly estimate the velocity of the slugs. With this new feature in mind, the DAS can be installed for existing and new pipelines, for which it can be used to not only track the already known applications but also the existence of slug flow. It can also be used for the same purpose as the subject of this project, namely detecting whether an added concentration of surfactant is sufficient to eliminate slug flow at current flow conditions.

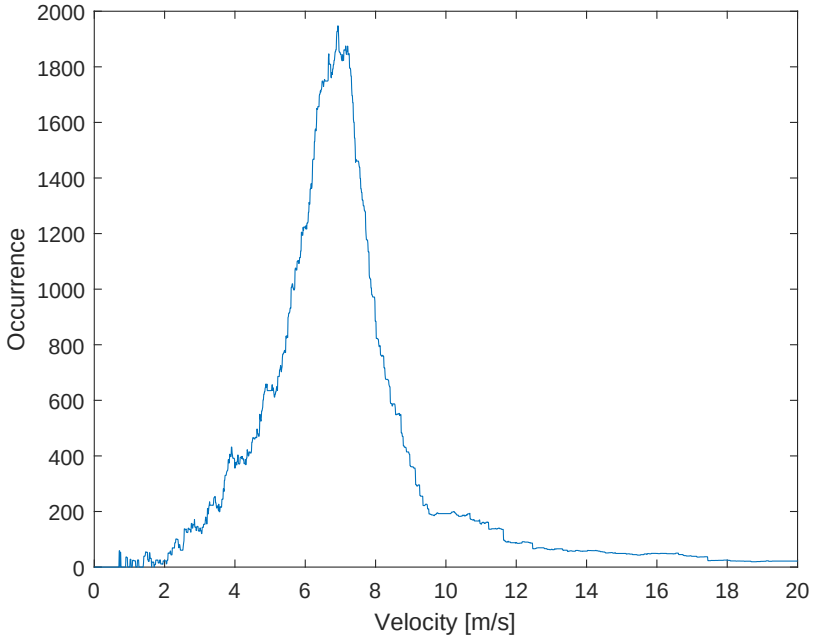

Figure 4.16: Velocity distribution

4.4. USED SURFACTANT

For the conducted experiments the main objectives were to find the surfactant concentration at which severe slugging was suppressed and to what extent slugging in the horizontal flowline is mitigated. The first objective had a good reference concentration, as such experiments have been done successfully in the past with a range of surfactants. This includes earlier experiments in the same flow loop as used in the present study. However suppression of hydrodynamic slugging in the horizontal flow line had a lack of reference concentrations. Only Wilkens et al. have reported the suppression of hydrodynamic slugging albeit with a different surfactant. Since it is not allowed to use any chemicals other than household detergents, the choice of surfactants was limited. Using SDS was not permitted. To have a rough estimation of the surfactant strength, the foaming factor introduced by Van Nimwegen et al.[24] was used. This foaming factor can predict the influence of a surfactant on slug flow in a vertical riser in comparison with Trifoam relatively accurately. The foaming factor is 3.6 for Dreft and 3.4 for SDS. This means that if the concentration of Dreft relative to the original concentration of SDS is increased by 5.9% the results should be the same for vertical slug flow.[24]
In order to find the right amount of surfactant, the concentration has been increased gradually. Due to a different type of Dreft that got delivered at one of the orders, two types of Dreft have been used namely Dreft Original and Dreft Professional. Verification by du Noüy ring experiments in the laboratory led to the conclusion that Dreft Original is almost twice (namely a factor 1.85) more concentrated than Dreft Professional. A straight line has been fitted to the linear part of the static surface tension graph on a concentration log scale, see figure 4.17. From the displacement between the two lines and noting that the slope is equal, the difference in concentration can be determined. The results are in agreement with what has been observed from the flow loop experiments.

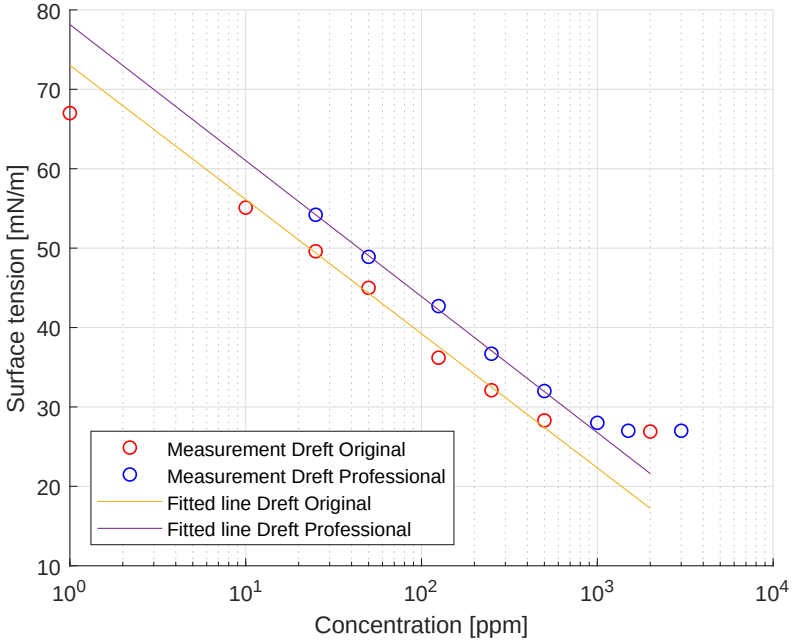

Figure 4.17: Static surface tension experiments conducted in the laboratory at STCA for Dreft Original and Dreft Professional at 20 °C

The used concentrations of Dreft Professional converted into effective Dreft Original concentrations are specified in table 4.1.

Table 4.1: Conversion of Dreft Professional concentrations into equivalent Dreft Original concentrations

$C_{\text{Dreft Professional}}$	$C_{\text{Dreft Original}}$
1000 ppm	540 ppm
1500 ppm	810 ppm

5

RESULTS

5.1. SINGLE PHASE

Before the multiphase experiments were started, single-phase experiments were conducted to ensure that the wall roughness and inclination were within the acceptable ranges. The flow loop had completely been drained and slowly been refilled with water. Because of the layout of the Severe Slugging Loop, some air gets trapped in the flowline. This air will be entrained in the water flow as the volumetric flow rate is increased or exits through venting of the tubes at the DPI sensors. The measured pressure drop for single-phase flow can be seen in figure 5.1.

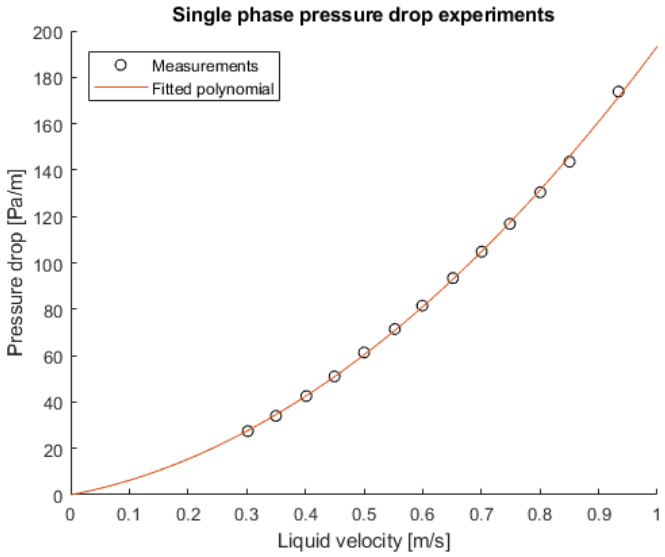

Figure 5.1: Pressure drop per meter measured halfway along the flowline for single phase water flow

The comparison of the measured pressure drop data with predictions from Shell Flow Explorer or from the OLGA Multiphase Toolkit, the measured values seem to be lower than the results from the existing correlations for a wall roughness of 30 μm and 45 μm which are standard values for commercial steel. The fitted polynomial passes through zero, hence a declination of the pipe is unlikely. However adding a small amount of air to the single phase water flow and forcing stratified smooth flow in the model gives similar results.

Table 5.1: Pressure drop as measured and as obtained from correlations with and without a small added gas flow for $u_{sl} = 0.93$ m/s

Method	**Pressure drop [Pa/m]**
Measurement	173.8
SFE	195.8
OLGA	194
SFE with $u_{sg} = 0.005$ m/s	176.7
OLGA with $u_{sg} = 0.005$ m/s	175.5

Also the pressure at the start and end of the flowline has been measured without flow and with either air or water at different pressures. The difference in pressure between the PI-300 at the start of the flowline and PI-210 is constant, regardless of the substance and pressure. From these pressure measurements it can be concluded that the difference in density between the water and air does not lead to a difference in the pressure drop between the two pressure indicators. This means that the inclination or declination of the horizontal flowline is within the accuracy of the pressure indicators. The combined accuracy of the measured pressure difference by the two pressure indicators is constrained by the combined error margin, which is ±0.02 bar per indicator. This leads to a combined error margin of ±0.04 bar or 40 cm water height, which corresponds to ±0.45°.
The same pressure measurement has been done using the differential pressure indicators DPI-430 and DPI-102, located halfway along the flowline and at the end of the flowline located respectively. These sensors are more accurate, but have the drawback that they only measure a part of the flowline. The measured pressure drop over 3 m is within the error margin of the differential pressure indicator. This means that the hydrostatic head should be smaller than 1.25 Pa/m, which shows that the inclination at these two locations is negligible. Visual inspection of the flowline leads to the conclusion that height differences along the flowline are too small to be seen by the naked eye. From the measurements and visual inspection it has been concluded that the flowline can assumed to be horizontal.

5.2. RE-ANALYSIS OF THE EXPERIMENTS BY PRONK

Experiments by Pronk[1] where growing slugs were reported for $u_{SL} = 0.4$ m/s and $u_{SG} = 1.21$ m/s have been re-analysed. From the original data of the measured volumetric flow rates for the gas and liquid it can be concluded that there are inconsistencies in the determination of the superficial gas velocity. A match was found between the pressure measurements over the riser that was reported by Pronk, which can be seen in figure 5.2, and the original pressure measurement data. In this experiment a volumetric normal gas flow rate of 9.99 Nm^3/hr and a volumetric liquid flow rate of 2.92 m^3/hr have been measured. Converting these flow rates into superficial velocities by using equation 4.3 for the gas and liquid gives: $u_{SL} = 0.4$ m/s and $u_{SG} = 0.55$ m/s, using $p = 2.7$ bar, $T = 20\,°C$ and $D = 0.0508$ m. The superficial gas velocity of 0.55 m/s as obtained here is lower than the value of 1.21 m/s reported by Pronk. The value of Pronk was most likely obtained by not correcting for the normal conditions and by using a larger diameter (0.054 m). This applies to all superficial gas velocities reported by Pronk.

The same experiment has been repeated as part of the current research, leading to similar pressure measurements with the same periodic behaviour. Growing slugs could not be seen, instead there were severe slugs observed. The pressure data from figure 5.2 shows that the pressure drop in the riser varied between 1500 and 9800 Pa/m at a period of around 90 s. A pressure drop of 9800 Pa/m indicates that the riser was filled with liquid at this point, which in combination with the long period suggests that severe slugs were measured. The severe slugging number for this experiment using equation 2.65 is: $\Pi_{ss} = 0.47$. This satisfies the first condition for severe slugging and therefore it can be concluded that no growing slugs were measured nor observed, but that severe slugging was measured and suppressed by Pronk. The concentrations reported by Pronk in this graph should be handled with caution; from the original data it is most likely that effective concentrations of 1000 ppm and 1500 ppm were used, corresponding to 278 ppm and 417 ppm of actual concentration of Dreft Original. Due to limited reporting and the absence of a logbook it is not possible to draw hard conclusions on the validity of the used concentrations. The surface tension values measured and reported for different concentrations of Dreft Original by Pronk (see Table 5.2 and figure 5.3) are larger than what would be expected for this type of surfactant. The surface tension for Dreft Original has also been measured in the laboratory at STCA for different concentrations as part of the present study, which can be seen in figure 4.17. Our measurements give a behaviour of the surface tension versus the concentration that is expected: when the concentration of surfactant is increased the surface tension decreases at an increasing

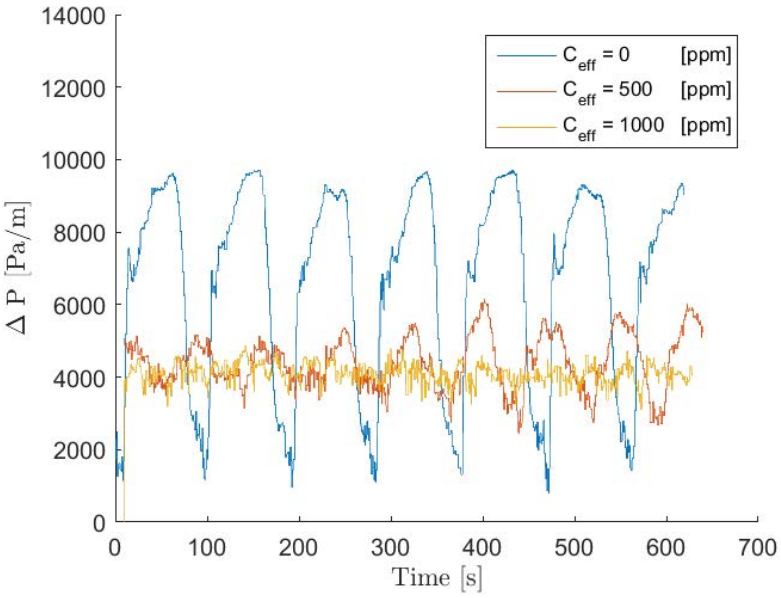

Figure 5.2: Figure taken from Master Thesis of Pronk with the following original description: "Pressure measurements for multiple effective surfactant concentrations and with $u_{SG} = 1.21$ m/s and $u_{SL} = 0.40$ m/s." Pronk[1]

rate in the first section, it continues at a constant rate and once the cmc value is reached, the rate decreases until the minimum value is obtained. From the laboratory experiments it can be concluded that the values of the surface tension as reported by Pronk are too large. This could be explained by a different (i.e. lower) actual concentration of the surfactant or the presence of dirt in the system that bounded the surfactant to itself and thereby reduced the amount of free moving surfactant molecules that could have influence on the surface tension.

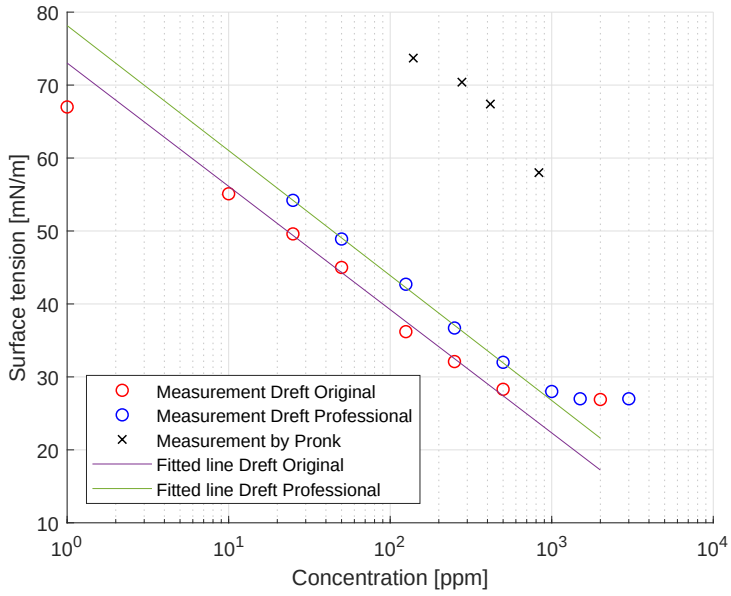

Figure 5.3: Static surface tension experiments conducted in the laboratory at STCA for Dreft Original and Dreft Professional at 20°C and the static surface tension experiments conducted by Pronk [1]

Table 5.2: The measured surface tension of the surfactant-water mixtures used during the experiment by Pronk [1]

$C_{\text{Dreft Original}}$	Static surface tension (γ) [mN/m]
0	76.5
139	73.7
278	70.4
417	67.4
833	58.0

5.3. HYDRODYNAMIC SLUGGING

5.3.1. EFFECT OF SURFACTANT ON THE PRESSURE DROP

Increasing the concentration of the surfactant (Dreft Original) to 2000 ppm leads to the suppression of slug flow for a range of flow rates, which can be seen in figure 5.4. This effect is best visible when looking at the spread in the measurements by the differential pressure indicators along the flow line. The pressure drop for the experiment without surfactant is highly unstable and reaches values between 130 and 580 Pa/m at the DPI430 sensor. In contrast to this, during the experiment with 2000 ppm surfactant the measured pressure drop is much more stable and it gives values around 200 Pa/m at the DPI430 sensor.

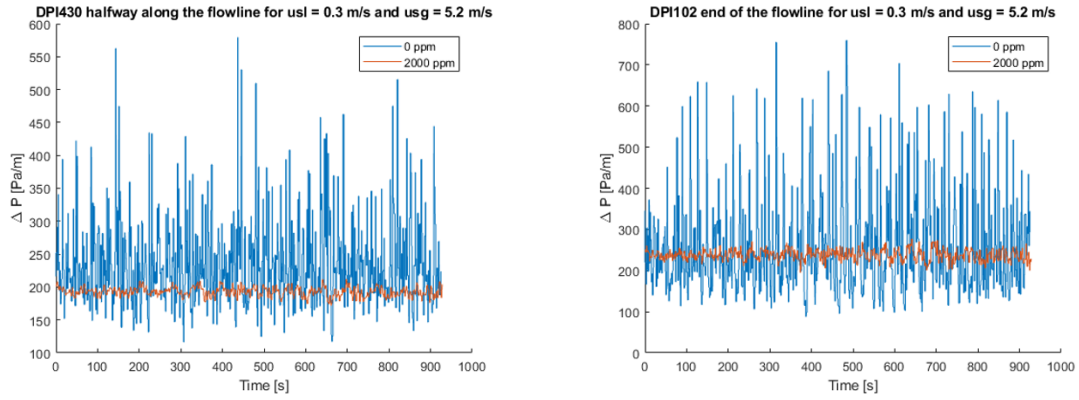

(a) DPI-430 (b) DPI-102

Figure 5.4: Pressure drop for an experiment without and with surfactant at $u_{SL} = 0.3$ m/s and $u_{SG} = 5.2$ m/s

Looking at the whole range of superficial liquid velocities for $u_{SG} = 5.2$ m/s in figure 5.5, it can be seen that the spread in the pressure drop measured by DPI430 is much smaller in the 2000 ppm case when compared to the reference case with just air and water, for all of the possible flow rates. The averaged pressure drop over 15 minutes is equal for both cases until $u_{SL} = 0.2$ m/s; from that point onward the added surfactant leads to a reduction in the pressure drop. This is in line with results from Wilkens et al. [8], where the reduction in pressure drop started at around $u_{SL} = 0.3$ m/s using a different surfactant. It is likely that the surfactant needs to be sufficiently agitated before it starts to reduce the averaged pressure drop. The fluctuations caused by the slug flow are reduced even when there is little agitation.

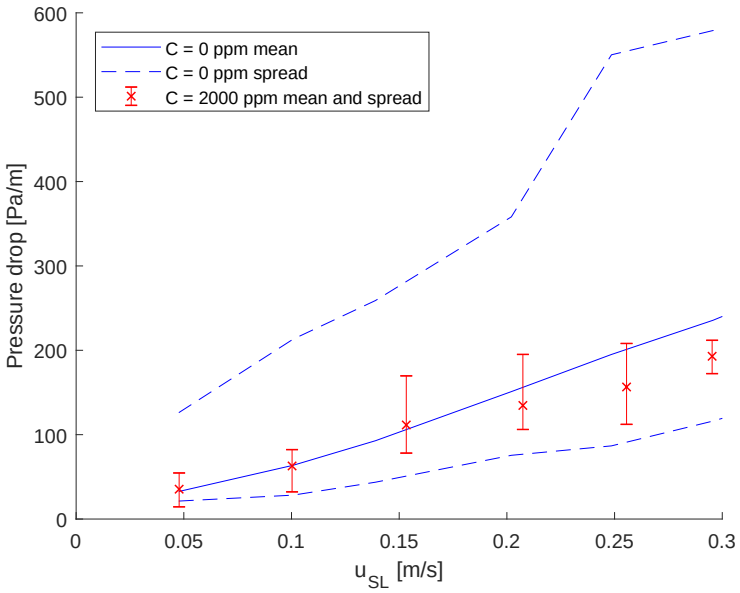

Figure 5.5: Mean and spread of the pressure drop measured by the differential pressure indicator halfway along the flow line for the case without surfactant and for the case with 2000 ppm Dreft Original at $u_{SG} = 5.2$ m/s.

In figure 5.6 the case without surfactant is compared to the case with 1500 ppm of Dreft Professional; with surfactant the fluctuations are reduced starting from $u_{SL} = 0.25$ m/s. At superficial liquid velocities lower than this value the fluctuations are larger than measured in the case without surfactant. The reduction in surface tension and therefore the lower suppression of the wave growth could serve as a possible explanation. At higher velocities the surfactant is sufficiently agitated to start with the reduction of the fluctuations caused by the slug flow. A reduction of the averaged pressure drop is not measured at this surfactant concentration of surfactant and at the possible flow rates. The spread in the pressure drop increases from $u_{SL} = 0.25$ m/s to 0.4 m/s. This is most likely caused by the energy in the slug flow, which is increasing as the flow rate increases; this balances with the amount of agitation caused by the flow.

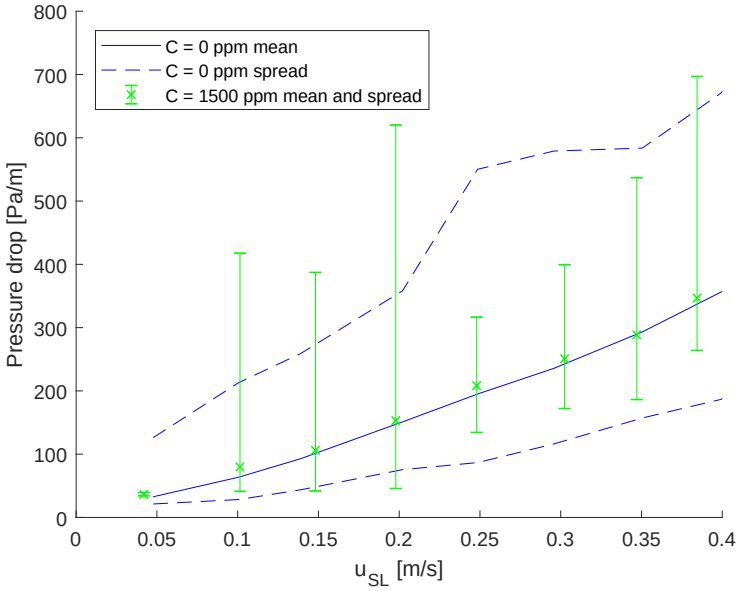

Figure 5.6: Mean and spread of the pressure drop measured by the differential pressure indicator halfway along the flow line for the case without surfactant and for the case with 1500 ppm Dreft Professional at $u_{SG} = 5.2$ m/s.

From the comparison between the case without surfactant and the case with 175 ppm of Dreft Original in figure 5.7, it can be concluded that the pressure drop fluctuations of the slug flow have increased. Using figure 4.17, we see that the surface tension σ has dropped from 73 to 35 N/m. This, combined with the influence of the surface tension on the stability analysis of the Kelvin-Helmholtz relation, which predicts that the waves become unstable earlier when the surface tension is lower, explains the increase of the fluctuations. The foam that is created leads to an increase of the wall friction, which translates to the increased averaged pressure drop at velocities of $u_{SG} = 0.4$ m/s and higher. The difference between the fluctuations in the case without surfactant and in the 175 ppm case reduced when the superficial liquid velocity increases, though it is still present at the highest measured velocities.

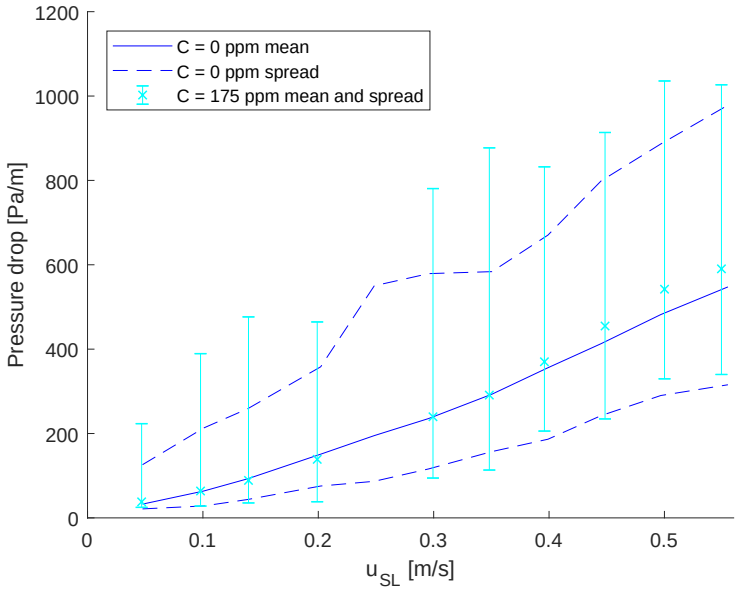

Figure 5.7: Mean and spread of the pressure drop measured by the differential pressure indicator halfway along the flow line for the case without surfactant and for the case with 175 ppm of Dreft Original at $u_{SG} = 5.2$ m/s.

At a lower super velocity of $u_{SG} = 3.8$ m/s the comparison between the reference case and the 175 ppm case gives the same picture, this can be seen in figure 5.8. Again the spread is larger with the added surfactant, and also the average pressure drop is larger at $u_{SL} = 0.2$ m/s and higher. The difference between the two cases for the average pressure drops and fluctuations decreases at the highest velocity, but still here the added surfactant leads to slightly larger fluctuations and a larger average pressure drop. Here the surface tension seems to play a role, similarly to previous findings.

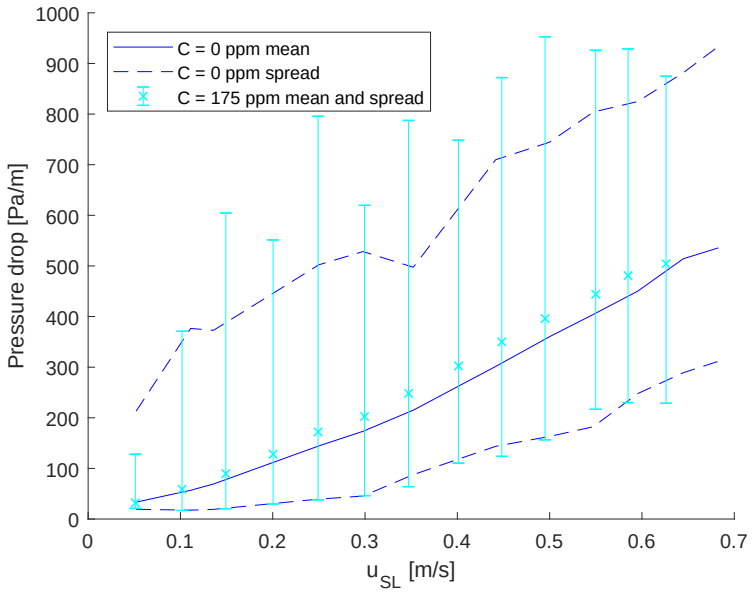

Figure 5.8: Mean and spread of the pressure drop measured by the differential pressure indicator halfway along the flow line for the case without surfactant and for the case with 175 ppm of Dreft Original at $u_{SL} = 3.8$ m/s.

When the surfactant concentration of 2000 ppm is compared with the reference case for the same superficial gas velocity of $u_{SG} = 3.8$ m/s, this can be seen in figure 5.9. The added surfactant seems to have an effect similarly to the same comparison with the superficial gas velocity of $u_{SG} = 5.2$ m/s. Apart from the lowest measured superficial liquid velocity of $u_{SL} = 0.04$ m/s, the fluctuations have been largely reduced. The average pressure drop seems to be similar to the reference case, apart from $u_{SL} = 0.15$ and 0.3 m/s, where the pressure drop has been reduced due to the added surfactant. Here the reduction of the average pressure drop is in line with the findings from Wilkens et al. [8]. The balance between agitation and energy in the slugs could be a possible explanation for the reduction of the averaged pressure drop and spread of the pressure drop.

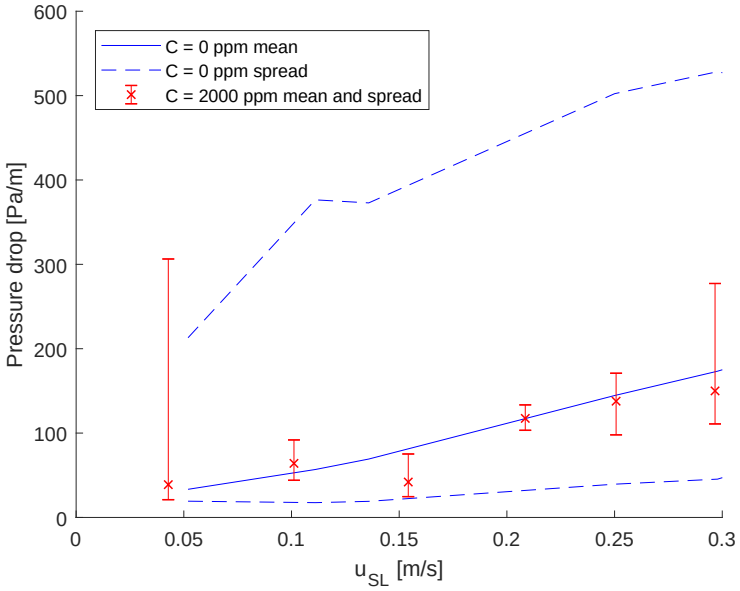

Figure 5.9: Mean and spread of the pressure drop measured by the differential pressure indicator halfway along the flow line for the case without surfactant and for the case with 2000 ppm of Dreft Original at $u_{SL} = 3.8$ m/s.

5.3.2. EFFECT OF SURFACTANT ON ACOUSTIC SIGNAL

The invidual slugs can be derived from the sensor data measured by the DAS system. In the graphs with the DAS data (such as figure 5.10) the x-axis is the time and the y-axis is the distance along the optical fibre. As mentioned in section 4.3, the fibre is attached to the flowline multiple times and the two visible sections are both at the top of the flowline back and forth. The slope of the lines determines the velocity of the flow features (such as the slug velocity) and indicates that they exist all the way along the flow line.
By using a Frequency Band Extraction of the frequencies between 0 and 7 Hz, the best signal to noise ratio was achieved. It should be noted that these frequencies can be different for every experimental setup. When

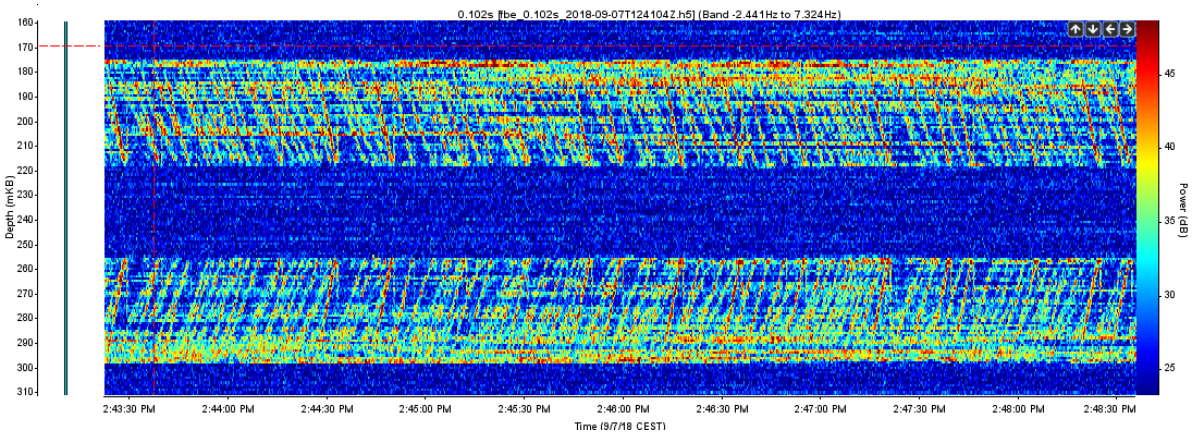

Figure 5.10: Signal measured by the two top fibres of the DAS system for u_{sl} = 0.3 m/s, u_{sg} = 5.2 m/s and 0 ppm concentration of surfactant

the concentration of surfactant is increased to 2000 ppm, similarly to the pressure measurements, the slugs disappear. The colours of figures 5.10 and 5.11 can be misleading; in fact the largest measured power that is related to the flow correspond to a measured acoustic energy of 45 dB in figure 5.10 and to a measured acoustic energy of 25 dB in figure 5.11. Hence the signal is greatly dampened; this suggests that the slugs have been suppressed, which is in line with what the pressure data and videos show. Here it should be noted that the horizontal red stripes in both figures are related to the acoustic energy produced by the environment. In contrast to measured acoustic energy produced by the flow, which moves at a non-zero velocity through the system.

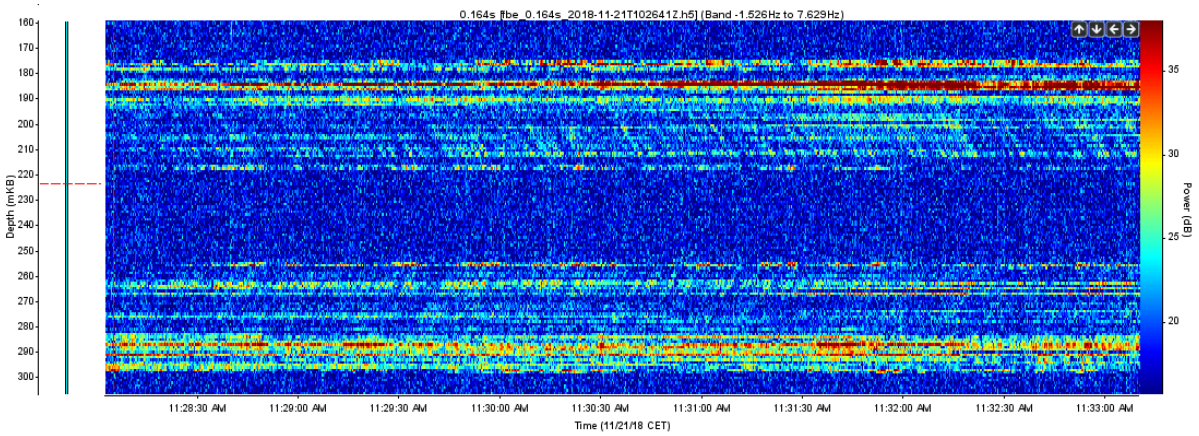

Figure 5.11: Signal measured by the two top fibres of the DAS system for u_{sl} = 0.3 m/s, u_{sg} = 5.2 m/s and 2000 ppm concentration of Dreft Original

As mentioned earlier in this section, the velocity of the flow features can be determined from the filtered datasets. The most basic approach is to select two points and determine the slope, which has the advantage that it is easy to do, but it is very inaccurate.
By using a MATLAB script that first splits the measured data into multiple windows, which should each have such a size that it contains one single feature. Then the time lag between two channels is estimated by cross

correlation. This is done for every distance between 3 and 30, the latter being the maximum channel separation for our measurements. In the correlations a threshold of 0.8 is used; this threshold is a trade-off between filtering out false noise or noise produced by the surrounding environment, while preserving the slug velocity measurements.
The velocity measurements have been plotted as the distribution of number of occurrences (divided by the total number of measurements), shown on the vertical axis, against the measured velocity, shown on the horizontal axis. The distribution plot shows a clear distinction between the air-water experiment and the 2000 ppm Dreft original experiment, and can be seen in figure 5.12.

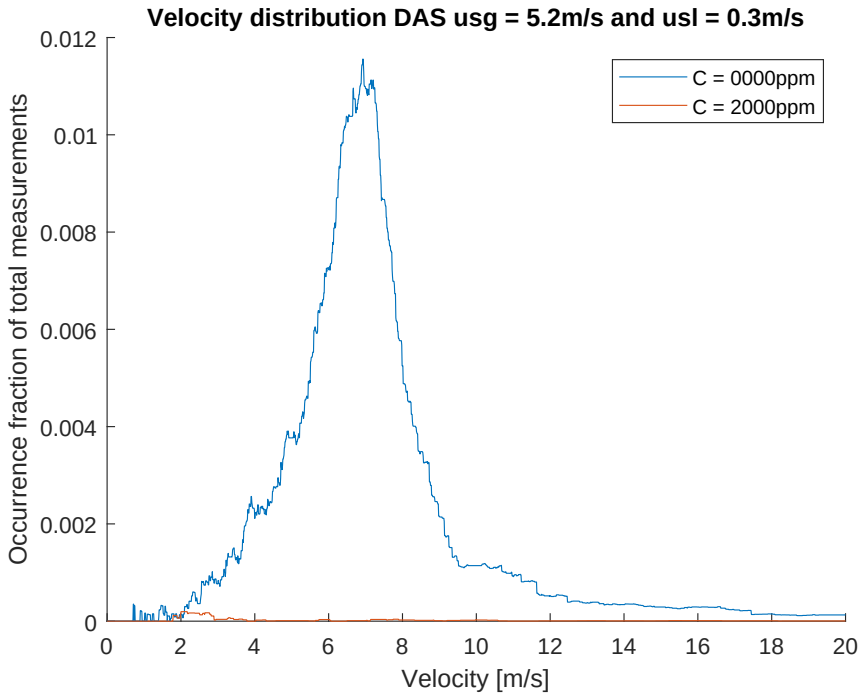

Figure 5.12: Signal measured by the two top fibres of the DAS system for u_{sl} = 0.3 m/s, u_{sg} = 5.2 m/s and 2000 ppm concentration of Dreft Original

Multiple experiments with different concentrations of surfactant have been compared using the velocity distribution with a normalized occurrence fraction. From this comparison it can be seen that the shape of the velocity distribution does not solely decrease between 0 and 2000 ppm. When the concentration is increased from 0 to 175 and to 500 ppm of Dreft Original, the occurrence fraction increases. This means that the velocity tracking algorithm tracks more moving features that satisfy the thresholds and this may help in explaining the effect that the surfactant has on slug flow for different concentrations. This is most likely caused by the reduction in surface tension, that is known to increase the development of the Kelvin-Helmholtz instabilities at the interface [37]. When the concentration is further increased to 1500 ppm Dreft Professional and 2000 ppm Dreft Original, enough foam is being produced at these flow conditions to have an effect on the measured velocity distribution, this can be seen in figure 5.14. The produced foam forms a third layer between the liquid and gas. This can be seen in figure 5.13 and is in agreement with what was described by Wilkens et al. [8].

Figure 5.13: Visual observation by the GoPro camera at the end of the flowline for u_{SG} = 5.2 m/s, u_{SL} = 0.3 m/s and 2000 ppm concentration of the surfactant Dreft Original

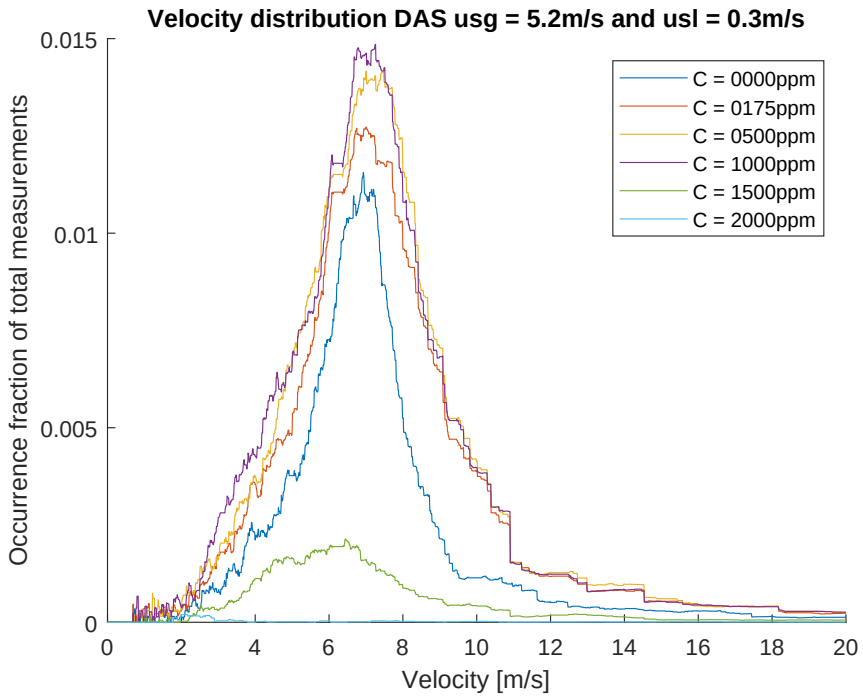

Figure 5.14: Signal measured by the two top fibres of the DAS system for u_{sl} = 0.3 m/s, u_{sg} = 5.2 m/s. Experiments without surfactant as well as containing 175, 500 and 2000 ppm concentration of Dreft Original, 1000 and 1500 ppm of Dreft Professional.

5.3.3. DETECTING HYDRODYNAMIC SLUG FLOW WITH DAS

To determine when slug flow occurs using the measurements by the Distributed Acoustic Sensing system, a sensitivity analysis has been done for several parameters. The value with the highest occurrence rate measured by the algorithm is the most likely slug velocity. For cases where the measured slug velocity is larger than the mixture velocity, there is a strong indication that slug flow exists for the flow rates used in the experiments. The experiments without surfactants have one false-positive and no false-negatives for 30 experiments measured with DAS and analysed with the velocity tracking algorithm. In figure 5.15 it can be seen that there is a clear distinction between the experiments without and with slug flow. The experiments that revealed slug flow almost fall on a linear line, which is close to the existing linear correlation (2.59) for the slug velocity. The experiments where no slug flow was observed have a much lower velocity than the one obtained for the slug velocity from correlation (2.59). The only false-positive is an experiment in the transition region from stratified flow to slug flow.

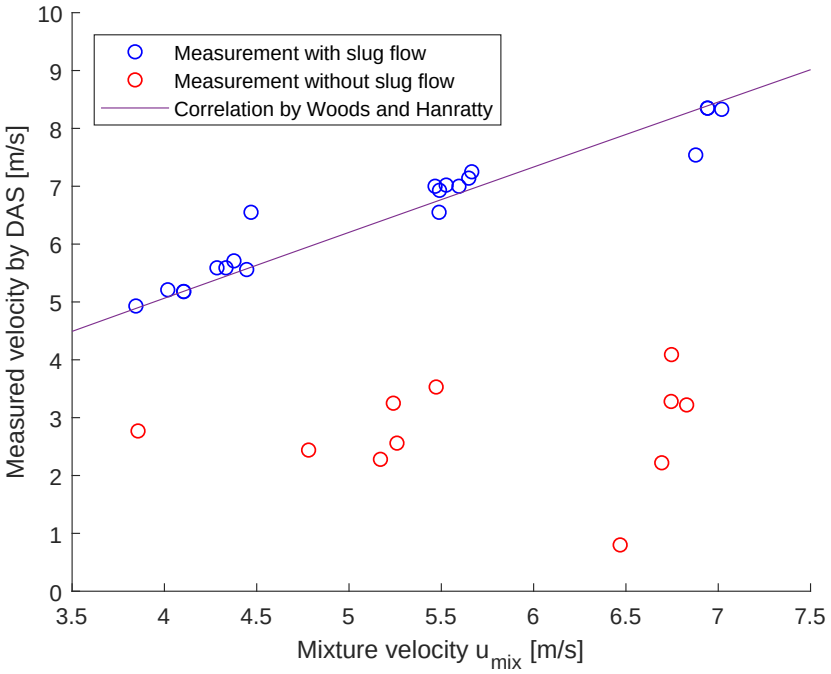

Figure 5.15: Scatter plot for all experiments with the superficial gas velocities of $u_{SG} = 3.8, 5.2, 6.6$ m/s of the slug velocity measured by DAS against the mixture velocity. In blue are the experiments where slug flow occurs, in red the experiments where no slug flow was measured and the purple line indicates the correlation by Woods and Hanratty from equation 2.59 [12]

For every experiment without surfactant the measured velocity and occurrence of the peak divided by the total number of measurements is obtained. This represents the number of features that meet the thresholds during an experiment corrected by the total number of measurements and could be a predictor for the determination of the flow pattern. However, this parameter is not a good indicator to determine whether slug flow exists in the system. As is shown in figure 5.16, the parameter varies for experiments without slug flow from 0 to $6 \cdot 10^{-3}$, while for experiments with slug flow it varies from $1.8 \cdot 10^{-3}$ to $8.5 \cdot 10^{-3}$. The measured velocity seems to be better at distinguishing between stratified flow and slug flow.

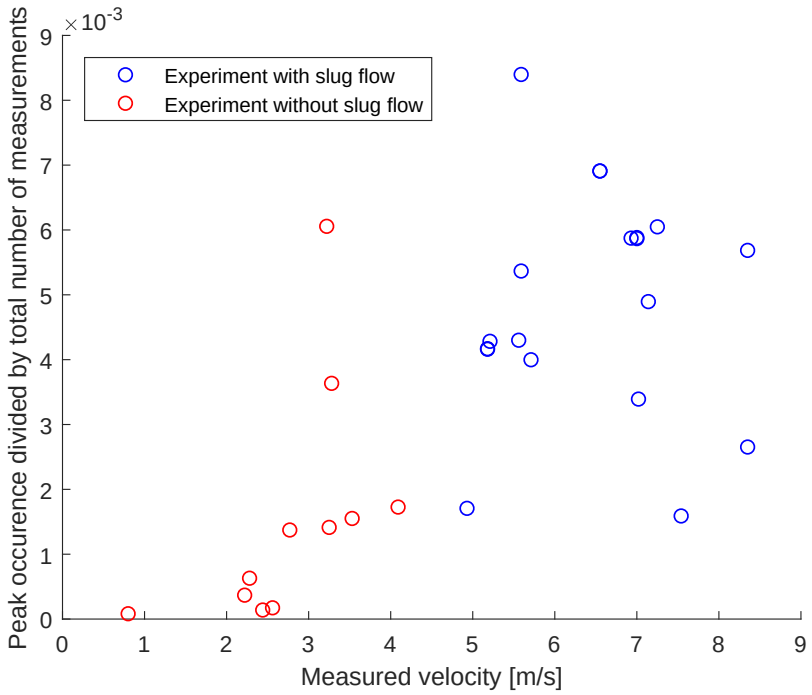

Figure 5.16: Scatter plot for all experiments with the superficial gas velocities of u_{SG} = 3.8, 5.2, 6.6 m/s of the slug velocity measured by DAS against the number of measurements where the most occurring velocity was measured divided by the total number of measurements. In blue are the experiments where slug flow occurs and in red the experiments where no slug flow was measured.

The explanation for this finding is that the algorithm is good in detecting moving features or events in the flowline. Especially in the transition region from stratified flow to slug flow there are slugs being created that are dampened out or merged into another slug. This is why they do not reach to the fully developed slug velocity and lead to measurements of events with a lower velocity than for flow that is clearly in the slug flow region. Once there are fully developed slugs moving through the system, the most measured velocity will be higher and will be near to other slug velocities with similar mixture velocities. Also the often measured velocity is close to the correlations that can be found in the literature.

5.3.4. SLUG VELOCITY ESTIMATION USING PRESSURE MEASUREMENTS

The determination of the slug velocity by using the two differential pressure indicators, DPI-430 halfway along the flowline and DPI-102 at the end of the horizontal flowline, and cross correlating between the measured data turns out to be not reliable, as can be seen in figure 5.17. The differential pressure indicators measure over a distance of 3 m and are able to make an accurate distinction between slug flow and stratified flow. However, the sampling frequency of 1 Hz is unfortunately too low to produce an accurate estimation of the slug velocity. The characteristics of slug flow, such as the multi modal behaviour, differences between the velocities of the slugs, differences between the velocity of the nose and tail of the slug, and merging of two slugs moving at different speeds, make the slug velocity a difficult to measure quantity.

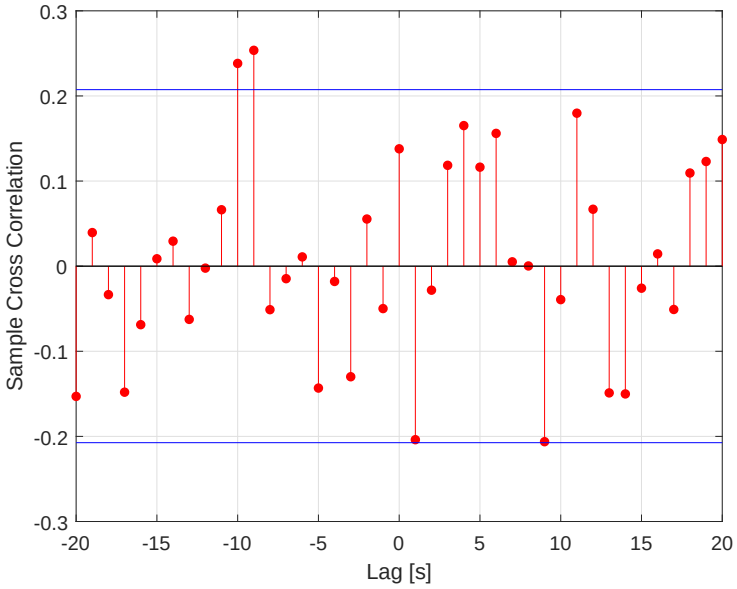

Figure 5.17: Cross correlation between DPI-430 halfway along the flowline and DPI-102 at the end of the flowline for $u_{SL} = 0.3$ m/s and $u_{SG} = 5.2$ m/s

When the slug velocity is determined using the pressure indicators PI-300 at the start of the flowline and PI-210 at the end of the horizontal flowline using the cross correlation method, the lag with the highest correlation is 0 s, as can be seen in figure 5.18. This is a unrealistic outcome, which is most likely caused by the reasons given in the section about the cross correlation between the DPI sensors in combination with a lower accuracy of the PI sensors.

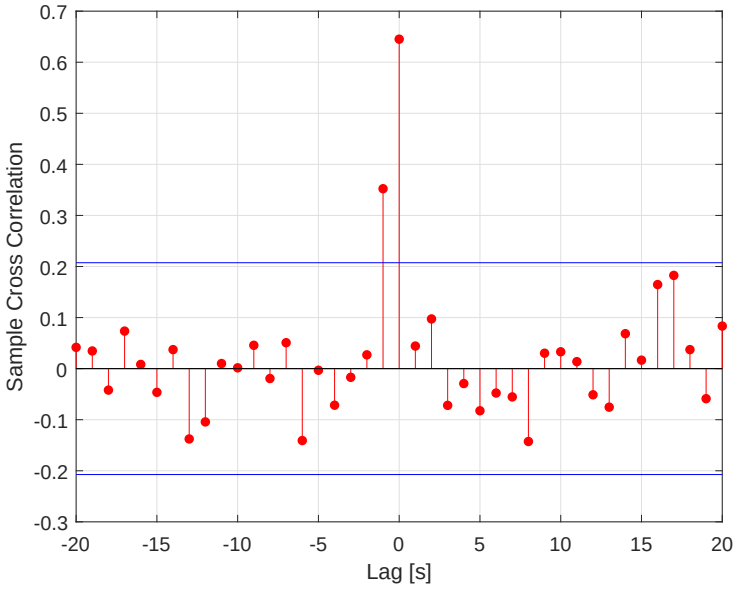

Figure 5.18: Cross correlation between PI-300 at the start of the flowline and PI-210 at the end of the flowline for $u_{SL} = 0.3$ m/s and $u_{SG} = 5.2$ m/s

5.3.5. COMPARISON WITH THE EXPERIMENTS BY WILKENS AND THOMAS

The experimental setup that was used by Wilkens and Thomas has a diameter of 52 mm, which is close to the diameter used in the experiment in the current research. The main difference between the two studies is the used surfactant: Wilkens and Thomas used SDS, while for this research Dreft was used.
In figure 5.19 a comparison of the pressure drop measurements can be seen. In black are the results from the experiments by Wilkens and Thomas [7] and the coloured filled dots are the results from the current research. The mitigation of slug flow that was achieved at a concentration of 2000 ppm of Dreft Original confirms the findings by Wilkens and Thomas that slugs can be suppressed using surfactants. The conversion between different types of surfactants that has been done by van Nimwegen et al. for vertical flows [5] does not hold for horizontal flows. Wilkens and Thomas achieved slug suppression and a reduction of the pressure drop already by using a concentration of 400 ppm of SDS. This corresponds to a concentration of 500 ppm Dreft Original.
The most interesting region of superficial liquid velocities could not be achieved for experiments with a 2000 ppm concentration of Dreft Original in our experimental setup due to a reduction of the pump efficiency. However, there is a clear distinction between the pressure drop measurements where an insufficient amount of surfactant was added and experiments where the concentration of surfactant was high enough to suppress slug flow, which is similar to the findings of Wilkens and Thomas. In our experiments an increase of the pressure drop for a small concentration of surfactant above $u_{SL} = 0.4$ m/s was found, which is similar to what was measured by Wilkens and Thomas, although their measured increase of the pressure drop was smaller. This effect could be caused by an increase of the wall friction caused by the foam layer and a reduction of the surface tension due to the added surfactant. From visual observations it could be seen that the foam rolled over the surface and at larger liquid superficial velocities it partly sticked to the pipe wall.

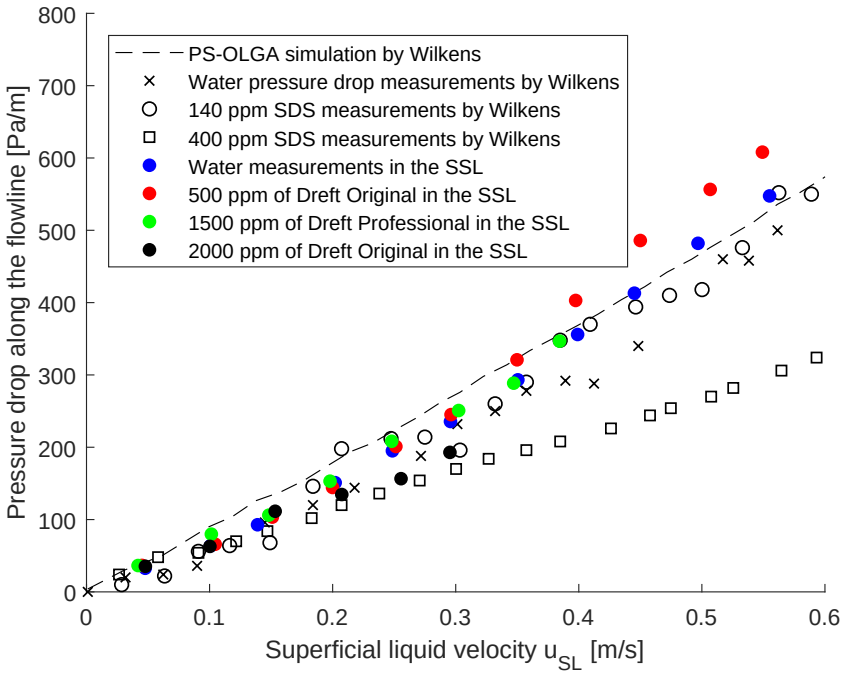

Figure 5.19: Comparison of the experiments and simulations by Wilkens and Thomas[7] with the experiments from the current research for a constant superficial gas velocity of $u_{SG} = 5.2$ m/s

5.3.6. COMPARISON WITH THE SHELL FLOW EXPLORER

The Shell Flow Explorer can be used to calculate the characteristics of single-phase and multiphase flow in pipelines. Since the 2017 version a foam model has been incorporated, which is able to calculate the flow characteristics for vertical flow with added surfactants. The input parameter for surfactants is the effective concentration in ppm, which is based on the research by van Nimwegen et al. [5].

The model automatically switches flow patterns, based on the input parameters. A comparison has been made between the measured pressure drop and the value as calculated by the Shell Flow Explorer; this comparison can be seen in figure 5.20. To give a better representation of the effect of the surfactant on the pressure drop, both the slug flow regime and the stratified flow regime have been imposed in the SFE simulations for all superficial liquid velocities.

The estimated pressure drop represented by the blue line does not give a good estimation of the actual pressure drop. The transition from stratified flow to slug flow is in reality much smoother than estimated by the model. The measured pressure drop for the water measurements is closer to the slug flow results than to the unforced flow pattern results, until the model switches to slug flow at $u_{SL} = 0.45$ m/s.

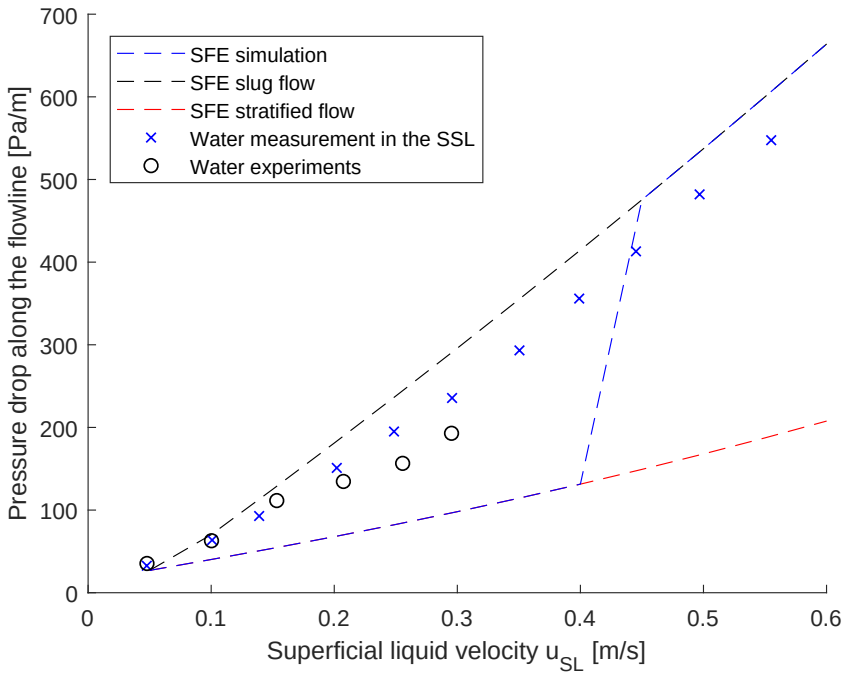

Figure 5.20: A comparison of the calculations from the Shell Flow Explorer for unforced and forced flow patterns with the experimental results for the case without surfactant and for the case with 2000 ppm of Dreft Original at $u_{SG} = 5.2$ m/s

5.4. SEVERE SLUGGING

In all experiments where initially severe slugging was reported, the slugging was mitigated by increasing the concentration of the surfactant. In the figures 5.21 and 5.22, the measured pressure drop over the full length of the riser (16.8 m) is shown for air-water flow without surfactant, with 1500 ppm of Dreft Professional and with 2000 ppm of Dreft Original. The two considered flow conditions are u_{SL} = 0.2 m/s with u_{SG} = 0.66 m/s and u_{SG} = 1.16 m/s. The 2000 ppm of Dreft Original is sufficient in both cases to prevent the severe slugging cycle. Therefore the minimum concentration at which severe slugging is suppressed most likely is located somewhere between 810 and 2000 ppm of the Dreft Original concentration.

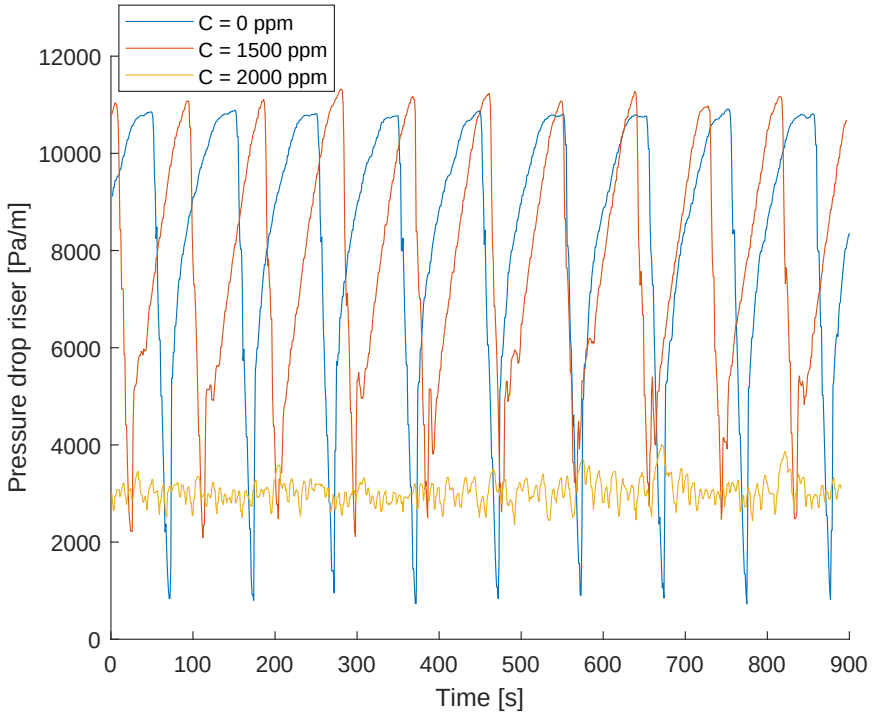

Figure 5.21: Pressure drop along the riser for different concentrations of the surfactant at u_{sl} = 0.2 m/s and u_{sg} = 0.66 m/s (no surfactant, 1500 ppm of Dreft Professional, 2000 ppm of Dreft Original)

Figure 5.21 clearly shows that 2000 ppm of Dreft Original completely suppresses the severe slugging cycle. Using 1500 ppm of Dreft Professional does not prevent the severe slugging, but only increases the frequency of the cycle and reduces the difference between the maximum and minimum pressure drop. Also the build up phase for that concentration seems to be more unstable, as shown by the wiggles in the pressure drop after the minimum has been reached.

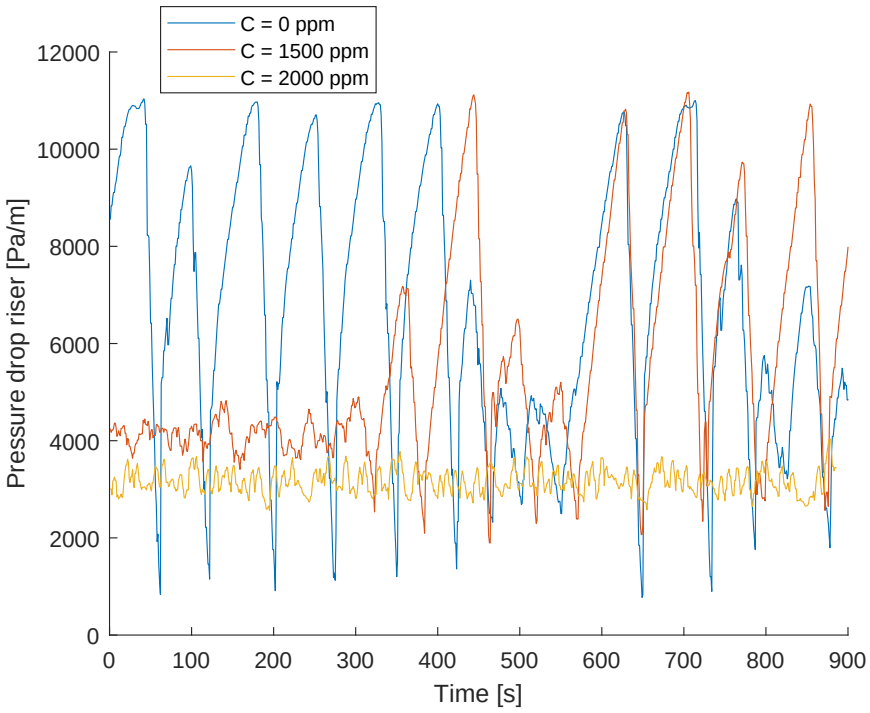

Figure 5.22: Pressure drop along the riser for different concentrations of the surfactant at u_{sl} = 0.2 m/s and u_{sg} = 1.16 m/s (no surfactant, 1500 ppm of Dreft Professional, 2000 ppm of Dreft Original)

When increasing the superficial gas velocity and keeping the superficial liquid velocity the same as shown in figure 5.22, the severe slugging cycle already becomes more unstable if surfactant is added at a 1500 ppm concentration. In fact when 1500 ppm of Dreft Professional is added, the cycle seemed to be suppressed until after 5 minutes the severe slugging suddenly started again. At 2000 ppm of Dreft Original the whole cycle is completely suppressed.
Increasing the concentration of Dreft Original unfortunately reduced the maximum achievable superficial liquid velocity. Therefore some experiments could not be reproduced at that concentration. It was found that the minimum gas to liquid ratio (GLR), that was needed to prevent severe slugging reduced with an increase of the surfactant concentration. At 2000 ppm Dreft Original, severe slugging was even suppressed at a gas to liquid ratio of 2, instead of 16, which is the minimum without surfactant. The pump was very unstable at 2000 ppm surfactant. Therefore these conditions did not satisfy the requirements for a reliable experiment.

5.5. PHYSICAL INTERPRETATION

The results obtained from the conducted experiments together with the visual observations can be used to give a physical interpretation.
When surfactant is added to stratified flow, the surface tension decreases and a third layer with foam is formed. This foam is generated by the pump or has been created earlier and is circulated through the experimental setup. The thickness of the foam layer increases and the foam bubble size decreases with the concentration of the surfactant. A change in flow pattern from stratified flow to wavy stratified flow leads to more foam being produced as well as to a smaller foam bubble size. When the flow pattern changes to slug flow these effects become larger.
If the agitation by the flow is large enough, i.e. with superficial velocities that are large enough, the foam layer is able to suppress the initiation of slugs as well as to dampen slugs that have been formed by the geometry of the flowline.
As van Nimwegen mentioned [5], unlike the gas and liquid that form the foam, foam itself is not a Newtonian fluid. It is often modelled as a Hershel-Bulkley fluid [38]. This means that foam has a non-zero yield stress

and that, above this stress value, foam is shear thinning:

$$\tau = \tau_y + \mu_{yb}\left(\frac{\partial u}{\partial y}\right)^n, \tag{5.1}$$

where τ_y is the yield stress, μ_{yb} is the plastic or Bingham viscosity, and n is the shear index ($n < 1$ for shear thinning fluids). Van Nimwegen defined the effective foam viscosity as:

$$\mu_f = \frac{\tau}{\frac{\partial u}{\partial y}} \tag{5.2}$$

Because of the non-zero yield stress of the foam layer, the foam is able to absorb shear stresses initiated by the difference in velocity between the different fluid layers. Waves are no longer initiated by the Kelvin-Helmholtz instability, as these require a yield stress that is very small or equal to zero in order to grow.
Already existing slugs in the system lead to extra foam formation in comparison to stratified flow. This additional foam layer becomes so large that the fluid waves are no longer able to fill the pipe cross section completely and the waves are bounded by both the geometry of the pipe and the height of the foam layer. The foam layer allows the gas, that normally is blocked in case of slug flow, to pass at the top side of the pipe. In the new situation the flow returns to wavy stratified flow with foam as a third layer.
If the foam is unable to dampen the slug flow, the flow pattern is comparable with slug flow without surfactant. Most of the foam accumulates at the tail of the slug and during periods between two slugs, there is a three layer stratified flow with foam between the gas and liquid layer.
In the case of severe slugging there is an imbalance between the volumetric flow rate of liquid that is arriving at the riser base and the volumetric flow rate of liquid that the riser is able to transport upwards for given flow conditions. This volumetric flow rate of liquid for the riser is smaller than the amount of liquid arriving at the riser base and with the right geometry the liquid then starts blocking the riser base. This is the moment that the severe slugging cycle starts, until the imbalance is neutralized.
When surfactant is added the volumetric flow rate of liquid that the gas is able to transport upwards increases because of an increase of interfacial friction between the gas and liquid and a reduction of the liquid holdup fraction. Both effects are caused by the formation of foam.
A comparison between the visual observations by the GoPro camera for the case with 500 ppm of Dreft Original where slug flow was not suppressed and the case with 2000 ppm of Dreft Original where slug flow was suppressed can be seen in figure 5.23.

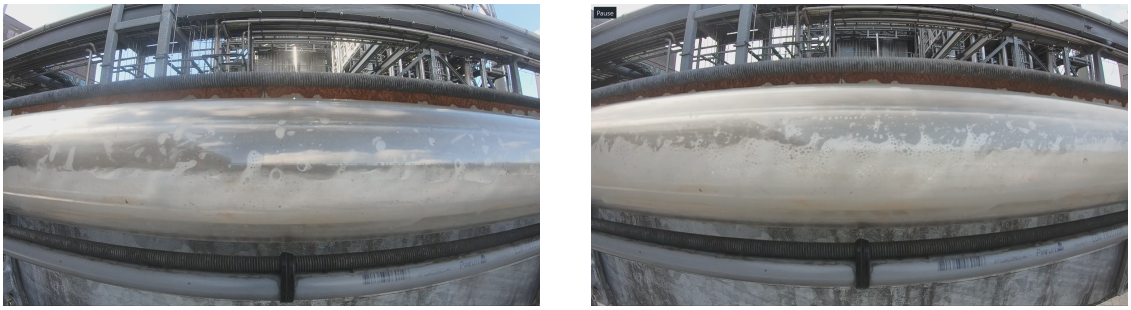

(a) 500 ppm of Dreft Original

(b) 2000 ppm of Dreft Original

Figure 5.23: Visual observation by the GoPro camera at the end of the flowline for $u_{SG} = 5.2$ m/s, $u_{SL} = 0.3$ m/s

6

CONCLUSIONS

Promising applications of surfactants in wells and vertical risers, as well as previous work on the influence of surfactants on two-phase air-water mixtures in flowlines and risers, has led to the interest in further exploring the influence of surfactants on slug flow in horizontal pipelines and on severe slugging in flowline-riser systems.
To investigate the effect of surfactants on gas-liquid flows, lab experiments were carried out using the Severe Slugging Loop at the Shell Technology Centre Amsterdam. This flow loop consists of a 50 meter long horizontal flowline, followed by a U-turn, a 15 meter horizontal section, a 30 meter 2.54° declined section, and multiple vertical risers of 16.8 m height with 32 mm and 44 mm diameters. Air and water were used as gas and liquid in combination with various concentrations of the dish washing detergent Dreft, which produced more foam as the concentration was increased. Multiple measurement devices were used: (Differential) Pressure Indicators (DPIs and PIs), Distributed Acoustic Sensing (DAS) system by Optasense and a GoPro Hero 6 camera at 1080p240fps for flow visualisation.
From the conducted experiments and data analysis the following conclusions can be drawn for the effect of surfactants on gas-liquid flows in horizontal flowlines and in flowline-riser systems:

- The results and conclusions of the Master's thesis by Pronk are inconsistent.
  Where growing slugs were reported, there were in fact severe slugs measured. Therefore the conclusion on growing slugs is no longer valid and the conclusion on suppression of severe slugging using surfactants, where no suppression was reported, should be revised. The superficial gas velocities that were reported were not converted from normal to actual conditions. This has been shown by a re-analysis of the original measurement data and by repeating the experiments where growing slugs were reported.

- Hydrodynamic slugging in horizontal pipelines can be suppressed by using surfactants.
  Adding a sufficient amount of surfactant can suppress the formation of slugs in horizontal flow lines, which confirms the findings by Wilkens et al.[8]. The concentration of Dreft Original that was used to obtain the suppression was 2000 ppm, whereas a concentration of 1500 ppm Dreft Professional and 500 ppm of Dreft Original did not lead to the mitigation of hydrodynamic slugs.

- Severe slugging in flow line-riser systems can be suppressed by using surfactants.
  Also severe slugging can be suppressed by adding a sufficient amount of surfactant. An increase in the concentration of surfactant leads to a lower gas-liquid ratio at which the severe slugging cycle is suppressed. When the severe slugging cycle is not completely suppressed, the surfactant can induce instabilities in the build up phase and it will reduce the amplitude of the oscillations in the pressure drop over the riser, which indicates that the riser gets not filled completely with liquid anymore. When severe slugging is suppressed, the average pressure drop is much lower than during the presence of the severe slugging cycle.

- The DAS system can be used to:

  - Determine whether or not slug flow is present.
    From the acoustic signal of the flow in horizontal pipelines, the presence of slug flow can be determined relatively easily. The improved velocity tracking algorithm is able to detect specific flow

features, which are, when the right values for the thresholds are chosen, mostly slugs moving through the flowline. For this analysis either sensor data or frequency band extraction data can be used, with the latter requiring much less computational time. When the number of measured features is significant and the velocity is within the expected range for the transport of slugs, the tool can reliably predict the presence of slugs. The tool has a robust method and a high accuracy to predict whether there is slug flow or stratified flow in our experimental setup and therefore looks promising to be able to provide the same results in operational pipelines.

  - Derive the slug velocity, if slug flow exists.
    The velocity tracking algorithm can provide a velocity distribution for each measurement, which gives a good representation of the most probable slug velocities.

- The foaming factor is not a good predictor for the performance of a surfactant in suppressing hydrodynamic slugging.
  The findings by Wilkens et al. [8] and by van Nimwegen et al. [24] can be combined to convert the concentration of SDS as applied by Wilkens et al. in their experiments, through using the foaming factor of Van Nimwegen et al., to the concentration of Dreft with similar foaming behaviour and similar influence on vertical flow. Wilkens et al. found hydrodynamic slug mitigation in horizontal flow lines for 400 ppm and 800 ppm SDS, and van Nimwegen et al. proposed a foaming factor, which could convert the influence of surfactants on vertical flow for different types of surfactants. The foaming factor is 3.6 for Dreft Original and 3.4 for SDS, so converting 400 and 800 ppm SDS leads to 376 and 752 ppm Dreft Original. The results from the conducted experiments indicate that at the converted surfactant concentrations, hydrodynamic slug flow was not suppressed. To be more precise, at 810 ppm Dreft Original concentration the surfactant started to have a slug suppression effect, which is much higher than the 376 ppm Dreft Original predicted by the experiments base on Wilkens et al. using the foaming factor.

- Adding surfactants in a sufficient concentration to gas-liquid flows can suppress slugs. A foam layer is formed as a third layer between the gas and the liquid layers due to agitation of the surfactant by the flow. This foam layer behaves as a non-Newtonian fluid that is able to absorb stresses below its yield stress and has been modelled by van Nimwegen et al. [5] as a Hershel-Bulkley fluid. Once the foam layer has grown sufficiently in volume, it is able to suppress slug flow and replace it by stratified wavy flow.

7

RECOMMENDATIONS

7.1. RECOMMENDATIONS FOR THE EXPERIMENTS

- The surfactant concentration that was used to suppress hydrodynamic slug flow in horizontal pipelines had to be guessed, as the foaming factor did not give a reliable indication to convert the results in the literature with SDS to our experimental setup. It is advised to conduct further research on the suppression of hydrodynamic slug flow using surfactants at concentrations of Dreft Original between 800 and 2000 ppm. According to the literature, concentrations of surfactant that are higher than needed impose more wall friction and, according to the findings during the experiments, the performance of the pump is reduced when more surfactant is used. Finding the optimal concentration could lead to a better understanding of the behaviour of different surfactants under the same flow conditions, just like what has been done with vertical flow.

- To be able to better analyse the influence of surfactants on hydrodynamic slug flow in horizontal pipelines, using a different experimental setup is suggested. The available flow loop has sections with horizontal, downward and vertical sections. This increases the complexity of the flow behaviour inside the system, as disturbances in the riser section also influence the flow in the horizontal flowline. Using a transparent flow loop could lead to a better understanding of the start-up behaviour of slug flow with lower concentrations of the surfactant, as well as of the suppression of hydrodynamic slugs at the start of the pipe. In our setup it was only possible to view the flow through the inspection glass at the end of the first horizontal section, just before the U-turn. The DAS data suggest that, for flow conditions in the transition region between stratified flow and slug flow, once the surfactant was added, several slugs travelling at different velocities merged together in the first half of the horizontal section.

- More experiments should be conducted on the effect of surfactants on severe slugging in flowline-riser systems. The minimum gas-to-liquid ratio that was needed to prevent severe slugging reduced with an increase of the surfactant concentration. The total mitigation of severe slugging has been reported for a 2000 ppm concentration of Dreft Original and the influence on the frequency and behaviour of the severe slugging cycle has been reported for lower concentrations of surfactant. Understanding the mechanisms involved and building a model to predict the effect that different surfactants have on severe slug flow, would be useful to apply in full size flowline-riser systems where severe slug flow limits the production rate.

- During the experiments excessive foam was formed and measures had to be taken to accommodate this. Thereto a flexible hose was installed from the air exhaust at the top of the platform to the mixing vessel at the ground level. Also the pump efficiency dropped severely as the concentration of the surfactant was increased. In possible further research it is advised to use an experimental setup that is equipped to handle the amount of foam that is formed. A modification to the current experimental setup could be the injection of the surfactant at a proper location after the pump, while not circulating the water. In this way the pump is able to produce a stable inflow of water and the influence of the surfactant on solely the flow in the horizontal section can be determined.

7.2. OTHER RECOMMENDATIONS

- Using a surfactant with different properties could lead to a much better understanding of the influence of surfactants on hydrodynamic slug flow in horizontal pipelines as well as on severe slugging in flowline-riser systems. Van Nimwegen et al. and Wilkens et al. both reported that dynamic surface tension and the tendency to foam likely are the most influencing properties of surfactants on gas-liquid flows. It is recommended to carry out experiments with surfactants that foam much more or much less and determine for various surfactant concentrations with identical dynamic surface tension if this has an effect on the flow behaviour for a range of flow rates.

- The results from this research indicate that the foaming factor introduced by van Nimwegen et al. to convert concentrations of different surfactants when applied to vertical flows does not hold when converting the results obtained by Wilkens et al. with SDS to the experiments using Dreft Original. One of the possible reasons, besides the differences in experimental setup, is that it is possible that a different conversion factor is needed for flows lower than 45 degrees inclination. It could be of great interest to investigate if there are differences in foam formation between vertical and horizontal slug flow for different surfactants. One of the possible ways to investigate this is to build a similar test as the shaker test (Bikerman) by van Boven [22]. However, instead of a straight pipe segment, a pipe in the form of a closed circular loop with a reasonable diameter could be oscillated at a specific frequency to induce a flow behaviour that is similar to hydrodynamic slug flow.

- Creating a model of the effect of surfactants on hydrodynamic slug flow in horizontal pipes could be a next step for this project. In this research the remaining time left was too limited to start with creating a model, but a description of the physical interpretation has been produced. The similarities and differences with respect to the research by van Nimwegen et al. [5] and the conclusion that the described foaming factor does not hold for horizontal flow should be used as a starting point. The suggested model is a three-phase model with liquid at the bottom of the pipe, foam in the middle and gas at the top. A closure model is needed for the amount of foam produced and the characteristics of the foam for different superficial velocities. A closure model is also needed for the interfacial stress between the liquid layer and the foam layer and between the foam layer and the gas layer.

- In actual field operations the pipelines are larger in diameter and are much longer than in our experimental setup, which means that not all the effects of surfactants could be tested. Using the DAS system to detect and determine the slug properties during field trials is possibly a valuable approach, as real-time measurements of acoustics through a long fibre length could lead to even more valuable insights. As the foaming factor leads to an underestimation of the required concentration, it is advised to prepare for the use of higher concentrations of the surfactants.

- Before implementing the DAS system on large-scale systems that are in operation to determine whether the flow pattern is slug flow or stratified flow, it is advised to start with a field test. It could be possible that the different composition of the fluids and the larger diameter of the pipes lead to challenges regarding the measurements of the slug velocity. The thresholds for the velocity tracking tool should be adjusted accordingly to filter out the noise and retain the velocities of the features in the flow.

NOMENCLATURE

α_f	Liquid holdup fraction in the flowline	[m]
α_G	Gas holdup	[-]
α_L	Liquid holdup	[-]
δz	Spatial resolution	[m]
$\dot{m}_G$	Gas mass flux	[$\mathrm{kg\,s^{-1}}$]
$\dot{m}_L$	Liquid mass flux	[$\mathrm{kg\,s^{-1}}$]
$\dot{q}$	Internal heat source	[$\mathrm{kW\,m^{-3}}$]
λ	Thermal conductivity	[$\mathrm{W\,m^{-1}\,K}$]
μ	Viscosity	[Pa s]
μ_G	Gas viscosity	[Pa s]
μ_L	Liquid viscosity	[Pa s]
ϕ	Angle of the riser with respect to the horizontal	[°]
Π_{ss}	Severe slugging number	[-]
ρ	Density	[$\mathrm{kg\,m^{-3}}$]
ρ_G	Gas density	[$\mathrm{kg\,m^{-3}}$]
ρ_L	Liquid density	[$\mathrm{kg\,m^{-3}}$]
σ	Surface tension	[$\mathrm{N\,m^{-1}}$]
$\sum \mathbf{F}$	All the body forces	[N]
τ	Tangential stress	[$\mathrm{N\,m^{-2}}$]
τ_G	Tangential stress between the gas phase and pipe wall	[$\mathrm{N\,m^{-2}}$]
τ_L	Tangential stress between the liquid phase and pipe wall	[$\mathrm{N\,m^{-2}}$]
τ_{LG}	Tangential stress between the gas and liquid phase	[$\mathrm{N\,m^{-2}}$]
$\mathbf{g}$	Gravitational force vector	[$\mathrm{m\,s^{-2}}$]
$\mathbf{n}$	Normal vector	[-]
$\mathbf{u}$	Velocity vector	[$\mathrm{m\,s^{-1}}$]
$\mathbf{u}_G$	Gas velocity vector	[$\mathrm{m\,s^{-1}}$]
$\mathbf{u}_L$	Liquid velocity vector	[$\mathrm{m\,s^{-1}}$]
$\tilde{\rho}$	Dimensionless density	[-]
$\tilde{\rho}_G$	Normalized gas density	[-]
$\tilde{\rho}_L$	Normalized liquid density	[-]

$\tilde{\mathbf{u}}$	Dimensionless velocity vector	[-]
$\tilde{\mathbf{u}}_G$	Normalized gas velocity	[-]
$\tilde{\mathbf{u}}_L$	Normalized liquid velocity	[-]
$\tilde{p}$	Dimensionless pressure	[-]
$\tilde{p}_G$	Normalized gas pressure	[-]
$\tilde{p}_G$	Normalized liquid pressure	[-]
$\tilde{t}$	Dimensionless time	[-]
A	Cross sectional area of the pipe	[m^2]
A_G	Cross sectional area of the part pipe filled with gas	[m^2]
c	Speed of light in vacuum	[$m\,s^{-1}$]
c_p	Heat capacity	[$J\,K^{-1}$]
$c_{surfactant}$	Concentration of the surfactant	[-]
D	Diameter of the pipe	[m]
d	Pulse length	[m]
Eu	Euler number	[-]
f	Fanning friction factor	[-]
F_p	Pulse frequency	[Hz]
f_s	Slug frequency	[Hz]
Fr	Froude number	[-]
h	Enthalpy	[$kJ\,kg^{-1}$]
I	Ittermittency factor	[-]
L	Characteristic length	[m]
L_f	Length of the flowline upstream of the riser	[m]
L_s	Fully developed slug length	[m]
n	Refractive index of a material	[-]
n_{risers}	Number of risers	[-]
p_G	Gas pressure	[$N\,m^{-2}$]
P_N	Pressure at normal conditions	[Pa]
P_{actual}	Actual pressure	[Pa]
Q	Volumetric flow rate	[$m^3\,s^{-1}$]
Re	Reynolds number	[-]
Re_G	Reynolds number for the gas phase	[-]
Re_L	Reynolds number for the liquid phase	[-]
S	Perimeter of the pipe	[m]

s	Slip between the gas and liquid phases within the slug	
S_G	Perimeter of the gas touching the wall of the pipe in the cross sectional plane	[m]
S_L	Perimeter of the gas touching the liquid phase in the cross sectional plane	[m]
t	Time	[s]
T_N	Temperature at normal conditions	[K]
T_{actual}	Actual temperature	[K]
U	Characteristic velocity	$[\mathrm{m\,s^{-1}}]$
U_G	Average velocity of the gas phase	$[\mathrm{m\,s^{-1}}]$
u_G	Gas velocity	$[\mathrm{m\,s^{-1}}]$
U_L	Average velocity of the liquid phase	$[\mathrm{m\,s^{-1}}]$
u_L	Liquid velocity	$[\mathrm{m\,s^{-1}}]$
U_t	Slug nose velocity	$[\mathrm{m\,s^{-1}}]$
u_{mix}	Mixture velocity	$[\mathrm{m\,s^{-1}}]$
u_{SG}	Superficial gas velocity	$[\mathrm{m\,s^{-1}}]$
u_{SL}	Superficial liquid velocity	$[\mathrm{m\,s^{-1}}]$
V	Volume of the liquid in the mixing vessel	$[\mathrm{m^3}]$
v	Speed of light in glass	$[\mathrm{m\,s^{-1}}]$
$V_{surfactant}$	Volume of the surfactant	$[\mathrm{m^3}]$
We	Weber number	[-]

ABBREVIATIONS

CMC	Critical Micelle Concentration
DAS	Distributed Acoustic Sensing
DPI	Differential Pressure Indicator
DTS	Distributed Temperature Sensing
FFT	Fast Fourier Transform
GLR	Gas-Liquid Ratio
PI	Pressure Indicator
SDS	Sodium Dodecyl Sulfate
SFC	Shell Flow Correlations
SSL	Severe Slugging Loop
STCA	Shell Technology Centre Amsterdam

BIBLIOGRAPHY

[1] E. J. Pronk. The effect of surfactants on slugs in two-phase flows in flowlines and risers. Master's thesis, Delft University of Technology, 2017.

[2] S.A. Hosseini and A.A. Jalali Khalilian. Considerations in designing multiphase flow lines. *Pipeline and Gas Journal*, 239(8), 2012.

[3] R. A. W. M. Henkes. Guidelines for the hydraulic design and operation of multiphase flow pipeline systems. Shell Report SR.14.12950, 2014.

[4] A.T. van Nimwegen. *The Effect of Surfactants on Gas-Liquid Pipe Flows*. PhD thesis, Delft University of Technology, 2015.

[5] A. T. van Nimwegen, L. M. Portela, and R. A.W.M. Henkes. Modelling of upwards gas-liquid annular and churn flow with surfactants in vertical pipes. *International Journal of Multiphase Flow*, 105:1–14, 2018.

[6] Xia Guo-dong and Chai Lei. Influence of surfactant on two-phase flow regime and pressure drop in upward inclined pipes. *Journal of Hydrodynamics*, 24:39–49, 2012.

[7] R.J. Wilkens and D.K. Thomas. Multiphase drag reduction: Effect of eliminating slugs. *International Journal of Multiphase Flow*, 33:134–146, 2007.

[8] R.J. Wilkens, D.K. Thomas, and S.R. Glassmeyer. Surfactant use for slug flow pattern suppression and new flow pattern types in a horizontal pipe. *Journal of Fluids Engineering*, 128:164–169, 2006.

[9] R. V. A. Oliemans. *Applied Multiphase Flows*. Delft University of Technology, 2001.

[10] R.H.A. IJzermans and R. Lacy. Technical description shell flow correlations. Shell Report GS.09.51663, 2009.

[11] S. Chandrasekhar. *Hydrodynamic and Hydromagnetic Stability*. Clarendon Press, 1961.

[12] B.D. Woods and T.J. Hanratty. Relation of slug stability to shedding rate. *International Journal of Multiphase Flow*, 22(5):809 – 828, 1996.

[13] G. Gregory, M. Nicholson, and K. Aziz. Correlation of the liquid volume fraction in the slug for horizontal gas-liquid slug flow. *International Journal of Multiphase Flow*, 4(1):33 – 39, 1978.

[14] B.D. Woods, Z. Fan, and T.J. Hanratty. Frequency and development of slugs in a horizontal pipe at large liquid flows. *International Journal of Multiphase Flow*, 32:902–925, 2006.

[15] J.T. Fokkema. *Long liquid slugs in stratified gas/liquid flow in horizontal and slightly inclined pipes*. PhD thesis, Delft University of Technology, 2009.

[16] R. Malekzadeh. *Severe slugging in gas-liquid two-phase pipe flow*. PhD thesis, Delft University of Technology, 2012.

[17] Pyotr M. Kruglyakov Dotchi Exerowa. *Foam and Foam Films*. Elsevier, 1998.

[18] Tharwat F. Tadros. *Introduction to Surfactants*. De Gruyter, 2014.

[19] K. Lunkenheimer and K. Malysa. Simple and generally applicable method of determination and evaluation of foam properties. *Journal of Surfactants and Detergents*, 6(1):69–74, 2003.

[20] R.J. Pugh. *Bubble and Foam Chemistry*. Cambridge University Press, 2016.

[21] S. Bechan. Development of a small-scale shaking test to evaluate foamability. Bachelor's thesis, Delft University of Technology, 2014.

[22] G. M. van Boven. Prediction of the foamability of surfactants in pipe flows using a shaking test. Master's thesis, Delft University of Technology, 2015.

[23] D. Kawale. Influence of dynamic surface tension on foams: Application in gas well deliquification. Master's thesis, Delft University of Technology, 2012.

[24] A. T. van Nimwegen, L. M. Portela, and R. A.W.M. Henkes. Modelling of upwards gas-liquid annular and churn flow with surfactants in vertical pipes. *International Journal of Multiphase Flow*, 105:1–14, 2018.

[25] J. Weisman, D. Duncan, J. Gibson, and T. Crawford. Effect of fluid properties and pipe diameter on two-phase flow patterns in horizontal lines. *Int. J. Multiphase Flow*, 5:437–462, 1979.

[26] N.P. Hand, P.L. Spedding, and S.J. Ralph. The effect of surface tension on flow pattern, holdup and pressure drop during horizontal air-water pipe flow at atmospheric conditions. *The Chemical Engineering Journal*, 48:192–210, 1992.

[27] P.L. Spedding and N.P. Hand. A revised analysis of the effect of surfactants on two-phase phenomena in horizontal air-water pipe flow. *Dev. Chem. Eng. Mineral Process*, 5(3/4):267–279, 1997.

[28] R.J. Wilkens and D.K. Thomas. A simple technique for determining slug frequency using differential pressure. *Journal of Energy Resources Technology*, 130, 2008.

[29] J.P.A. Beekers. An experimental and numerical investigation of multiphase flow splitting at an impacting tjunction between a single flowline and two risers. Master's thesis, Delft University of Technology, 2016.

[30] M. L. Huber, R. A. Perkins, A. Laesecke, D. G. Friend, J. V. Sengers, M. J. Assael, I. N. Metaxa, E. Vogel, R. Mareš, and K. Miyagawa. New international formulation for the viscosity of h2o. *Journal of Physical and Chemical Reference Data*, 38(2):101–125, 2009.

[31] P. in 't Panhuis. Distributed acoustic sensing - a primer on the application of das for downhole flow monitoring. Shell Report SR.15.11964, 2015.

[32] P. in 't panhuis, R. Kusters, and L. Groen. Second das field trial for flow assurance in brunei zonal production allocation and multi-phase flow characterization. Shell Report SR.12.10291, 2012.

[33] P. in 't panhuis, D. Roy, and R. Kusters. An integrated analysis of das and dts for production profiling and monitoring in deviated tight gas wells. Shell Report SR.13.12851, 2014.

[34] N. S. Neidell and M. Turhan Taner. Semblance and other coherency measures for multichannel data. *GEOPHYSICS*, 36(3):482–497, 1971.

[35] R. Paleja, D. Mustafina, P. in 't panhuis, T. Park, D. Randell, J. van der Horst, and R. Crickmore. Velocity tracking for flow monitoring and production profiling using distributed acoustic sensing. Conference paper SPE Annual Technical Conference and Exhibition, SPE-170917-MS, January, 2015.

[36] R. J. Paleja, D. Randell, A. G. Askegar, P. P. H. M. W. Panhuis, and D. A. Mustafina. Das technology: Algorithms to estimate velocities of sound and hydrocarbons. Shell Report SR.14.11106, 2015.

[37] H. Geun Lee and J. Kim. Two-dimensional kelvin–helmholtz instabilities of multi-component fluids. *European Journal of Mechanics - B/Fluids*, 49:77 – 88, 2015.

[38] D. Weaire, S. Hutzler, W. Drenckhan-Andreatta, A. Saugey, and S. Cox. The rheology of foams. *Prog. Colloid Polym. Sci.*, 133:100–105, 01 1970.

A

VIDEO IMAGES

Figure A.1: Visual observation by the GoPro camera at the end of the flowline for u_{SG} = 5.2 m/s, u_{SL} = 0.3 m/s and no surfactant was added

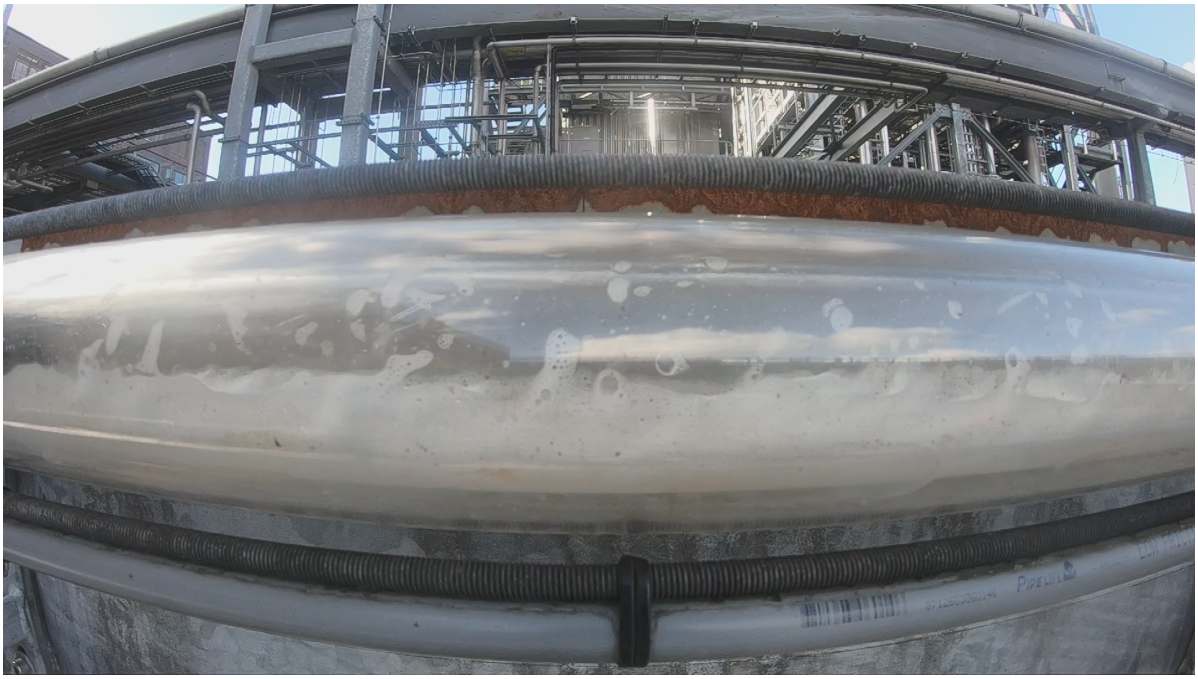

Figure A.2: Visual observation by the GoPro camera at the end of the flowline for u_{SG} = 5.2 m/s, u_{SL} = 0.3 m/s and 500 ppm concentration of the surfactant Dreft Original

Figure A.3: Visual observation by the GoPro camera at the end of the flowline for u_{SG} = 5.2 m/s, u_{SL} = 0.3 m/s and 1000 ppm concentration of the surfactant Dreft Professional

Figure A.4: Visual observation by the GoPro camera at the end of the flowline for u_{SG} = 5.2 m/s, u_{SL} = 0.3 m/s and 1500 ppm concentration of the surfactant Dreft Professional

Figure A.5: Visual observation by the GoPro camera at the end of the flowline for u_{SG} = 5.2 m/s, u_{SL} = 0.3 m/s and 2000 ppm concentration of the surfactant Dreft Original

B

PRESSURE DROP ALONG THE HORIZONTAL FLOWLINE

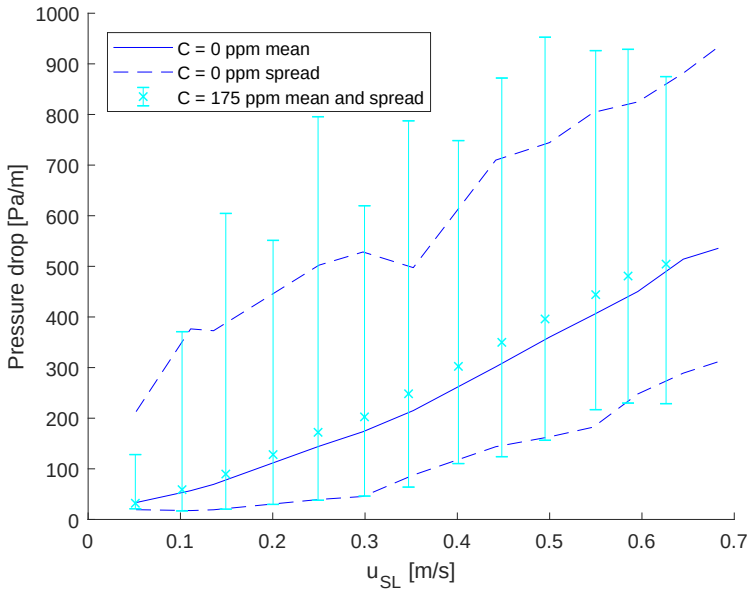

Figure B.1: Mean and spread of the pressure drop measured by the differential pressure indicator halfway along the flow line for the case without surfactant and for the case with 175 ppm of Dreft Original at $u_{SG} = 3.8$ m/s.

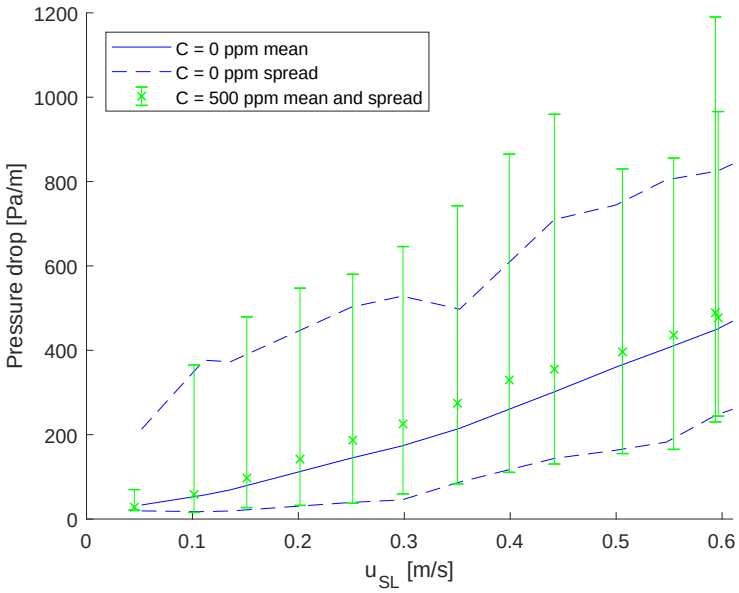

Figure B.2: Mean and spread of the pressure drop measured by the differential pressure indicator halfway along the flow line for the case without surfactant and for the case with 500 ppm of Dreft Original at $u_{SG} = 3.8$ m/s.

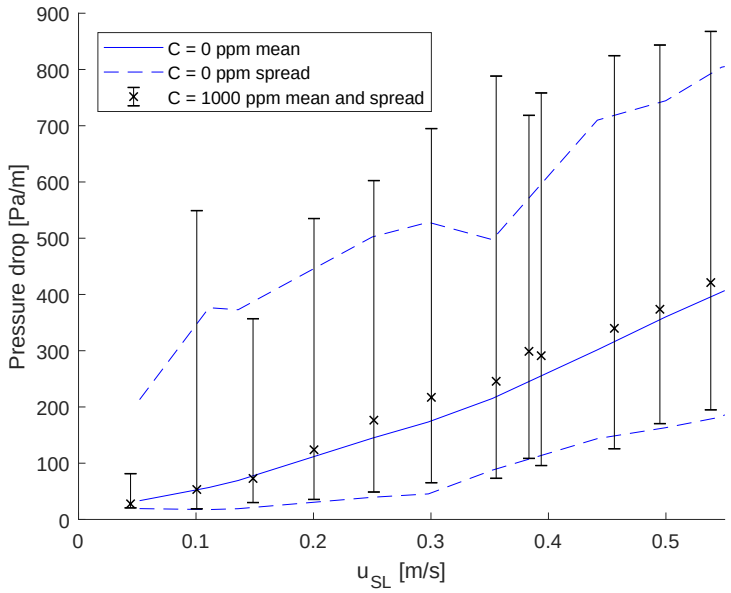

Figure B.3: Mean and spread of the pressure drop measured by the differential pressure indicator halfway along the flow line for the case without surfactant and for the case with 1000 ppm of Dreft Professional at $u_{SG} = 3.8$ m/s.

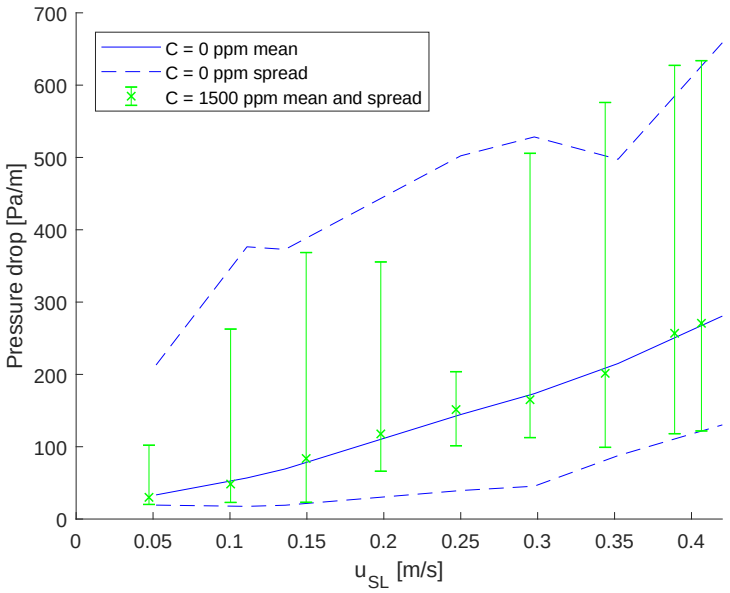

Figure B.4: Mean and spread of the pressure drop measured by the differential pressure indicator halfway along the flow line for the case without surfactant and for the case with 1500 ppm of Dreft Professional at $u_{SG} = 3.8$ m/s.

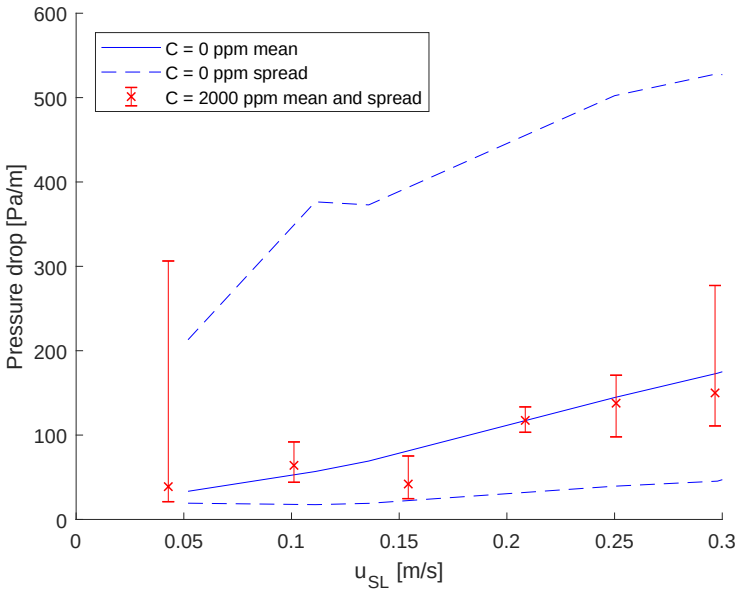

Figure B.5: Mean and spread of the pressure drop measured by the differential pressure indicator halfway along the flow line for the case without surfactant and for the case with 2000 ppm of Dreft Original at $u_{SG} = 3.8$ m/s.

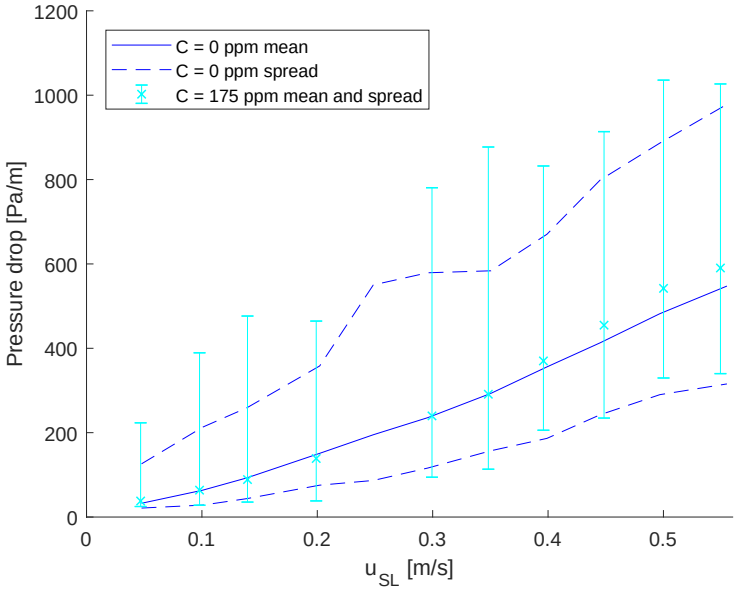

Figure B.6: Mean and spread of the pressure drop measured by the differential pressure indicator halfway along the flow line for the case without surfactant and for the case with 175 ppm of Dreft Original at $u_{SG} = 5.2$ m/s.

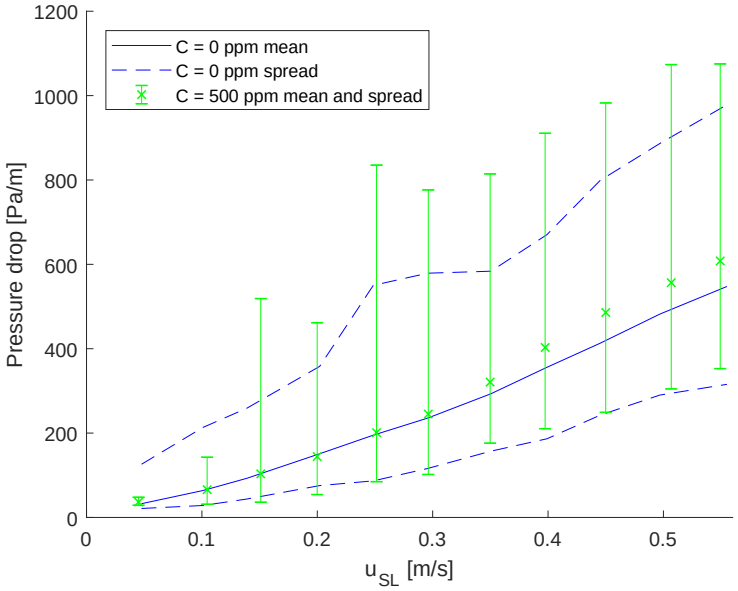

Figure B.7: Mean and spread of the pressure drop measured by the differential pressure indicator halfway along the flow line for the case without surfactant and for the case with 500 ppm of Dreft Original at $u_{SG} = 5.2$ m/s.

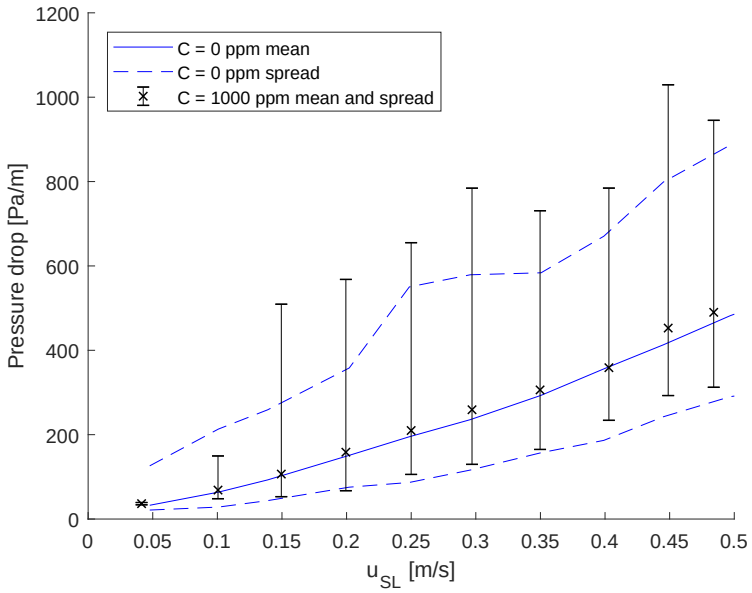

Figure B.8: Mean and spread of the pressure drop measured by the differential pressure indicator halfway along the flow line for the case without surfactant and for the case with 1000 ppm of Dreft Professional at $u_{SG} = 5.2$ m/s.

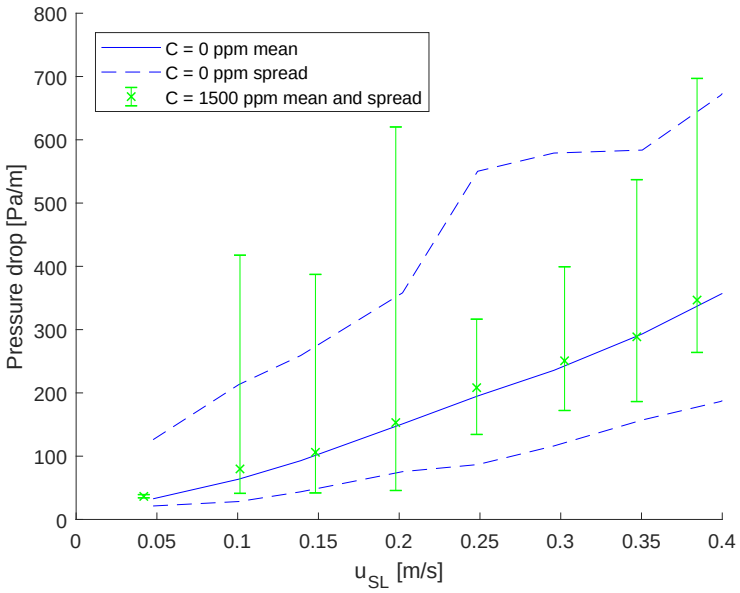

Figure B.9: Mean and spread of the pressure drop measured by the differential pressure indicator halfway along the flow line for the case without surfactant and for the case with 1500 ppm of Dreft Professional at $u_{SG} = 5.2$ m/s.

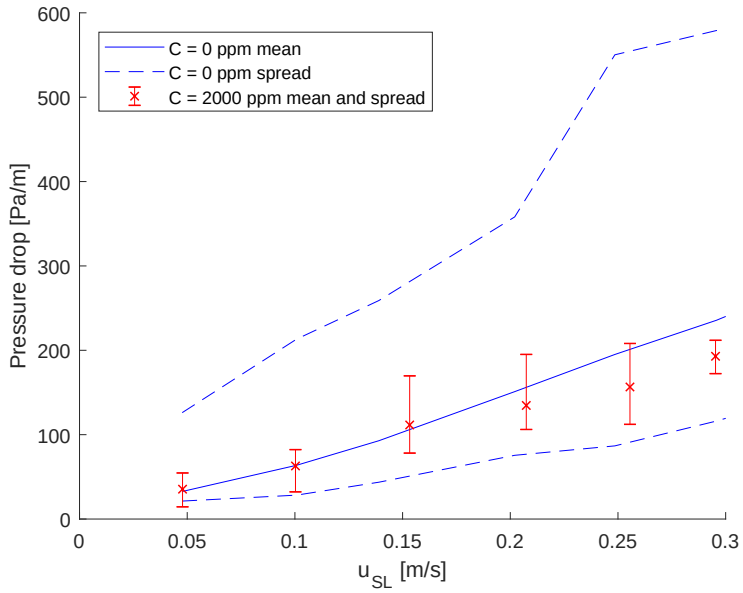

Figure B.10: Mean and spread of the pressure drop measured by the differential pressure indicator halfway along the flow line for the case without surfactant and for the case with 2000 ppm of Dreft Original at $u_{SG} = 5.2$ m/s.

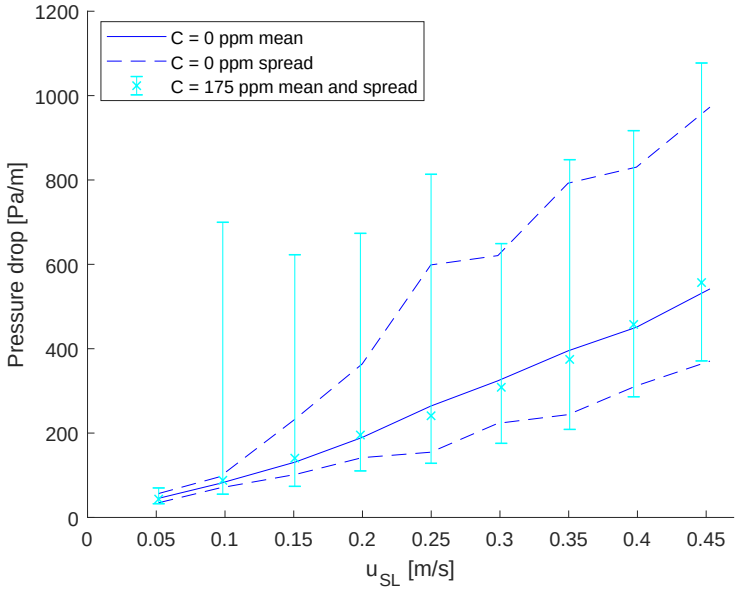

Figure B.11: Mean and spread of the pressure drop measured by the differential pressure indicator halfway along the flow line for the case without surfactant and for the case with 175 ppm of Dreft Original at $u_{SG} = 6.6$ m/s.

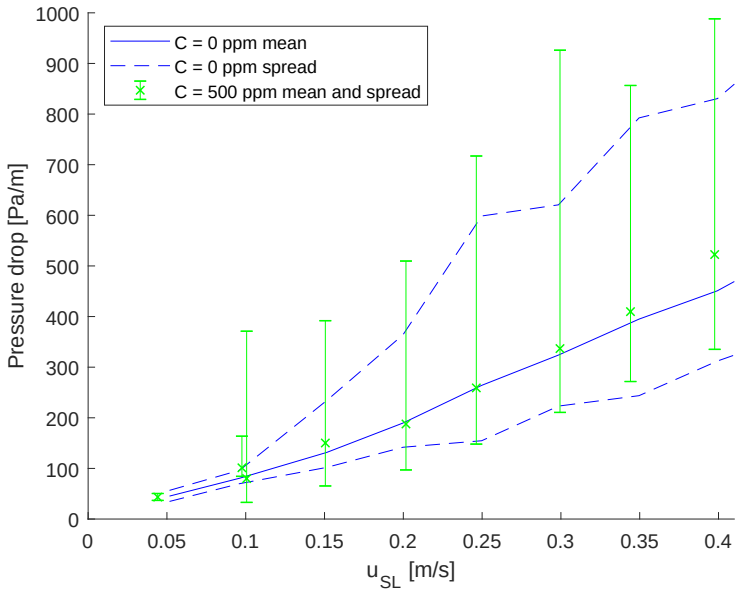

Figure B.12: Mean and spread of the pressure drop measured by the differential pressure indicator halfway along the flow line for the case without surfactant and for the case with 500 ppm of Dreft Original at $u_{SG} = 6.6$ m/s.

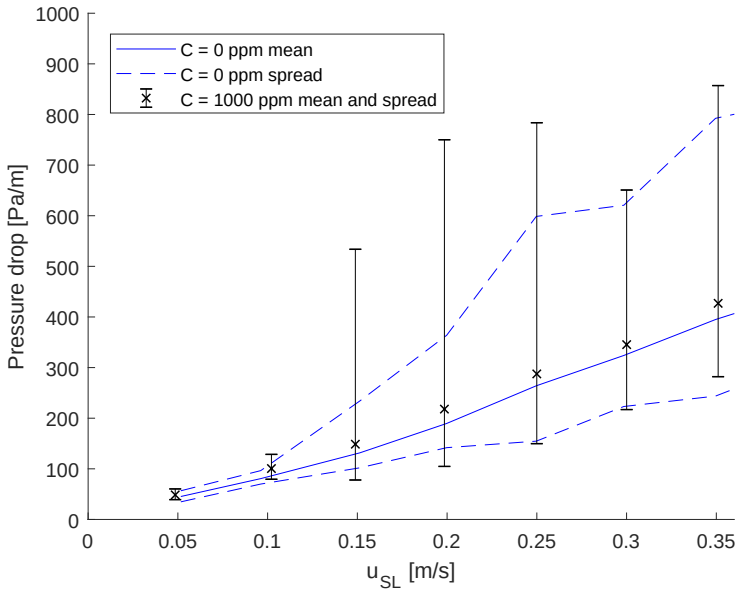

Figure B.13: Mean and spread of the pressure drop measured by the differential pressure indicator halfway along the flow line for the case without surfactant and for the case with 1000 ppm of Dreft Professional at $u_{SG} = 6.6$ m/s.

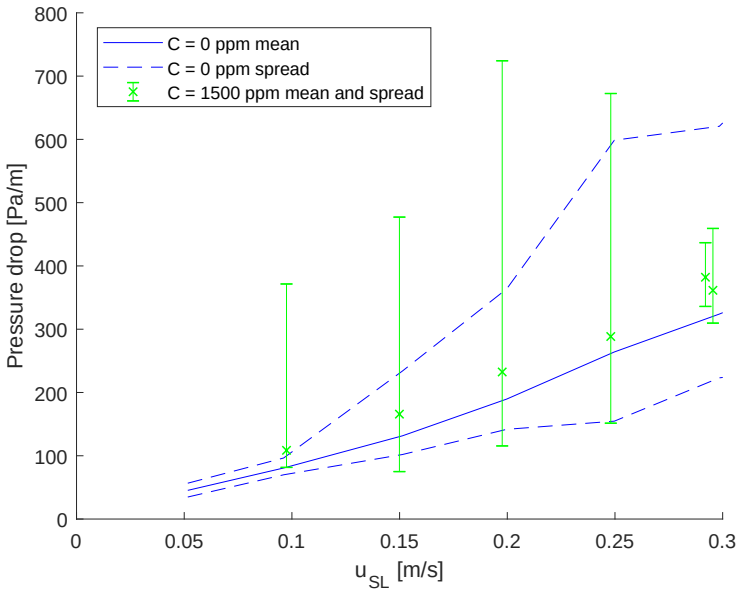

Figure B.14: Mean and spread of the pressure drop measured by the differential pressure indicator halfway along the flow line for the case without surfactant and for the case with 1500 ppm of Dreft Professional at $u_{SG} = 6.6$ m/s.

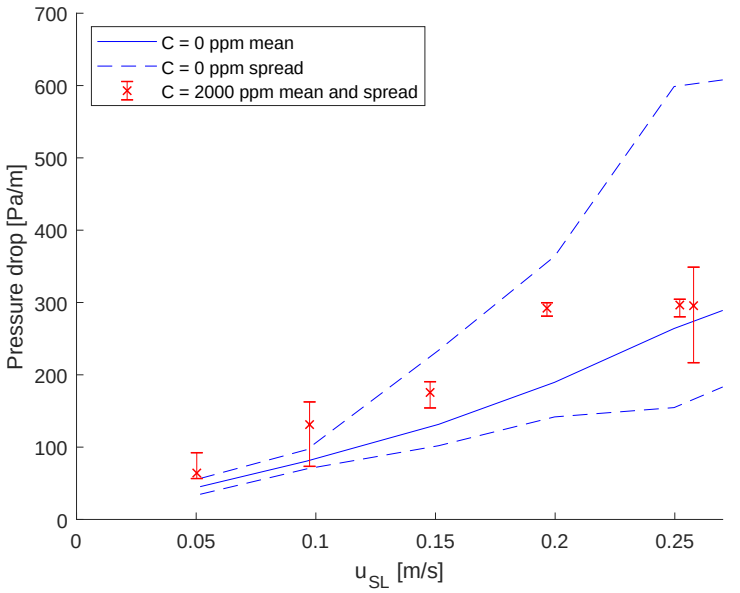

Figure B.15: Mean and spread of the pressure drop measured by the differential pressure indicator halfway along the flow line for the case without surfactant and for the case with 2000 ppm of Dreft Original at $u_{SG} = 6.6$ m/s.

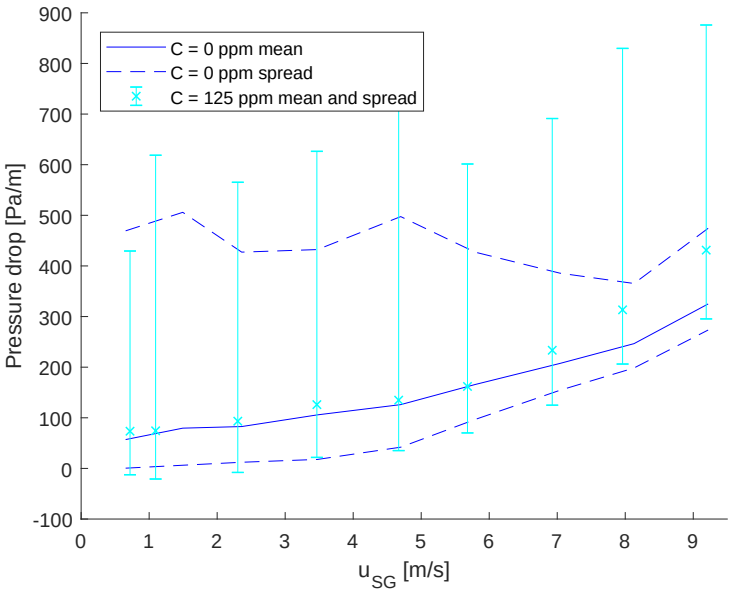

Figure B.16: Mean and spread of the pressure drop measured by the differential pressure indicator halfway along the flow line for the case without surfactant and for the case with 125 ppm of Dreft Original at $u_{SL} = 0.2$ m/s.

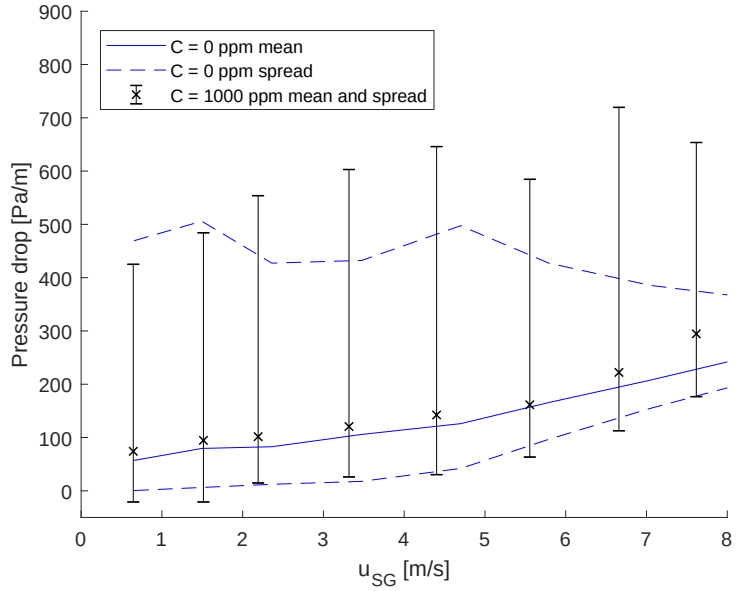

Figure B.17: Mean and spread of the pressure drop measured by the differential pressure indicator halfway along the flow line for the case without surfactant and for the case with 1000 ppm of Dreft Professional at $u_{SL} = 0.2$ m/s.

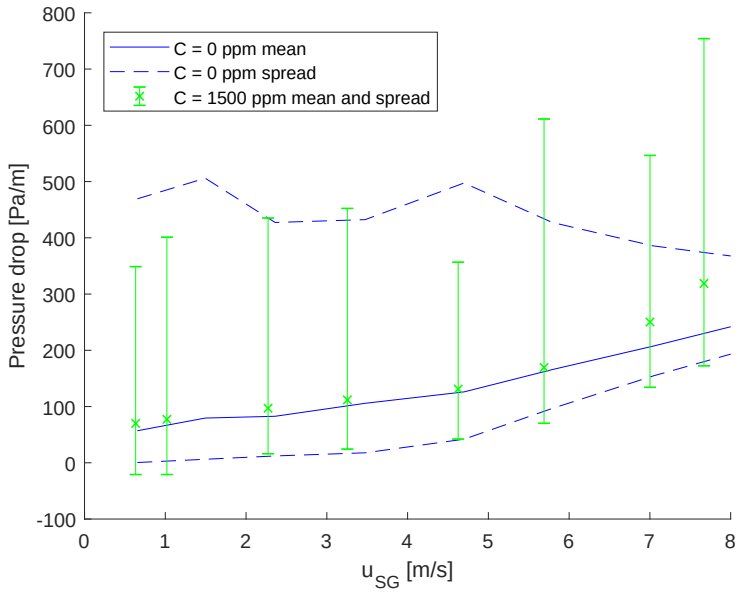

Figure B.18: Mean and spread of the pressure drop measured by the differential pressure indicator halfway along the flow line for the case without surfactant and for the case with 1500 ppm of Dreft Professional at $u_{SL} = 0.2$ m/s.

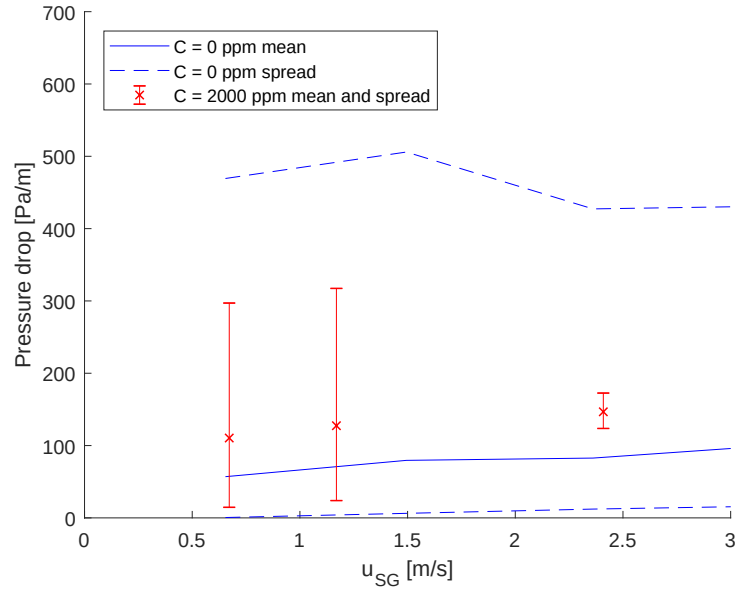

Figure B.19: Mean and spread of the pressure drop measured by the differential pressure indicator halfway along the flow line for the case without surfactant and for the case with 2000 ppm of Dreft Original at $u_{SL} = 0.2$ m/s.

C

PRESSURE DROP ALONG THE RISER

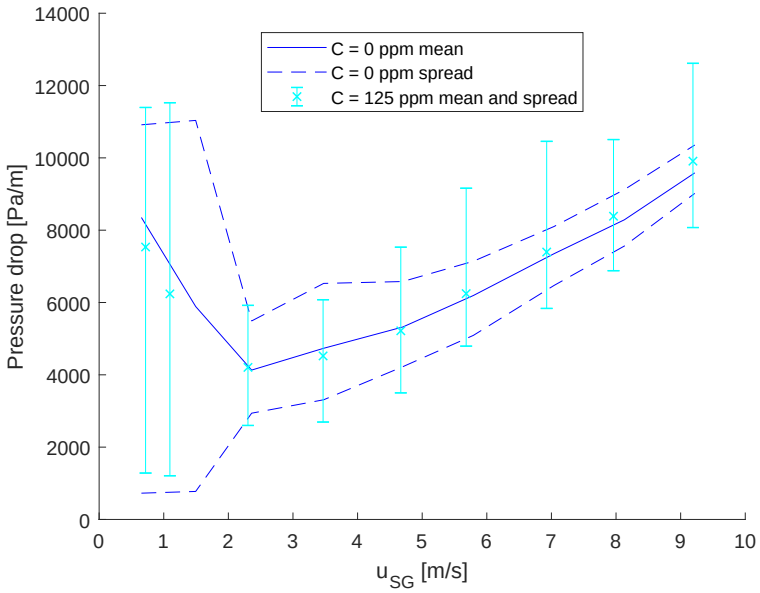

Figure C.1: Mean and spread of the pressure drop measured between the riser bottom and top, divided by the length of the riser, for the case without surfactant and for the case with 125 ppm of Dreft Original at $u_{SL} = 0.2$ m/s.

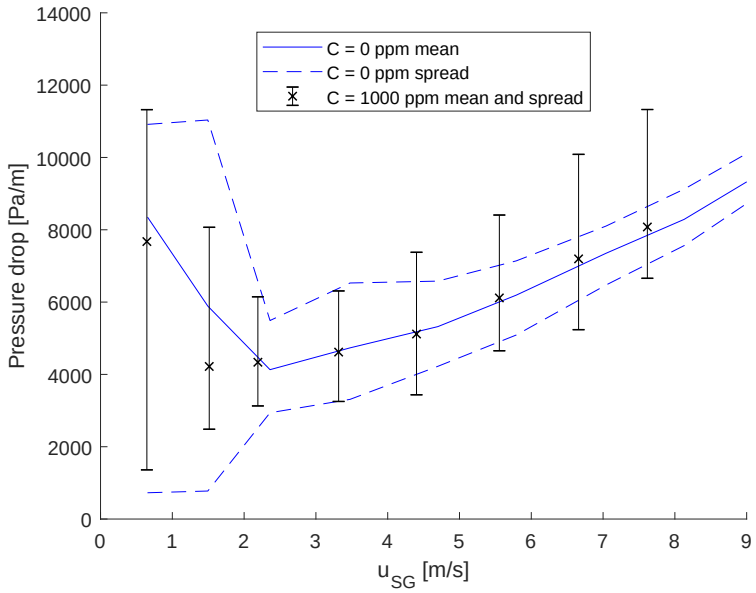

Figure C.2: Mean and spread of the pressure drop measured between the riser bottom and top, divided by the length of the riser, for the case without surfactant and for the case with 1000 ppm of Dreft Professional at $u_{SL} = 0.2$ m/s.

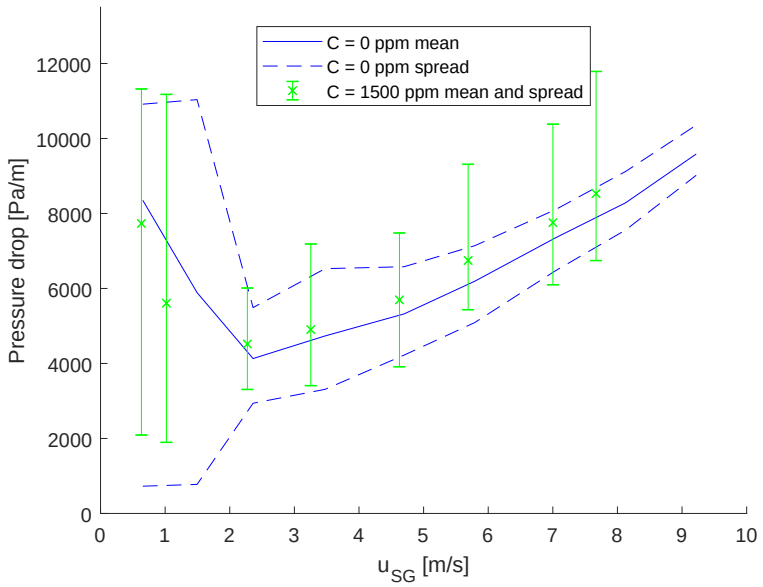

Figure C.3: Mean and spread of the pressure drop measured between the riser bottom and top, divided by the length of the riser, for the case without surfactant and for the case with 1500 ppm of Dreft Professional at $u_{SL} = 0.2$ m/s.

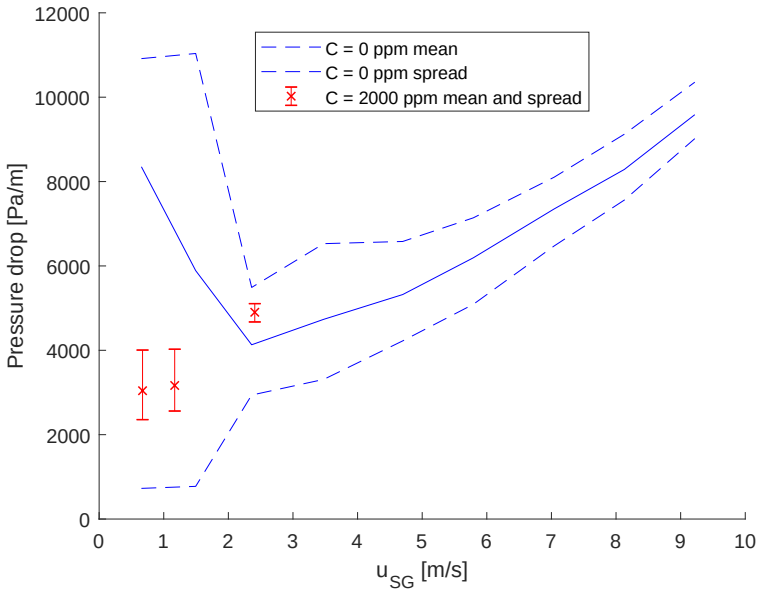

Figure C.4: Mean and spread of the pressure drop measured between the riser bottom and top, divided by the length of the riser, for the case without surfactant and for the case with 2000 ppm of Dreft Original at $u_{SL} = 0.2$ m/s.